Supplementary Information

Conserved ancestral tropical niche but different continental histories explain the latitudinal diversity gradient in brush-footed butterflies

Nicolas Chazot, Fabien L. Condamine, Gytis Dudas, Carlos Peña, Ullasa Kodandaramaiah, Pavel Matos-Maraví, Kwaku Aduse-Poku, Marianne Elias, Andrew D. Warren, David J. Lohman, Carla M. Penz, Phil DeVries, Zdenek F. Fric, Soren Nylin, Chris Müller, Akito Y. Kawahara, Karina L. Silva-Brandão, Gerardo Lamas, Irena Kleckova, Anna Zubek, Elena Ortiz-Acevedo, Roger Vila, Richard I Vane-Wright, Sean P. Mullen, Chris D. Jiggins, Christopher W. Wheat, Andre V. L. Freitas, Niklas Wahlberg.

Supplementary Methods 1 - Gene and taxon sampling

We based our analyses on 11 gene regions: the mitochondrial COI gene (1473 bp) and the nuclear genes ArgKin (596 bp), CAD (850 bp), DDC (373 bp), EF1a (1240 bp), GAPDH (691 bp), IDH (710 bp), MDH (733 bp), RpS5 (617 bp), RpS2 (411 bp), and wingless (412 bp). These gene regions have been used extensively in molecular systematic studies of Nymphalidae. Most unpublished sequences that we use have been generated according to protocols reported in [1].

We assembled our dataset from two databases: our own VoSeq [2] and BoLD [3]. From each of these databases we extracted all the individuals classified as "Nymphalidae", which gave us 10,477 individuals and 23,138 individuals respectively (as of May 2016). In the VoSeq dataset, we filtered multiple hits of species names by keeping only one species representative having the highest number of base pairs available. This first list of taxa was compared to the dataset imported from BoLD, which allowed adding 415 taxa absent from VoSeq for a total of 3,070 taxa. This list of taxa was further cleaned by checking for misspellings of names leading to multiple representatives per species. We also removed all the barcode sequences imported from BoLD that were not associated with a published paper on GenBank. We checked for the validity of all species names, mostly relying on online resources (e.g. http://ftp.funet.fi/pub/sci/bio/life/insecta/lepidoptera/ditrysia/papilionoidea/nymphalidae/). When we encountered a disagreement on taxon assignment we searched for the most recent relevant source of information to decide whether the taxon was included as a valid species or removed. All these sequences were aligned in Codon Code v.7.1.2 (CodonCode Corporation, www.codoncode.com) and uploaded into our VoSeq database. Finally, we used RAxML v.8.2.12 [4] on the full dataset, to search for the best scoring topology. We partitioned the dataset into 4 subsets: 1st position of all nuclear genes, 2nd position of all nuclear genes, 3rd position of all nuclear genes, 1st and 2nd position of COI (3rd position of COI was excluded). We selected a GTR+G to model substitution rates for each partition. This RAxML analysis was used to identify misidentifications, rogue taxa, and other species with unexpected phylogenetic positions likely resulting from human/laboratory error and to check for misalignments. Rogue taxa were removed from the dataset. After these cleaning steps, we ended up with a final taxon sampling of 2,866 species (Supplementary Data 1).

Supplementary Methods 2 - Time-calibrated phylogeny

1 - Overview

The scale of our dataset prevented us from a direct timing of divergence analysis of the full dataset. Therefore, we adopted a tree grafting procedure (e.g., [5–7]). We first built a backbone tree, based on a dataset of 800 taxa with at least 6 sequenced gene regions available. This backbone was time-calibrated using a set of 20 secondary calibrations from a recent genus level time-calibrated tree of all Papilionoidea [8]. We then inferred 15 species-level trees, corresponding often to the different subfamilies. For these trees, we included as many species as possible regardless of the amount of molecular information available, and we estimated relative times of divergence. Finally, these subclade trees were rescaled using the age of the root estimated in the backbone analysis, to be grafted on the backbone tree. This process was performed on the posterior distributions of both the backbone and the subclades to build a posterior distribution of grafted trees, each tree with 2,866 species.

2 - *Backbone dataset*

To build a robust time-calibrated backbone tree, we created a subset of taxa that had at least 6 gene regions out of 11 to limit the potential effect of missing information in our molecular dataset. All genera were represented in this subset, which contained 1,172 taxa. We further refined this list by removing some taxa from clades that were overrepresented. As such, our final dataset contained 789 species classified as Nymphalidae (Supplementary Data 1). We added 11 outgroups, including Lycaenidae and Riodinidae – the two sister families of Nymphalidae - and Pieridae, sister family to Lycaenidae + Riodinidae + Nymphalidae. Preliminary analyses revealed potential saturation with the 3rd codon position of COI for the time-calibration analysis. Thus, we excluded this position from the backbone analyses.

3 - Time-calibrated backbone phylogeny

For the backbone tree, we followed [8]'s partitioning strategy for the backbone: 1st position of all nuclear genes, 2nd position of all nuclear genes, 3rd position of all nuclear genes, 1st and 2nd position of COI. For each subset, the substitution rate was modelled by a GTR+G. First, we performed a maximum likelihood search with RAxML v.8.2.12 [4] to obtain a topology. This topology was almost identical to that obtained in [8]'s time calibration of butterflies, which is our source of secondary calibrations for this study. To ensure correct estimation of the crown and stem ages of the subclades that were to be grafted, we compared the subclade tree topologies (see below), and checked that the deepest node within each subclade was included.

This backbone topology was then time-calibrated using BEAST 1.8.3. [9]. To time-calibrate the backbone tree we used the same partitioning strategy as for RAxML and GTR+G to model the rates of substitution. For each subset, we set an uncorrelated lognormal relaxed clock (unlinked across partitions, four independent clocks). For calibrating the clocks, we relied on secondary calibrations taken from [8]. The butterfly fossil record is depauperate, which drastically limits their use in time-calibrations [10]. [8] estimated a time-calibrated genus-level tree of butterflies, using the most complete set of fossils up to date, which provides the most robust age estimates for the root of Nymphalidae and internal relationships to date. Using these estimations, we defined a set of 20 calibration points across the tree (Supplementary Table 2. 1). We used normal priors for these calibration points, where the mean and standard deviation were adjusted to recover the age and credibility interval from [8]. We ran eight independent BEAST analyses for 40 million generations each, sampling every 40,000 generations. We checked for convergence of the Markov chains Monte Carlo (MCMC) using Tracer v.1.6. After removing the first 10 million generations as burn-in we combined the different runs using LogCombiner 1.8.3 [9]. Posterior distributions of node ages were synthesized by extracting the median and 95% credibility interval (CI) for each node. This tree was compared to that of [8] to ensure that we recovered expected ages.

Supplementary Table 2. 1. Clades corresponding to the nodes constrained for time-calibrating the backbone tree. Information about the shape of normal prior (mean and standard deviation) is also given.

Clade	mean	stdev
root	83	120
Apaturinae	33.6	4.00
Biblidinae	40.1	4.00
Charaxinae	41	4.0
Cyrestinae	33.4	4.0
Danainae	42	4
Heliconiinae	47.7	4.5
Limenitidinae	48.7	4.5
Nymphalidae	82	7.5
Nymphalinae	47.5	4.5
Satyrinae	54.4	4.5
Ithomiini	25.6	2.8
Argynnini	29.2	3.0
Adoliadini	32.2	3.2
Limenitidini	16.3	2
Nymphalini	35	3.5

Melitaeini	27.4	2.5
Charaxini_Euxanthini	17.5	2.2
Mycalesina	24.2	2.2
Satyrini	37.2	3.5

4 - Subclade trees

We subdivided the whole family Nymphalidae into 15 monophyletic groups of species (sublades), all well defined by previous literature. These subclades corresponded to the Danaini, Ithomiini, Heliconiinae, Cyrestinae, Charaxinae, Libythaeinae, Nymphalinae, Apaturinae, Biblidinae, Calinaginae, Limenitidinae, Pseudergolinae, Satyrinae group I (*Heteropsis*+*Coenonympha*), Satyrinae group II (*Elymnias*+*Morpho*) and Satyrini. For each of them we included all the species available. We also added two outgroups, one from the sister clade of the focal subclade and one sister clade to the two previous ones. For each subclade dataset we started by assessing the best partitioning strategy using PartitionFinder 2 [11], allowing all possible combinations of genes and codon position and all substitution models available in BEAST. Partitioning strategies were identified using the *greedy* algorithm and BIC score. By default, we started by setting one molecular clock (uncorrelated relaxed clock with lognormal distribution) for each partition. If convergence or good mixing could not be obtained after running BEAST, we reduced the number of molecular clocks (see detailed description of subclade analyses). We did not add any time-calibration and therefore only estimated the relative divergence times. We enforced the monophyly of the clade to be grafted (i.e., excluding the outgroups); all other relationships were estimated by BEAST. We performed at least two independent runs with BEAST for each subclade. The length of the MCMC varied according to the size of the subclade (see detailed description of subclade analyses descriptions). We checked for convergence and mixing of the MCMC using Tracer v.1.6.0 (http://beast. bio. ed. ac. uk/tracer). Posterior distributions were finally combined after removing an appropriate burn-in fraction.

Details of the analysis for each subclade are provided hereafter.

a) Apaturinae

Dataset – The dataset for the Apaturinae consisted of 32 taxa to which two outgroups were added: *Marpesia eleuchea* (Cyrestinae), *Biblis hyperia* (Biblidinae).

Partition Finder – Partition Finder identified 10 subsets.

Subset #	Substitution model	Gene fragments and codon positions
Subset 1	GTR+I+G	MDH_pos1, IDH_pos1, CAD_pos1, GAPDH_pos1, ArgKin_pos1, RpS2_pos1, RpS5_pos1, EF1a_pos1
Subset 2	TRN+I	GAPDH_pos2, RpS5_pos2, EF1a_pos2, ArgKin_pos2, MDH_pos2, CAD_pos2, IDH_pos2
Subset 3	GTR+G	wingless_pos3, ArgKin_pos3, GAPDH_pos3, EF1a_pos3
Subset 4	HKY+I	CAD_pos3
Subset 5	HKY+G	COI-begin_pos3, COI-end_pos3
Subset 6	GTR+G	COI-begin_pos1, COI-end_pos1
Subset 7	HKY+I	COI-begin_pos2, COI-end_pos2
Subset 8	GTR+G	DDC_pos3, RpS2_pos3, RpS5_pos3, IDH_pos3, MDH_pos3
Subset 9	K80	DDC_pos1, wingless_pos2, wingless_pos1
Subset 10	JC	RpS2_pos2, DDC_pos2

BEAST analysis – In order to improve the quality of our runs we replaced the default priors for rates of substitutions by uniform prior ranging between 0 and 10 for the following cases: subset1.at, cg, gt, subset6.ac, at, cg, gt. We used a single molecular clock linked across all partition to obtain good mixing and convergence. We used a birth-death tree prior. We performed two runs of 60 million generations, sampling trees and parameters every 6000 generations.

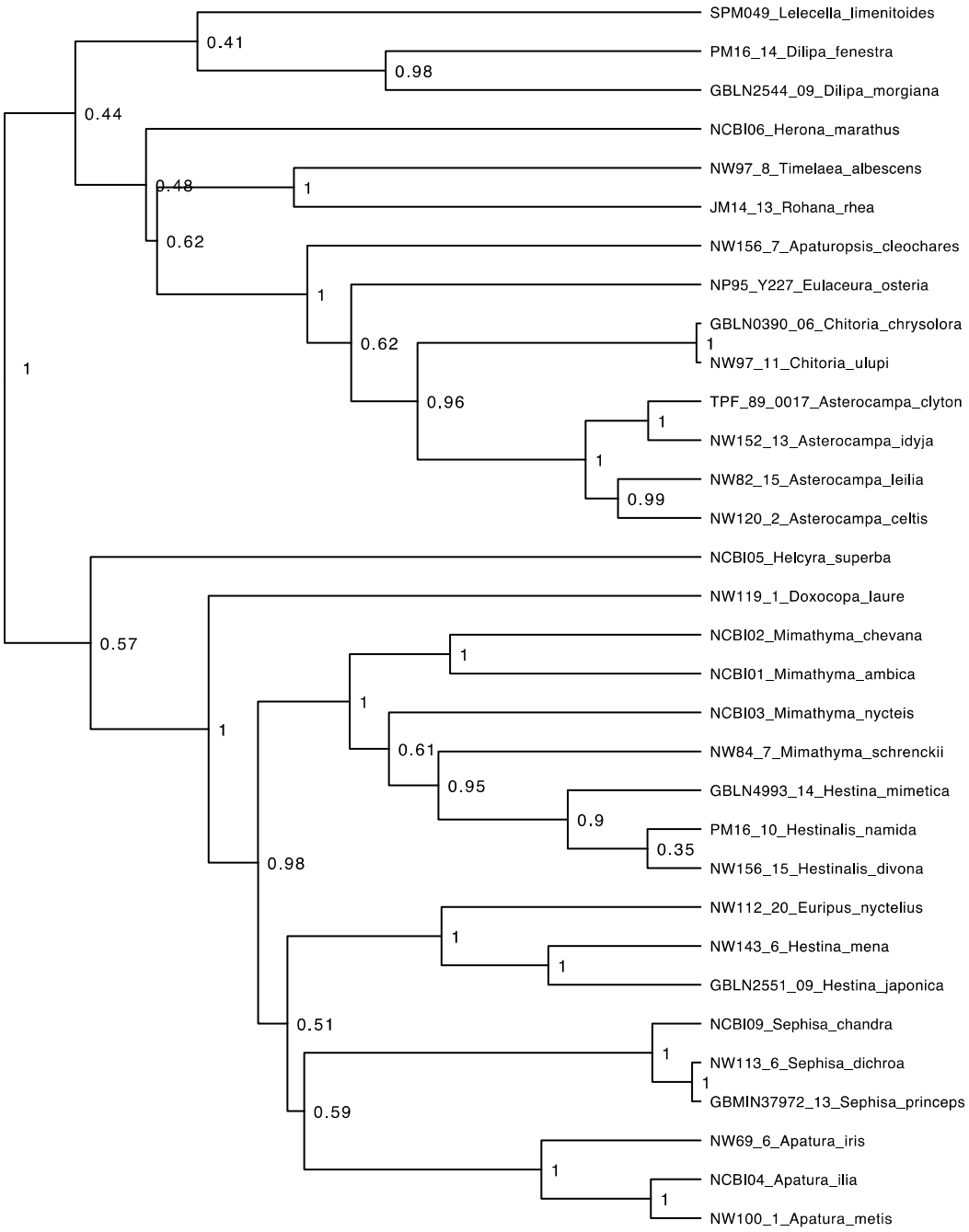

Supplementary Figure 2. 1. Maximum clade credibility tree for the Apaturinae subclade from BEAST. Posterior probabilities are indicated at the nodes.

b) Biblidinae

Dataset – The dataset for the Biblidinae consisted of 155 taxa to which two outgroups were added: *Marpesia eleuchea* (Cyrestinae), *Chitoria ulupi* (Apaturinae).

Partition Finder – Partition Finder identified 12 subsets.

Subset #	Substitution model	Gene fragments and codon positions
Subset 1	GTR+I+G	DDC_pos1, ArgKin_pos1, RpS2_pos1, MDH_pos1, RpS5_pos1, IDH_pos1, wingless_pos1, CAD_pos1
Subset 2	GTR+I+G	COI-begin_pos2, EF1a_pos2, GAPDH_pos2, RpS5_pos2, ArgKin_pos2, DDC_pos2, IDH_pos2, CAD_pos2, MDH_pos2, COI-end_pos2
Subset 3	GTR+G	ArgKin_pos3
Subset 4	HKY+I+G	MDH_pos3, CAD_pos3
Subset 5	GTR+I+G	COI-begin_pos3
Subset 6	GTR+I+G	COI-end_pos1, COI-begin_pos1
Subset 7	HKY+G	COI-end_pos3
Subset 8	GTR+I+G	DDC_pos3, IDH_pos3, GAPDH_pos3
Subset 9	GTR+G	EF1a_pos3
Subset 10	TRN+I+G	GAPDH_pos1, EF1a_pos1
Subset 11	JC+G	RpS2_pos2, wingless_pos2
Subset 12	HKY+G	wingless_pos3, RpS5_pos3, RpS2_pos3

BEAST analysis – In order to improve the quality of our runs we replaced the default priors for rates of substitutions by uniform prior ranging between 0 and 10 for the following cases: subset3.cg, gt, subset5.at, ag, cg. We used one molecular clock per subset identified by Partition Finder and obtained good mixing and convergence. We used a birth-death tree prior. We performed two runs of 150 million generations, sampling trees and parameters every 15000 generations.

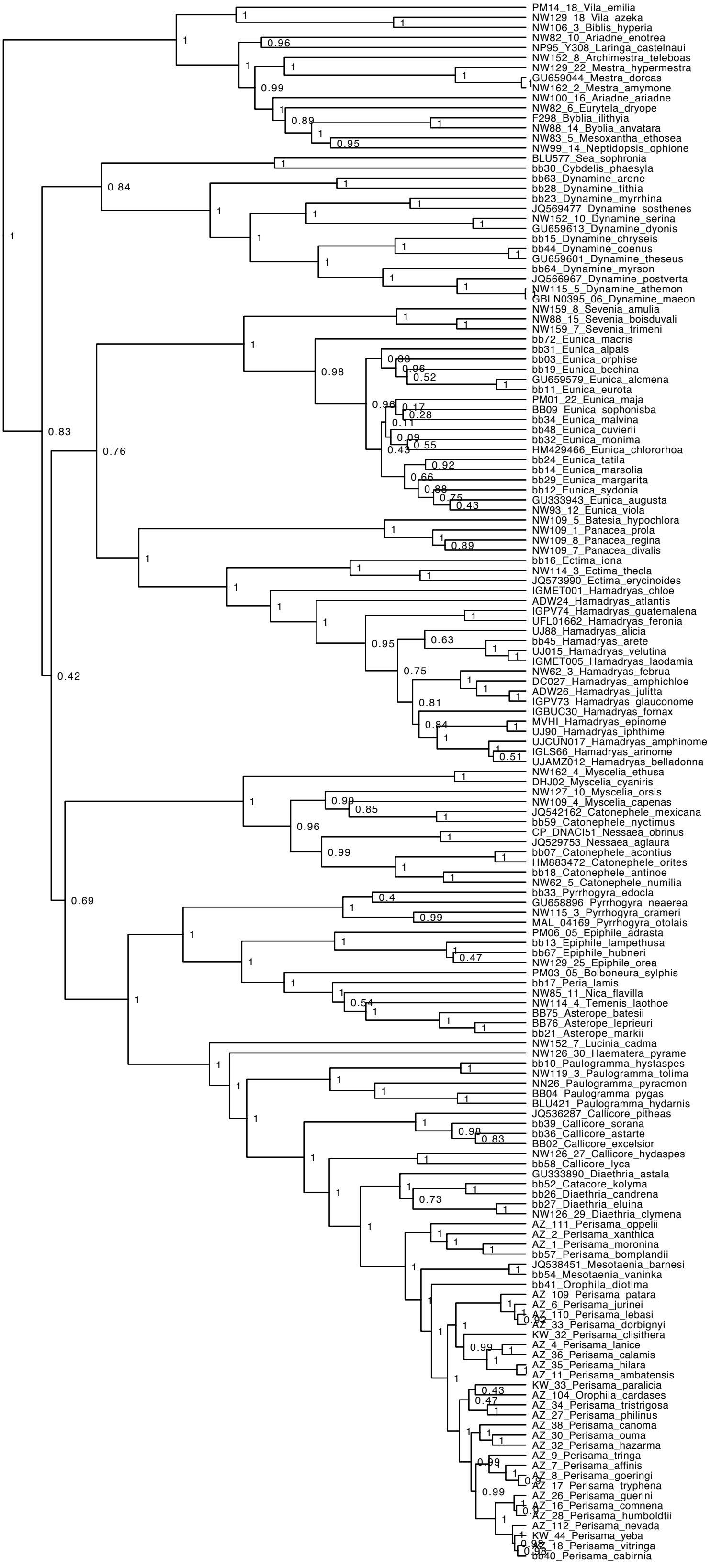
PM14_18_Vila_emilia
NW129_18_Vila_azeka
NW106_3_Biblis_hyperia
NW82_10_Ariadne_enotrea
NP95_Y308_Laringa_castelnaui
NW152_8_Archimestra_teleboas
NW129_22_Mestra_hypermestra
GU659044_Mestra_dorcas
NW162_2_Mestra_amymone
NW100_16_Ariadne_ariadne
NW82_6_Eurytela_dryope
F298_Byblia_ilithyia
NW88_14_Byblia_anvatara
NW83_5_Mesoxantha_ethosea
NW99_14_Neptidopsis_ophione
BLU577_Sea_sophronia
bb30_Cybdelis_phaesyla
bb63_Dynamine_arene
bb28_Dynamine_tithia
bb23_Dynamine_myrrhina
JQ569477_Dynamine_sosthenes
NW152_10_Dynamine_serina
GU659613_Dynamine_dyonis
bb15_Dynamine_chryseis
bb44_Dynamine_coenus
GU659601_Dynamine_theseus
bb64_Dynamine_myrson
JQ566967_Dynamine_postverta
NW115_5_Dynamine_athemon
GBLN0395_06_Dynamine_maeon
NW159_8_Sevenia_amulia
NW88_15_Sevenia_boisduvali
NW159_7_Sevenia_trimeni
bb72_Eunica_macris
bb31_Eunica_alpais
bb03_Eunica_orphise
bb19_Eunica_bechina
GU659579_Eunica_alcmena
bb11_Eunica_eurota
PM01_22_Eunica_maja
BB09_Eunica_sophonisba
bb34_Eunica_malvina
bb48_Eunica_cuvierii
bb32_Eunica_monima
HM429466_Eunica_chlororhoa
bb24_Eunica_tatila
bb14_Eunica_marsolia
bb29_Eunica_margarita
bb12_Eunica_sydonia
GU333943_Eunica_augusta
NW93_12_Eunica_viola
NW109_5_Batesia_hypochlora
NW109_1_Panacea_prola
NW109_8_Panacea_regina
NW109_7_Panacea_divalis
bb16_Ectima_iona
NW114_3_Ectima_thecla
JQ573990_Ectima_erycinoides
IGMET001_Hamadryas_chloe
ADW24_Hamadryas_atlantis
IGPV74_Hamadryas_guatemalena
UFL01662_Hamadryas_feronia
UJ88_Hamadryas_alicia
bb45_Hamadryas_arete
UJ015_Hamadryas_velutina
IGMET005_Hamadryas_laodamia
NW62_3_Hamadryas_februa
DC027_Hamadryas_amphichloe
ADW26_Hamadryas_julitta
IGPV73_Hamadryas_glauconome
IGBUC30_Hamadryas_fornax
MVHI_Hamadryas_epinome
UJ90_Hamadryas_iphthime
UJCUN017_Hamadryas_amphinome
IGLS66_Hamadryas_arinome
UJAMZ012_Hamadryas_belladonna
NW162_4_Myscelia_ethusa
DHJ02_Myscelia_cyaniris
NW127_10_Myscelia_orsis
NW109_4_Myscelia_capenas
JQ542162_Catonephele_mexicana
bb59_Catonephele_nyctimus
CP_DNACI51_Nessaea_obrinus
JQ529753_Nessaea_aglaura
bb07_Catonephele_acontius
HM883472_Catonephele_orites
bb18_Catonephele_antinoe
NW62_5_Catonephele_numilia
bb33_Pyrrhogyra_edocla
GU658896_Pyrrhogyra_neaerea
NW115_3_Pyrrhogyra_crameri
MAL_04169_Pyrrhogyra_otolais
PM06_05_Epiphile_adrasta
bb13_Epiphile_lampethusa
bb67_Epiphile_hubneri
NW129_25_Epiphile_orea
PM03_05_Bolboneura_sylphis
bb17_Peria_lamis
NW85_11_Nica_flavilla
NW114_4_Temenis_laothoe
BB75_Asterope_batesii
BB76_Asterope_leprieuri
bb21_Asterope_markii
NW152_7_Lucinia_cadma
NW126_30_Haematera_pyrame
bb10_Paulogramma_hystaspes
NW119_3_Paulogramma_tolima
NN26_Paulogramma_pyracmon
BB04_Paulogramma_pygas
BLU421_Paulogramma_hydarnis
JQ536287_Callicore_pitheas
bb39_Callicore_sorana
bb36_Callicore_astarte
BB02_Callicore_excelsior
NW126_27_Callicore_hydaspes
bb58_Callicore_lyca
GU333890_Diaethria_astala
bb52_Catacore_kolyma
bb26_Diaethria_candrena
bb27_Diaethria_eluina
NW126_29_Diaethria_clymena
AZ_111_Perisama_oppelii
AZ_2_Perisama_xanthica
AZ_1_Perisama_moronina
bb57_Perisama_bomplandii
JQ538451_Mesotaenia_barnesi
bb54_Mesotaenia_vaninka
bb41_Orophila_diotima
AZ_109_Perisama_patara
AZ_6_Perisama_jurinei
AZ_110_Perisama_lebasi
AZ_33_Perisama_dorbignyi
KW_32_Perisama_clisithera
AZ_4_Perisama_lanice
AZ_36_Perisama_calamis
AZ_35_Perisama_hilara
AZ_11_Perisama_ambatensis
KW_33_Perisama_paralicia
AZ_104_Orophila_cardases
AZ_34_Perisama_tristrigosa
AZ_27_Perisama_philinus
AZ_38_Perisama_canoma
AZ_30_Perisama_ouma
AZ_32_Perisama_hazarma
AZ_9_Perisama_tringa
AZ_7_Perisama_affinis
AZ_8_Perisama_goeringi
AZ_17_Perisama_tryphena
AZ_26_Perisama_guerini
AZ_16_Perisama_comnena
AZ_28_Perisama_humboldtii
AZ_112_Perisama_nevada
KW_44_Perisama_yeba
AZ_18_Perisama_vitringa
bb40_Perisama_cabirnia

Supplementary Figure 2. 2. (page before). Maximum clade credibility tree for the Biblidinae subclade from BEAST. Posterior probabilities are indicated at the nodes.

c) Calinaginae

Dataset – The dataset for the Calinaginae consisted of 6 taxa to which two outgroups were added: *Heliconius melpomene* (Heliconiinae), *Amathusia phidippus* (Satyrinae).

Partition Finder – Partition Finder identified 9 subsets.

Subset #	Substitution model	Gene fragments and codon positions
Subset 1	GTR	ArgKin_pos1, RpS2_pos1, EF1a_pos1, wingless_pos1, DDC_pos1, RpS5_pos1, GAPDH_pos1, CAD_pos1, MDH_pos1, IDH_pos1
Subset 2	HKY	RpS5_pos2, MDH_pos2, GAPDH_pos2, DDC_pos2, ArgKin_pos2, IDH_pos2, EF1a_pos2
Subset 3	GTR	EF1a_pos3, ArgKin_pos3
Subset 4	TRN	MDH_pos3, CAD_pos3
Subset 5	TRN+I	CAD_pos2, COI-end_pos1, COI-begin_pos1
Subset 6	HKY+I	COI-end_pos3, COI-begin_pos3
Subset 7	HKY	COI-end_pos2, COI-begin_pos2
Subset 8	GTR	RpS2_pos3, IDH_pos3, RpS5_pos3, GAPDH_pos3, DDC_pos3, wingless_pos3
Subset 9	JC	wingless_pos2, RpS2_pos2

BEAST analysis – In order to improve the quality of our runs, we replaced the default priors for rates of substitutions by uniform prior ranging between 0 and 10 for the following cases: subset3.cg, subset8.cg, subset1.at, gt. We used a single molecular clock linked across all partition to obtain good mixing and convergence. We used a birth-death tree prior. We performed two runs of 50 million generations, sampling trees and parameters every 5000 generations.

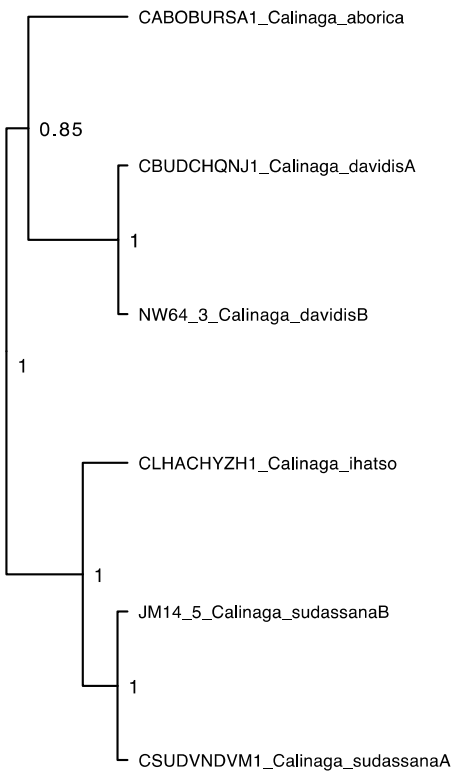

Supplementary Figure 2. 3. Maximum clade credibility tree for the Calinaginae subclade from BEAST. Posterior probabilities are indicated at the nodes.

d) Charaxinae

Dataset – The dataset for the Charaxinae consisted of 234 taxa to which two outgroups were added: *Calinaga davidis* (Calinaginae), *Amathusia phidippus* (Satyrinae).

Partition Finder – Partition Finder identified 11 subsets.

Subset #	Substitution model	Gene fragments and codon positions
Subset 1	TRN+I+G	ArgKin_pos1, GAPDH_pos1, MDH_pos1, EF1a_pos1, RpS2_pos1, RpS5_pos1
Subset 2	HKY+I+G	MDH_pos2, RpS5_pos2, EF1a_pos2, GAPDH_pos2, ArgKin_pos2, DDC_pos2, IDH_pos2
Subset 3	TRN	RpS2_pos2, wingless_pos2, ArgKin_pos3
Subset 4	HKY+I+G	MDH_pos3, CAD_pos3
Subset 5	GTR+G	DDC_pos1, wingless_pos1, CAD_pos1, IDH_pos1
Subset 6	TRN+I	CAD_pos2, COI-begin_pos2, COI-end_pos2
Subset 7	GTR+G	COI-end_pos3, COI-begin_pos3
Subset 8	TRN+I+G	COI-end_pos1, COI-begin_pos1
Subset 9	GTR+I+G	DDC_pos3, IDH_pos3, RpS2_pos3, GAPDH_pos3
Subset 10	GTR+I+G	EF1a_pos3, RpS5_pos3
Subset 11	K80+I+G	wingless_pos3

BEAST analysis – In order to improve the quality of our runs we replaced the substitution model of subset3 by K80. We used one molecular clock per subset identified by Partition Finder and obtained good mixing and convergence. We used a birth-death tree prior. We performed two runs of 100 million generations, sampling trees and parameters every 10000 generations.


LEP_03436_Archaeoprepona_phaedra
LEP_03505_Archaeoprepona_demophoon
NW81_9_Archaeoprepona_demophon
LEP_00521_Archaeoprepona_camilla
LEP_00542_Archaeoprepona_meander
PM14_26_Archaeoprepona_amphimachus
LEP_04034_Archaeoprepona_chalciope
LEP_03369_Archaeoprepona_licomedes
LEP_00554_Archaeoprepona_chromus
LEP_03519_Prepona_laertes
LEP_00539_Prepona_dexamenus
LEP_03428_Prepona_deiphile
LEP_03524_Prepona_pylene
LEP_04035_Prepona_werneri
LEP_03438_Prepona_praeneste
LEP_04033_Prepona_aedon
LEP_04218_Prepona_narcissus
PM21_35_Prepona_claudina
LEP_00515_Prepona_amydon
CP_M264_Prepona_hewitsonius
CP05_41_Anaeomorpha_splendida
PM14_27_Mesoprepona_pheridamas
NW127_11_Hypna_clytemnestra
CP_M269_Coenophlebia_archidona
PM19_26_Zaretis_itys
NW124_6_Siderone_galanthis
NW109_16_Consul_fabius
MHAAB893_06_Anaea_aidea
NW92_2_Anaea_troglodyta
PM19_46_Fountainea_halice
PM19_43_Fountainea_glycerium
PM19_05_Fountainea_eurypyle
NW106_1_Fountainea_ryphea
CP06_88_Polygrapha_tyrianthina
PM21_31_Fountainea_nessus
PM19_20_Fountainea_nobilis
PM21_48_Fountainea_sosippus
PM19_32_Memphis_glauce
PM21_21_Memphis_praxias
PM19_19_Memphis_acaudata
PM21_08_Memphis_artacaena
PM19_02_Memphis_pithyusa
PM21_57_Memphis_arginussa
PM19_36_Memphis_lemnos
NW127_6_Memphis_appias
PM21_25_Memphis_xenocles
PM21_12_Memphis_verticordia
LEP_05073_Memphis_aureola
PM19_21_Memphis_dia
PM21_22_Memphis_polyxo
PM19_30_Memphis_forreri
PM19_29_Memphis_hirta
PM21_07_Memphis_otrere
PM19_18_Memphis_anna
PM19_33_Memphis_philumena
PM19_23_Memphis_catinka
PM21_40_Memphis_polycarmes
PM19_37_Memphis_moruus
PM19_35_Memphis_offa
PM21_65_Memphis_grandis
PM21_44_Memphis_cerealia
PM19_24_Memphis_moeris
PM19_09_Memphis_acidalia
PM21_23_Memphis_phantes
PM21_20_Memphis_basilia
PM19_22_Memphis_anassa
PM21_30_Memphis_leonida
PM19_57_Memphis_editha
PM21_10_Memphis_lorna
PM21_19_Memphis_lineata
PM21_09_Memphis_ambrosia
PM21_11_Memphis_cluvia
NW111_8_Agatasa_calydonia
PM15_13_Prothoe_australis
NW103_5_Prothoe_franck
NW123_24_Palla_publius
NW123_22_Palla_ussheri
NW124_7_Palla_decius
KAP132_Palla_violinitens
EV_0010_Charaxes_zoolina
EV_0009_Charaxes_kahldeni
KAP100_Charaxes_pleione
KAP108_Charaxes_paphianus
NW114_19_Polyura_schreiber
ET0130_Polyura_luzonica
ET0026_Polyura_jalysus
ET0108_Polyura_moori
PS988_Polyura_agraria
NW121_24_Polyura_alphius
ET0027_Polyura_paulettae
ET0099_Polyura_athamas
AC901_Polyura_bharata
ET0107_Polyura_hebe
PV933_Polyura_arja
ET0014_Polyura_delphis
ET0029_Polyura_narcaea
ET0067_Polyura_dolon
ET0208_Polyura_posidonius
ET0075_Polyura_eudamippus
ET0040_Polyura_weismanni
ET0103_Polyura_nepenthes
ET0044_Polyura_cognata
ET0183_Polyura_dehanii
ET0211_Polyura_epigenes
ET0201_Polyura_gamma
ET0157_Polyura_attila
ET0213_Polyura_sacco
ET0165_Polyura_caphontis
ET0203_Polyura_clitarchus
ET0058_Polyura_gilolensis
ET0231_Polyura_jupiter
ET0042_Polyura_sempronius
ET0184_Polyura_pyrrhus
ET0186_Polyura_smilesi
EV_0044_Charaxes_montis
EZCHA039_07_Charaxes_schiltzei
EV_0043_Charaxes_subornatus
NW164_3_Charaxes_eupale
UN0509_Charaxes_dilutus
NW134_13_Charaxes_solon
KAP505_Charaxes_achaemenes
KAP149_Charaxes_etesipe
EV_0041_Charaxes_penricei
ABRI_025_Charaxes_jahlusa
KAP113_Charaxes_hildebrandti
ABRI_008_Charaxes_baumanni
KAP292_Charaxes_anticlea
ABRI_015_Charaxes_opinatus
ABRI_013_Charaxes_blanda
EV_0057_Charaxes_guderiana
ABRI_009_Charaxes_analava
EV_0027_Charaxes_phraortes
EV_0051_Charaxes_aubyni
KAP296_Charaxes_etheocles
EV_0049_Charaxes_petersi
EV_0067_Charaxes_pembanus
GBLN2362_09_Charaxes_mccleeryi
EV_0048_Charaxes_maccleeryi
EV_0042_Charaxes_cacuthis
EV_0053_Charaxes_congdoni
EV_0047_Charaxes_marieps
ABRI_001_Charaxes_ethalion
EV_0056_Charaxes_kirki
EV_0068_Charaxes_northcotti
ET0210_Charaxes_viola
ABRI_012_Charaxes_mafuga
ABRI_016_Charaxes_turlini
EV_0052_Charaxes_berkeleyi
EV_0050_Charaxes_sidamo
EV_0058_Charaxes_galawadiwosi
EV_0059_Charaxes_howarthi
KAP071_Charaxes_virilis
KAP507_Charaxes_plantroui
ABRI_004_Charaxes_nichetes
NW118_11_Charaxes_porthos
EV_0062_Charaxes_mycerina
KAP228_Charaxes_zelica
KAP506_Charaxes_lycurgus
FM_15_Euxanthe_trajanus
EV_0064_Euxanthe_tiberius
EV_0066_Euxanthe_madagascariensis
NW131_10_Euxanthe_eurinome
EV_0065_Euxanthe_wakefieldi
NW103_15_Euxanthe_crossleyi
KAP165_Charaxes_zingha
EV_0039_Charaxes_hadrianus
KAP163_Charaxes_protoclea
KAP050_Charaxes_boueti
NW107_11_Charaxes_cynthia
EV_0020_Charaxes_lasti
KAP299_Charaxes_fulvescens
KAP503_Charaxes_varanes
ABRI_010_Charaxes_acuminatus
NW78_3_Charaxes_castor
EV_0022_Charaxes_jasius
EV_0023_Charaxes_legeri
KAP069_Charaxes_lucretius
KAP081_Charaxes_brutus
EV_0029_Charaxes_ansorgei
ABRI_019_Charaxes_eudoxus
EV_0035_Charaxes_richelmanni
KAP501_Charaxes_pollux
EV_0025_Charaxes_lactetinctus
EV_0034_Charaxes_ducarmei
ABRI_032_Charaxes_druceanus
EV_0006_Charaxes_fournierae
EV_0007_Charaxes_acraeoides
EV_0002_Charaxes_nobilis
EV_0001_Charaxes_superbus
EV_0038_Charaxes_imperialis
EV_0037_Charaxes_pythodoris
KAP509_Charaxes_numenes
KAP280_Charaxes_ameliae
ABRI_005_Charaxes_phenix
KAP290_Charaxes_bipunctatus
ABRI_031_Charaxes_bohemani
EV_0036_Charaxes_mixtus
KAP502_Charaxes_smaragdalis
KAP098_Charaxes_tiridates
EV_0032_Charaxes_cithaeron
EV_0033_Charaxes_xiphares
EV_0031_Charaxes_nandina
ABRI_020_Charaxes_cowani
EV_0018_Charaxes_antamboulou
KAP273_Charaxes_candiope
CJM_148_001_Charaxes_marki
CJM_171_001_Charaxes_ocellatus
CJM_173_001_Charaxes_orilus
CJM_194_001_Charaxes_harmodius
CJM_186_001_Charaxes_distanti
CJM_199_004_Charaxes_mars
CJM_191_007_Charaxes_nitebis
CJM_175_002_Charaxes_amycus
CJM_202_001_Charaxes_sangana
CJM_179_002_Charaxes_antonius
CJM_189_001_Charaxes_elwesi
CJM_196_001_Charaxes_eurialus
CJM_177_002_Charaxes_madensis
CJM_181_007_Charaxes_latona
CJM_166_001_Charaxes_setan
CJM_192_001_Charaxes_musashi
CJM_170_005_Charaxes_affinis
CJM_185_001_Charaxes_kahruba
CJM_183_007_Charaxes_repetitus
CJM_209_002_Charaxes_plateni
CJM_188_001_Charaxes_bupalus
CJM_205_003_Charaxes_aristogiton
CJM_195_003_Charaxes_borneensis
NW134_10_Charaxes_bernardus
UN0479_Charaxes_marmax
CJM_206_002_Charaxes_fervens
CJM_210_003_Charaxes_bajula
CJM_212_001_Charaxes_durnfordi
CJM_204_002_Charaxes_psaphon

Supplementary Figure 2. 4. (page before). Maximum clade credibility tree for the Charaxinae subclade from BEAST. Posterior probabilities are indicated at the nodes.

e) Cyrestinae

Dataset – The dataset for the Cyrestinae consisted of 28 taxa to which two outgroups were added: *Antanartia delius* (Antanartia), *Chitoria ulupi* (Apaturinae).

Partition Finder – Partition Finder identified 11 subsets.

Subset #	Substitution model	Gene fragments and codon positions
Subset 1	GTR+G	wingless_pos1, RpS5_pos1, ArgKin_pos1, RpS2_pos1, MDH_pos1, CAD_pos1
Subset 2	HKY+I	DDC_pos2, ArgKin_pos2, CAD_pos2, IDH_pos2
Subset 3	GTR+G	EF1a_pos3, ArgKin_pos3
Subset 4	HKY+I+G	MDH_pos3, CAD_pos3
Subset 5	GTR+I+G	COI-end_pos3, COI-begin_pos3
Subset 6	TRN+I+G	COI-end_pos1, COI-begin_pos1
Subset 7	HKY+I	COI-begin_pos2, COI-end_pos2, RpS5_pos2, GAPDH_pos2, MDH_pos2, EF1a_pos2
Subset 8	TRN+G	wingless_pos3, DDC_pos3
Subset 9	TRN+I+G	wingless_pos2, DDC_pos1, IDH_pos1, GAPDH_pos1, EF1a_pos1
Subset 10	GTR+G	RpS5_pos3, RpS2_pos3, IDH_pos3, GAPDH_pos3
Subset 11	JC	RpS2_pos2

BEAST analysis – In order to improve the quality of our runs we replaced the default priors for rates of substitutions by uniform prior ranging between 0 and 10 for the following cases: subset5. at, cg, gt. We used one molecular clock per subset identified by Partition Finder and obtained good mixing and convergence. We used a birth-death tree prior. We performed two runs of 60 million generations, sampling trees and parameters every 6000 generations.

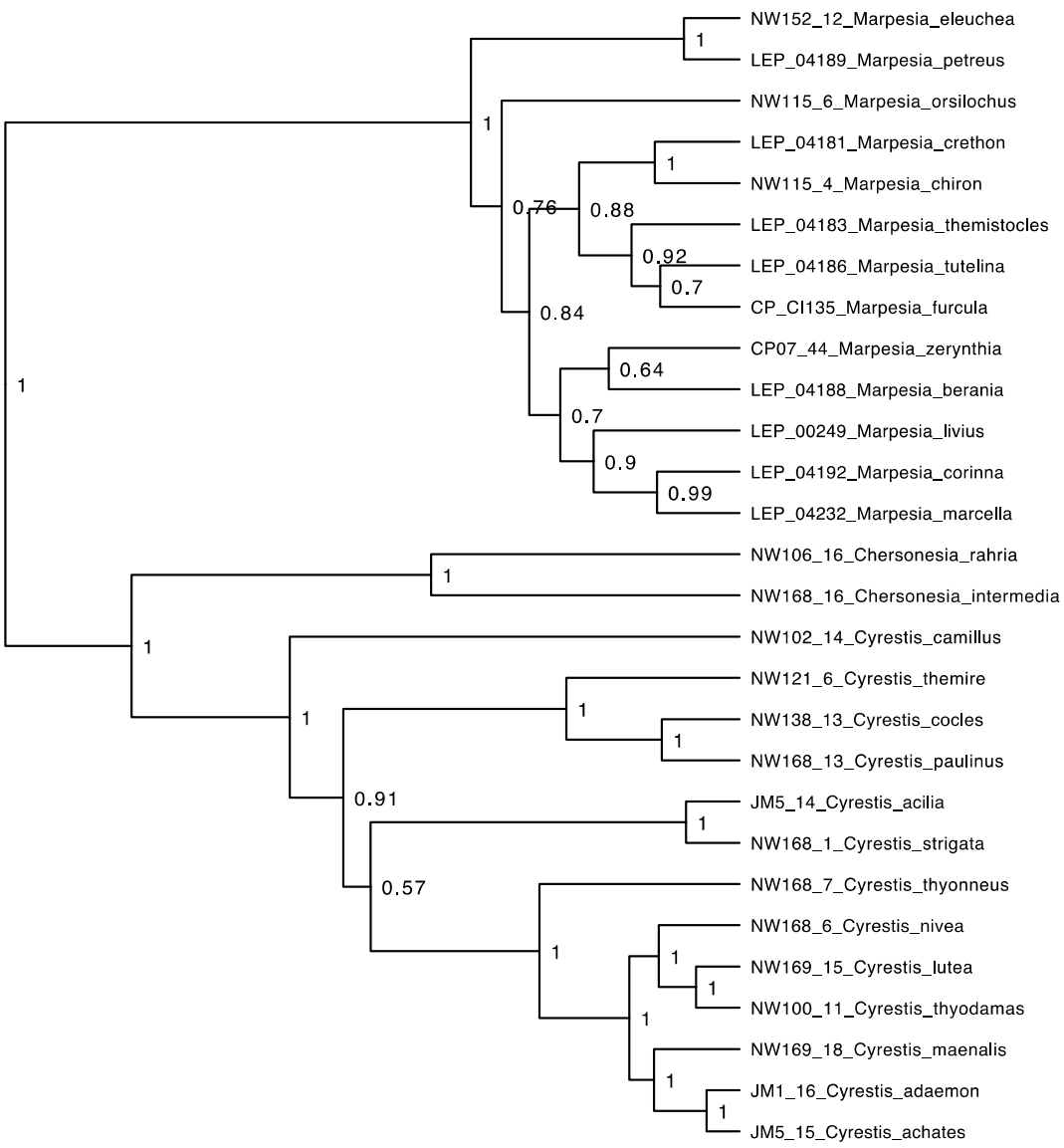

Supplementary Figure 2. 5. Maximum clade credibility tree for the Cyrestinae subclade from BEAST. Posterior probabilities are indicated at the nodes.

f) Danaini

Dataset – The dataset for the Danaini consisted of 46 taxa to which two outgroups were added: *Tellervo zoilus* (Tellervini), *Libythea celtis* (Libytheinae).

Partition Finder – Partition Finder identified 11 subsets.

Subset #	Substitution model	Gene fragments and codon positions
Subset 1	GTR+G	wingless_pos1, RpS5_pos1, ArgKin_pos1, RpS2_pos1, MDH_pos1, CAD_pos1
Subset 2	HKY+I	DDC_pos2, ArgKin_pos2, IDH_pos2, CAD_pos2
Subset 3	GTR+G	EF1a_pos3, ArgKin_pos3
Subset 4	HKY+I+G	MDH_pos3, CAD_pos3

Subset 5	GTR+I+G	COI-end_pos3, COI-begin_pos3
Subset 6	TRN+I+G	COI-end_pos1, COI-begin_pos1
Subset 7	HKY+I	COI-begin_pos2, COI-end_pos2, RpS5_pos2, GAPDH_pos2, MDH_pos2, EF1a_pos2
Subset 8	TRNEF+G	DDC_pos3, wingless_pos3
Subset 9	TRN+I+G	wingless_pos2, DDC_pos1, IDH_pos1, GAPDH_pos1, EF1a_pos1
Subset 10	GTR+G	RpS5_pos3, RpS2_pos3, IDH_pos3, GAPDH_pos3
Subset 11	JC	RpS2_pos2

BEAST analysis – In order to improve the quality of our runs we replaced the default priors for rates of substitutions by uniform prior ranging between 0 and 10 for the following cases: subset5.at, cg, gt, subset10.cg, subset1.cg. We used a single molecular clock linked across all partition to obtain good mixing and convergence. We used a birth-death tree prior. We performed two runs of 60 million generations, sampling trees and parameters every 7000 generations.

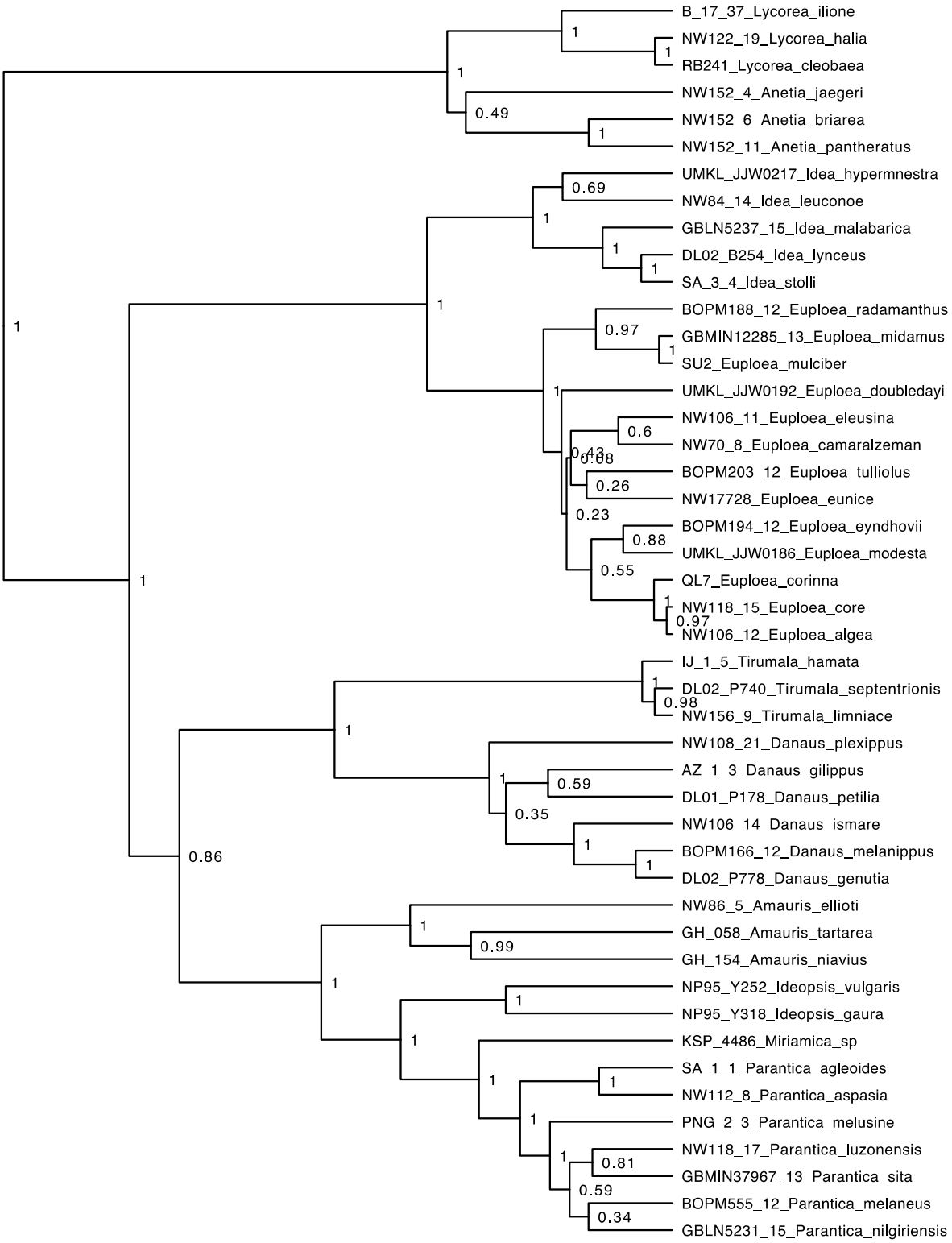

Supplementary Figure 2. 6. Maximum clade credibility tree for the Danaini subclade from BEAST. Posterior probabilities are indicated at the nodes.

g) Heliconiinae

Dataset – The dataset for the Heliconiinae consisted of 248 taxa to which two outgroups were added: *Pseudergolis wedah* (Pseudergolinae), *Cymothoe caenis* (Limenitidinae).

Partition Finder – Partition Finder identified 13 subsets.

Subset #	Substitution model	Gene fragments and codon positions
Subset 1	TRN+I+G	GAPDH_pos1, EF1a_pos1, ArgKin_pos1, RpS2_pos1, RpS5_pos1
Subset 2	TRN+I+G	RpS2_pos2, RpS5_pos2, EF1a_pos2, GAPDH_pos2, ArgKin_pos2
Subset 3	GTR+G	ArgKin_pos3
Subset 4	HKY+I+G	MDH_pos3, CAD_pos3
Subset 5	GTR+I+G	CAD_pos1, MDH_pos1, IDH_pos1
Subset 6	GTR+I+G	DDC_pos2, IDH_pos2, CAD_pos2, MDH_pos2, COI-begin_pos2, COI-end_pos2
Subset 7	GTR+G	COI-begin_pos3
Subset 8	TRN+I+G	COI-end_pos1, COI-begin_pos1
Subset 9	GTR+G	COI-end_pos3
Subset 10	GTR+I+G	IDH_pos3, DDC_pos3
Subset 11	SYM+G	wingless_pos2, DDC_pos1, wingless_pos1
Subset 12	GTR+I+G	RpS2_pos3, wingless_pos3, EF1a_pos3, RpS5_pos3
Subset 13	TRN+I+G	GAPDH_pos3

BEAST analysis – In order to improve the quality of our runs we replaced the default priors for rates of substitutions by uniform prior ranging between 0 and 10 for the following cases: subset9.cg. We used one molecular clock per subset identified by Partition Finder and obtained good mixing and convergence. We used a birth-death tree prior. We performed three runs of 100 million generations, sampling trees and parameters every 10000 generations.

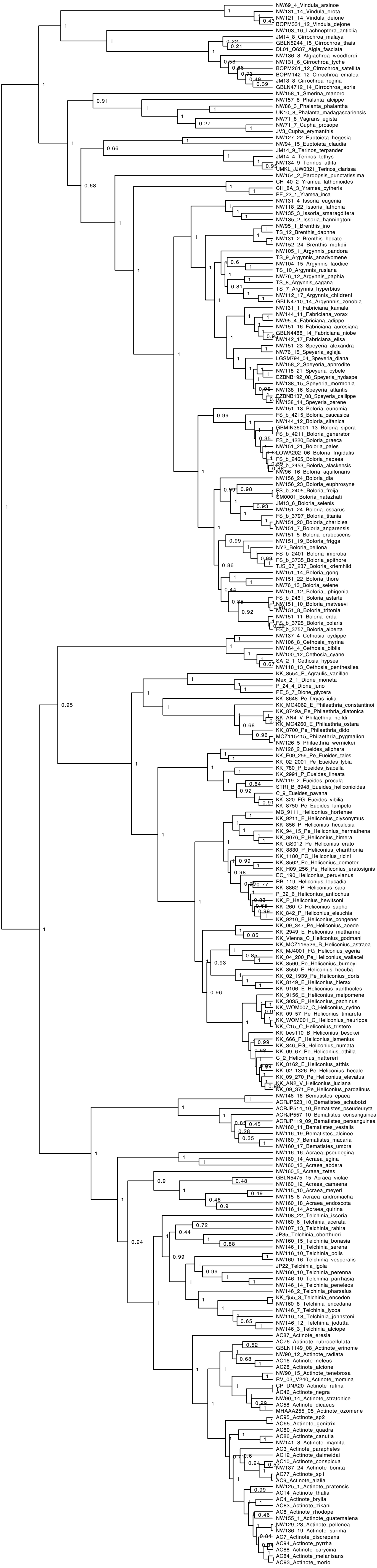
NW69_4_Vindula_arsinoe
NW131_14_Vindula_erota
NW121_14_Vindula_deione
BOPM331_12_Vindula_dejone
NW103_16_Lachnoptera_anticlia
JM14_8_Cirrochroa_malaya
GBLN5244_15_Cirrochroa_thais
DL01_Q637_Algia_fasciata
NW136_8_Algiachroa_woodfordi
NW131_6_Cirrochroa_tyche
BOPM261_12_Cirrochroa_satellita
BOPM142_12_Cirrochroa_emalea
JM13_8_Cirrochroa_regina
GBLN4712_14_Cirrochroa_aoris
NW158_1_Smerina_manoro
NW157_8_Phalanta_alcippe
NW86_3_Phalanta_phalantha
UK10_8_Phalanta_madagascariensis
NW71_8_Vagrans_egista
NW71_7_Cupha_prosope
JV3_Cupha_erymanthis
NW127_22_Euptoieta_hegesia
NW94_15_Euptoieta_claudia
JM14_9_Terinos_terpander
JM14_4_Terinos_tethys
NW134_9_Terinos_atlita
UMKL_JJW0321_Terinos_clarissa
NW154_2_Pardopsis_punctatissima
CH_40_2_Yramea_lathonioides
CH_8A_3_Yramea_cytheris
PE_22_1_Yramea_inca
NW131_4_Issoria_eugenia
NW118_22_Issoria_lathonia
NW135_3_Issoria_smaragdifera
NW135_2_Issoria_hanningtoni
NW95_1_Brenthis_ino
TS_12_Brenthis_daphne
NW131_2_Brenthis_hecate
NW152_24_Brenthis_mofidii
NW105_1_Argynnis_pandora
TS_9_Argynnis_anadyomene
NW104_15_Argynnis_laodice
TS_10_Argynnis_ruslana
NW76_12_Argynnis_paphia
TS_8_Argynnis_sagana
TS_7_Argynnis_hyperbius
NW112_17_Argynnis_childreni
GBLN4710_14_Argynnnis_zenobia
NW131_1_Fabriciana_kamala
NW144_11_Fabriciana_vorax
NW95_4_Fabriciana_adippe
NW151_16_Fabriciana_auresiana
GBLN4488_14_Fabriciana_niobe
NW142_17_Fabriciana_elisa
NW151_23_Speyeria_alexandra
NW76_15_Speyeria_aglaja
LGSM794_04_Speyeria_diana
NW158_2_Speyeria_aphrodite
NW118_21_Speyeria_cybele
EZBNB192_08_Speyeria_hydaspe
NW138_15_Speyeria_mormonia
NW138_16_Speyeria_atlantis
EZBNB137_08_Speyeria_callippe
NW138_14_Speyeria_zerene
NW151_13_Boloria_eunomia
FS_b_4215_Boloria_caucasica
NW144_12_Boloria_sifanica
GBMIN36001_13_Boloria_sipora
FS_b_4211_Boloria_generator
FS_b_4220_Boloria_graeca
NW151_21_Boloria_pales
LOWA202_06_Boloria_frigidalis
FS_b_2465_Boloria_napaea
FS_b_2453_Boloria_alaskensis
NW96_16_Boloria_aquilonaris
NW156_24_Boloria_dia
NW156_23_Boloria_euphrosyne
FS_b_2405_Boloria_freija
SM0001_Boloria_natazhati
JM13_6_Boloria_selenis
NW151_24_Boloria_oscarus
FS_b_3797_Boloria_titania
NW151_20_Boloria_chariclea
NW151_7_Boloria_angarensis
NW151_5_Boloria_erubescens
NW151_19_Boloria_frigga
NY2_Boloria_bellona
FS_b_2401_Boloria_improba
FS_b_3735_Boloria_epithore
TJS_07_237_Boloria_kriemhild
NW151_14_Boloria_gong
NW151_22_Boloria_thore
NW76_13_Boloria_selene
NW151_12_Boloria_iphigenia
FS_b_2461_Boloria_astarte
NW151_10_Boloria_matveevi
NW151_8_Boloria_tritonia
NW151_11_Boloria_erda
FS_b_3725_Boloria_polaris
FS_b_3757_Boloria_alberta
NW137_4_Cethosia_cydippe
NW106_8_Cethosia_myrina
NW164_4_Cethosia_biblis
NW100_12_Cethosia_cyane
SA_2_1_Cethosia_hypsea
NW118_13_Cethosia_penthesilea
KK_8554_P_Agraulis_vanillae
Mex_2_1_Dione_moneta
P_24_4_Dione_juno
PE_5_7_Dione_glycera
KK_8648_Pe_Dryas_iulia
KK_MG4062_E_Philaethria_constantinoi
KK_8749a_Pe_Philaethria_diatonica
KK_AN4_V_Philaethria_neildi
KK_MG4260_E_Philaethria_ostara
KK_8700_Pe_Philaethria_dido
MCZ115415_Philaethria_pygmalion
NW126_5_Philaethria_wernickei
NW126_2_Eueides_aliphera
KK_E09_256_Pe_Eueides_tales
KK_02_2001_Pe_Eueides_lybia
KK_780_P_Eueides_isabella
KK_2991_P_Eueides_lineata
NW119_2_Eueides_procula
STRI_B_8948_Eueides_heliconioides
C_9_Eueides_pavana
KK_320_FG_Eueides_vibilia
KK_8750_Pe_Eueides_lampeto
MB_9111_Heliconius_hortense
KK_9211_E_Heliconius_clysonymus
KK_856_P_Heliconius_hecalesia
KK_94_15_Pe_Heliconius_hermathena
KK_8076_P_Heliconius_himera
KK_GS012_Pe_Heliconius_erato
KK_8830_P_Heliconius_charithonia
KK_1180_FG_Heliconius_ricini
KK_8562_Pe_Heliconius_demeter
KK_H09_256_Pe_Heliconius_eratosignis
EC_190_Heliconius_peruvianus
RB_119_Heliconius_leucadia
KK_8862_P_Heliconius_sara
P_32_6_Heliconius_antiochus
KK_P_Heliconius_hewitsoni
KK_260_C_Heliconius_sapho
KK_842_P_Heliconius_eleuchia
KK_9210_E_Heliconius_congener
KK_09_347_Pe_Heliconius_aoede
KK_2949_E_Heliconius_metharme
KK_Vienna_C_Heliconius_godmani
KK_MCZ116526_B_Heliconius_astraea
KK_MJ4001_FG_Heliconius_egeria
KK_04_200_Pe_Heliconius_wallacei
KK_8560_Pe_Heliconius_burneyi
KK_8550_E_Heliconius_hecuba
KK_02_1939_Pe_Heliconius_doris
KK_8149_E_Heliconius_hierax
KK_9106_E_Heliconius_xanthocles
KK_9156_E_Heliconius_melpomene
KK_3035_P_Heliconius_pachinus
KK_WOM007_C_Heliconius_cydno
KK_09_57_Pe_Heliconius_timareta
KK_WOM001_C_Heliconius_heurippa
KK_C15_C_Heliconius_tristero
KK_bes110_B_Heliconius_besckei
KK_666_P_Heliconius_ismenius
KK_346_FG_Heliconius_numata
KK_09_67_Pe_Heliconius_ethilla
C_2_Heliconius_nattereri
KK_8162_E_Heliconius_atthis
KK_02_1326_Pe_Heliconius_hecale
KK_09_270_Pe_Heliconius_elevatus
KK_AN2_V_Heliconius_luciana
KK_09_371_Pe_Heliconius_pardalinus
NW146_16_Bematistes_epaea
ACRJP523_10_Bematistes_schubotzi
ACRJP514_10_Bematistes_pseudeuryta
ACRJP557_10_Bematistes_consanguinea
ACRJP119_09_Bematistes_persanguinea
NW160_11_Bematistes_vestalis
NW116_19_Bematistes_alcinoe
NW160_7_Bematistes_macaria
NW160_17_Bematistes_umbra
NW116_16_Acraea_pseudegina
NW160_14_Acraea_egina
NW160_13_Acraea_abdera
NW160_5_Acraea_zetes
GBLN5475_15_Acraea_violae
NW160_12_Acraea_camaena
NW115_10_Acraea_meyeri
NW115_8_Acraea_andromacha
NW160_18_Acraea_endoscota
NW116_14_Acraea_quirina
NW108_22_Telchinia_issoria
NW160_6_Telchinia_acerata
NW107_13_Telchinia_rahira
JP35_Telchinia_oberthueri
NW160_15_Telchinia_bonasia
NW146_11_Telchinia_serena
NW116_10_Telchinia_polis
NW160_16_Telchinia_vesperalis
JP22_Telchinia_igola
NW160_10_Telchinia_perenna
NW146_10_Telchinia_parrhasia
NW146_14_Telchinia_peneleos
NW146_2_Telchinia_pharsalus
KK_fj55_3_Telchinia_encedon
NW160_8_Telchinia_encedana
NW146_7_Telchinia_lycoa
NW116_18_Telchinia_johnstoni
NW146_12_Telchinia_jodutta
NW146_3_Telchinia_alciope
AC87_Actinote_eresia
AC76_Actinote_rubrocellulata
GBLN1149_08_Actinote_erinome
NW90_12_Actinote_radiata
AC16_Actinote_neleus
AC28_Actinote_alcione
NW90_15_Actinote_tenebrosa
RV_03_V240_Actinote_momina
CP_DNA20_Actinote_rufina
AC46_Actinote_negra
NW90_14_Actinote_stratonice
AC58_Actinote_dicaeus
MHAAA255_05_Actinote_ozomene
AC95_Actinote_sp2
AC65_Actinote_genitrix
AC80_Actinote_quadra
AC86_Actinote_canutia
NW141_8_Actinote_mamita
AC3_Actinote_parapheles
AC12_Actinote_dalmeidai
AC10_Actinote_conspicua
NW137_24_Actinote_bonita
AC77_Actinote_sp1
AC9_Actinote_alalia
NW125_1_Actinote_pratensis
AC14_Actinote_thalia
AC4_Actinote_brylla
AC83_Actinote_zikani
AC8_Actinote_rhodope
NW155_1_Actinote_guatemalena
NW129_23_Actinote_pellenea
NW136_19_Actinote_surima
AC7_Actinote_discrepans
AC94_Actinote_pyrrha
AC88_Actinote_carycina
AC84_Actinote_melanisans
AC93_Actinote_morio

Supplementary Figure 2. 7. (page before). Maximum clade credibility tree for the Heliconiinae subclade from BEAST. Posterior probabilities are indicated at the nodes.

h) Ithomiini

Dataset – The dataset for the Ithomiini consisted of 337 taxa to which two outgroups were added: *Danaus plexippus* (Danaini), *Tellervo zoilus* (Tellervini).

Partition Finder – Partition Finder identified 12 subsets.

Subset #	Substitution model	Gene fragments and codon positions
Subset 1	TRN+I+G	ArgKin_pos1, RpS2_pos1, EF1a_pos1
Subset 2	GTR+I+G	RpS5_pos2, GAPDH_pos2, DDC_pos2, CAD_pos2, IDH_pos2, ArgKin_pos2, EF1a_pos2
Subset 3	GTR	ArgKin_pos3
Subset 4	HKY+I+G	MDH_pos3, CAD_pos3
Subset 5	GTR+I+G	RpS5_pos1, GAPDH_pos1, wingless_pos1, MDH_pos1, CAD_pos1, IDH_pos1, DDC_pos1, wingless_pos2
Subset 6	GTR+I+G	COI-end_pos3, COI-begin_pos3
Subset 7	TRN+I+G	COI-end_pos1, COI-begin_pos1
Subset 8	TRN+I+G	MDH_pos2, COI-begin_pos2, COI-end_pos2
Subset 9	K80	DDC_pos3
Subset 10	GTR+I+G	EF1a_pos3, wingless_pos3, RpS5_pos3
Subset 11	GTR+G	IDH_pos3, GAPDH_pos3, RpS2_pos3
Subset 12	JC+I	RpS2_pos2

BEAST analysis – In order to improve the quality of our runs we replaced the default priors for rates of substitutions by uniform prior ranging between 0 and 10 for the following cases: subset3.at, cg, gt, subset3.ag, cg. We used one molecular clock per subset identified by Partition Finder and obtained good mixing and convergence. We used a birth-death tree prior. We performed two runs of 100 million generations, sampling trees and parameters every 10000 generations.

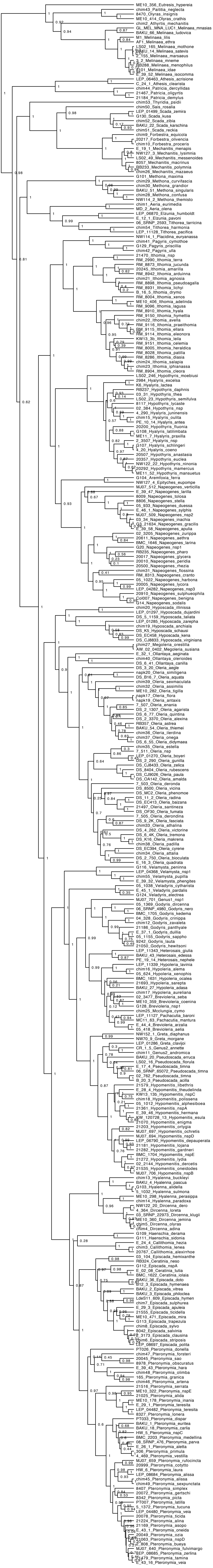
ME10_356_Eutresis_hypereia
chim43_Paititia_neglecta
8470_Olyras_insignis
ME10_414_Olyras_crathis
chim2_Athyrtis_mechanitis
GL_MEL_MNA_LUC1_Melinaea_mnasias
BAKU_66_Melinaea_ludovica
M1_Melinaea_lilis
AF1_Melinaea_ethra
LS02_165_Melinaea_mothone
BAKU_14_Melinaea_satevis
2_155_Melinaea_marsaeus
3_2_Melinaea_mneme
RB288_Melinaea_menophilus
8101_Melinaea_idae
E_39_52_Melinaea_isocomma
LEP_06463_Athesis_acrisione
C_24_1_Athesis_clearista
chim44_Patricia_dercyllidas
21467_Patricia_oligyrtis
21184_Patricia_demylus
chim53_Thyridia_psidii
chim50_Sais_rosalia
LEP_01499_Scada_zemira
G130_Scada_kusa
chim52_Scada_zibia
BAKU_22_Scada_karschina
chim51_Scada_reckia
chim9_Forbestra_equicola
20217_Forbestra_olivencia
chim10_Forbestra_proceris
E_19_1_Mechanitis_menapis
NW127_3_Mechanitis_lysimnia
LS02_49_Mechanitis_messenoides
8057_Mechanitis_macrinus
RB233_Mechanitis_polymnia
chim26_Mechanitis_mazaeus
G101_Methona_maxima
chim29_Methona_curvifascia
chim30_Methona_grandior
BAKU_51_Methona_singularis
chim28_Methona_confusa
NW114_2_Methona_themisto
chim1_Aeria_eurimedia
MD_2_Aeria_olena
LEP_06870_Elzunia_humboldt
E_12_1_Elzunia_pavoni
06_SRNP_2593_Tithorea_tarricina
chim54_Tithorea_harmonia
LEP_11128_Tithorea_pacifica
NW114_1_Placidina_euryanassa
chim41_Pagyris_cymothoe
G129_Pagyris_priscillia
chim42_Pagyris_ulla
21470_Ithomia_nsp
RM_2990_Ithomia_terra
RM_8873_Ithomia_jucunda
20245_Ithomia_amarilla
RM_8942_Ithomia_arduinna
chim21_Ithomia_agnosia
RM_8898_Ithomia_pseudoagalla
RM_8931_Ithomia_lichyi
B_16_5_Ithomia_drymo
RM_8004_Ithomia_xenos
ME10_406_Ithomia_adelinda
RM_9096_Ithomia_lagusa
RM_8910_Ithomia_hyala
RM_9150_Ithomia_hymettia
chim22_Ithomia_avella
RM_9116_Ithomia_praeithomia
RM_9115_Ithomia_ellara
RM_9114_Ithomia_eleonora
KW13_3b_Ithomia_leila
RM_9151_Ithomia_celemia
RM_8005_Ithomia_heraldica
RM_8028_Ithomia_patilla
RM_8286_Ithomia_diasia
chim24_Ithomia_salapia
chim23_Ithomia_iphianassa
RM_8904_Ithomia_cleora
LS02_246_Hypothyris_moebiusi
2984_Hyalyris_excelsa
K6_Hyalyris_lactea
RB237_Hypothyris_daphnis
03_31_Hypothyris_thea
LS02_23_Hypothyris_semifulva
8117_Hypothyris_lycaste
02_384_Hypothyris_nsp
4_290_Hyalyris_juninensis
chim15_Hyalyris_oulita
PE_10_14_Hyalyris_antea
20200_Hypothyris_fluonia
G108_Hyalyris_latilimbata
ME11_7_Hyalyris_praxilla
2_3507_Hyalyris_nsp
G107_Hyalyris_schlingeri
4_20_Hyalyris_coeno
20507_Hypothyris_anastasia
20357_Hypothyris_euclea
NW122_22_Hypothyris_ninonia
20292_Hypothyris_mamercus
ME11_52_Hypothyris_mansuetus
G104_Aremfoxia_ferra
NW127_4_Epityches_eupompe
MJ07_512_Napeogenes_verticilla
E_39_47_Napeogenes_larilla
8009_Napeogenes_tolosa
8806_Napeogenes_stella
05_933_Napeogenes_duessa
E_46_1_Napeogenes_sylphis
MJ07_509_Napeogenes_nsp2
03_34_Napeogenes_inachia
G3_21634_Napeogenes_gracilis
E_39_58_Napeogenes_apulia
02_3205_Napeogenes_zurippa
20611_Napeogenes_aethra
BMC_1646_Napeogenes_larina
G20_Napeogenes_nsp1
RB235_Napeogenes_pharo
20017_Napeogenes_glycera
20010_Napeogenes_peridia
20500_Napeogenes_rhezia
chim31_Napeogenes_flossina
RM_8313_Napeogenes_cranto
05_1022_Napeogenes_harbona
20005_Napeogenes_lycora
LEP_04282_Napeogenes_nsp3
20910_Napeogenes_sulphueophila
Col007_Napeogenes_benigna
G14_Napeogenes_sodalis
chim20_Hyposcada_illinissa
LEP_01297_Hyposcada_dujardini
DS_5_1159_Hyposcada_taliata
LEP_01285_Hyposcada_zarepha
chim19_Hyposcada_anchiala
DS_K5_Hyposcada_schausi
DS_EC458_Hyposcada_kena
DS_CJ8833_Hyposcada_virginiana
chim27_Megoleria_orestilla
AW_02_0402_Megoleria_susiana
E_32_1_Ollantaya_aeginata
chim40_Ollantaya_olerioides
DS_6_41_Ollantaya_canilla
DS_3_20_Oleria_aegle
napk20_Oleria_similigena
DS_B16_7_Oleria_aquata
chim39_Oleria_sexmaculata
chim32_Oleria_assimilis
ME10_282_Oleria_tigilla
napk17_Oleria_flora
napk19_Oleria_antaxis
7_507_Oleria_enania
DS_2_1307_Oleria_agarista
DS_6_77_Oleria_quintina
DS_2_3370_Oleria_alexina
RB357_Oleria_astrea
BAKU_54_Oleria_thiemei
chim36_Oleria_ilerdina
chim37_Oleria_onega
DS_6_55_Oleria_didymaea
chim35_Oleria_estella
7_511_Oleria_nsp
LEP_01270_Oleria_boyeri
DS_2_290_Oleria_gunilla
DS_CJ8433_Oleria_zelica
DS_8404_Oleria_rubescens
DS_CJ9026_Oleria_paula
DS_OA142_Oleria_amalda
7_503_Oleria_deronda
DS_8500_Oleria_vicina
DS_MC2_Oleria_phenomoe
DS_11_2_Oleria_radina
DS_EC413_Oleria_baizana
21497_Oleria_santineza
DS_OF30_Oleria_fumata
7_505_Oleria_derondina
DS_9_2K_Oleria_fasciata
chim33_Oleria_athalina
DS_4_262_Oleria_victorine
DS_6_4K_Oleria_tremona
DS_K16_Oleria_makrena
chim38_Oleria_padilla
DS_EC394_Oleria_cyrene
chim34_Oleria_attalia
DS_2_750_Oleria_bioculata
E_16_3_Oleria_quadrata
G116_Velamysta_peninna
LEP_04368_Velamysta_nsp1
chim55_Velamysta_pupilla
E_39_32_Velamysta_phengites
05_1038_Veladyris_cytharista
E_45_1_Veladyris_pardalis
G124_Veladyris_electrea
MJ07_701_Genus1_nsp1
05_1369_Godyris_dircenna
06_SRNP_4980_Godyris_nero
BMC_1705_Godyris_kedema
04_328_Godyris_crinippa
chim12_Godyris_zavaleta
21186_Godyris_panthyale
E_37_1_Godyris_duillia
05_1155_Godyris_sappho
9242_Godyris_lauta
21050_Godyris_hewitsoni
LEP_11343_Heterosais_giulia
BAKU_43_Heterosais_edessa
PE_19_14_Heterosais_nephele
LEP_11339_Hypoleria_lavinia
chim16_Hypoleria_alema
05_624_Hypoleria_xenophis
BMC_1631_Hypoleria_ocalea
21693_Hypoleria_sarepta
BAKU_27_Hypoleria_adasa
chim17_Hypoleria_aureliana
02_3477_Brevioleria_seba
ME10_359_Brevioleria_coenina
G128_Brevioleria_nsp1
chim25_Mcclungia_cymo
LEP_11127_Pachacutia_baroni
MC11_63_Pachacutia_mantura
E_44_4_Brevioleria_arzalia
05_418_Brevioleria_aelia
NW152_1_Greta_diaphanus
NW70_9_Greta_morgane
LEP_01286_Greta_clavijoi
CR_1_5_Genus2_annette
chim11_Genus2_andromica
BAKU_20_Pseudoscada_erruca
LS02_16_Pseudoscada_florula
E_17_4_Pseudoscada_timna
06_SRNP_65072_Pseudoscada_timna
02_762_Pseudoscada_timna
B_20_3_Pseudoscada_acilla
21579_Hypomenitis_libethris
E_28_4_Hypomenitis_theudelinda
KW13_13b_Hypomenitis_nspC
chim18_Hypomenitis_polissena
05_1012_Hypomenitis_alphesiboea
21361_Hypomenitis_nspA
E_39_46_Hypomenitis_hermana
KW_120728_13_Hypomenitis_esula
21070_Hypomenitis_enigma
21203_Hypomenitis_ortygia
MJ07_697_Hypomenitis_ochretis
MJ07_694_Hypomenitis_nspD
LEP_06790_Hypomenitis_depauperata
21181_Hypomenitis_lojana
21282_Hypomenitis_gardneri
BMC_1704_Hypomenitis_nspE
21272_Hypomenitis_lydia
02_2144_Hypomenitis_dercetis
21535_Hypomenitis_oneidodes
MJ07_706_Hypomenitis_nspB
chim13_Hyalenna_buckleyi
BAKU_4_Hyalenna_pascua
G103_Hyalenna_alidella
5_1032_Hyalenna_sulmona
ME10_298_Hyalenna_perasippa
chim14_Hyalenna_paradoxa
NW122_20_Dircenna_dero
4_364_Dircenna_loreta
03_SRNP_22973_Dircenna_klugii
ME10_360_Dircenna_jemina
chim5_Dircenna_olyras
chim4_Dircenna_adina
G109_Haenschia_derama
G111_Haenschia_sidonia
E_24_4_Callithomia_hezia
chim3_Callithomia_lenea
20767_Callithomia_alexirrhoe
03_104_Episcada_hemixanthe
RB324_Ceratinia_neso
G112_Episcada_nspA
E_02_08_Ceratinia_tutia
BMC_1622_Ceratinia_iolaia
BAKU_36_Episcada_doto
B12_3_Episcada_hymenaea
BAKU_2_Episcada_vitrea
BAKU_3_Episcada_philoclea
LdeS11_609_Episcada_hymen
chim7_Episcada_sulphurea
E_29_3_Episcada_apuleia
21555_Episcada_ticidella
ME10_471_Episcada_mira
G113_Episcada_trapezula
chim8_Episcada_sylvo
8042_Episcada_salvinia
2_3173_Episcada_clausina
chim6_Episcada_striposis
LEP_08697_Episcada_polita
PT026_Pteronymia_donella
chim47_Pteronymia_forsteri
20045_Pteronymia_sao
8978_Pteronymia_obscuratus
E_39_43_Pteronymia_hara
chim48_Pteronymia_olimba
165_Pteronymia_granica
chim46_Pteronymia_artena
21516_Pteronymia_serrata
ME10_322_Pteronymia_nspE
21025_Pteronymia_alida
ME10_178_Pteronymia_inania
E_29_1_Pteronymia_teresita
LEP_04482_Pteronymia_teresita
8327_Pteronymia_lonera
PT033_Pteronymia_dispar
BAKU_1_Pteronymia_euritea
BAKU_18_Pteronymia_carlia
HW_5_Pteronymia_nspC
BMC_2203_Pteronymia_medellina
08_SRNP_476_Pteronymia_parva
E_26_1_Pteronymia_aletta
306_Pteronymia_primula
4_469_Pteronymia_vestilla
MJ07_659_Pteronymia_rufocincta
20999_Pteronymia_cotytto
HW_6_Pteronymia_laura
LEP_08684_Pteronymia_alissa
chim45_Pteronymia_alissa
chim49_Pteronymia_sexpunctata
8407_Pteronymia_simplex
20072_Pteronymia_gertschi
8342_Pteronymia_picta
PT007_Pteronymia_latilla
5_1372_Pteronymia_tucuna
LEP_04480_Pteronymia_veia
20078_Pteronymia_ticida
21224_Pteronymia_alina
21169_Pteronymia_asopo
E_43_1_Pteronymia_oneida
20049_Pteronymia_ozia
21063_Pteronymia_nspD
2_808_Pteronymia_bueya
MJ07_640_Pteronymia_fulvimargo
LEP_08685_Pteronymia_zerlina
21479_Pteronymia_tamina
E_43_16_Pteronymia_veia

Supplementary Figure 2. 8. Maximum clade credibility tree for the Ithomiini subclade from BEAST. Posterior probabilities are indicated at the nodes.

i) Libytheinae

Dataset – The dataset for the Libytheinae consisted of 10 taxa to which two outgroups were added: *Danaus plexippus* (Danaini), *Heliconius melpomene* (Heliconinae).

Partition Finder – Partition Finder identified 10 subsets.

Subset #	Substitution model	Gene fragments and codon positions
Subset 1	GTR+G	DDC_pos1, CAD_pos1, MDH_pos1, IDH_pos1, wingless_pos1, ArgKin_pos1, RpS5_pos1, RpS2_pos1, EF1a_pos1, GAPDH_pos1
Subset 2	HKY+I	RpS5_pos2, GAPDH_pos2, MDH_pos2, ArgKin_pos2, EF1a_pos2, IDH_pos2, DDC_pos2, CAD_pos2
Subset 3	HKY	ArgKin_pos3
Subset 4	HKY+G	IDH_pos3, MDH_pos3, CAD_pos3
Subset 5	HKY+G	COI-end_pos3, COI-begin_pos3
Subset 6	TRN+G	COI-end_pos1, COI-begin_pos1
Subset 7	HKY	COI-begin_pos2, COI-end_pos2
Subset 8	GTR	RpS2_pos3, DDC_pos3, GAPDH_pos3, RpS5_pos3, wingless_pos3
Subset 9	HKY+G	EF1a_pos3
Subset 10	JC	RpS2_pos2, wingless_pos2

BEAST analysis – In order to improve the quality of our runs we replaced the default priors for rates of substitutions by uniform prior ranging between 0 and 10 for the following cases: subset1.at, cg, gt. We used a single molecular clock linked across all partition to obtain good mixing and convergence. We used a birth-death tree prior. We performed two runs of 30 million generations, sampling trees and parameters every 3000 generations.

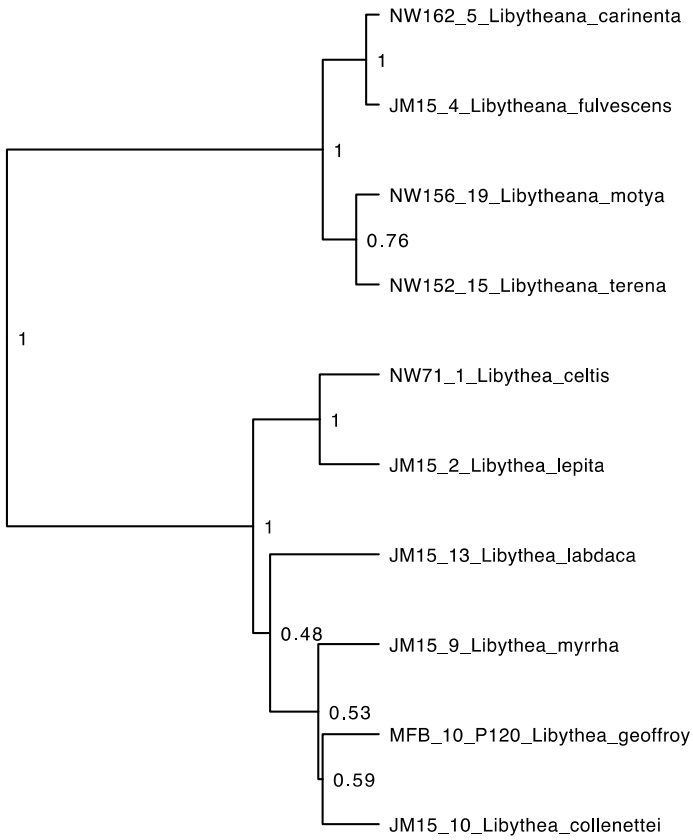

Supplementary Figure 2. 9. Maximum clade credibility tree for the Libytheinae subclade from BEAST. Posterior probabilities are indicated at the nodes.

j) Limenitidinae

Dataset – The dataset for the Limenitidinae consisted of 311 taxa to which two outgroups were added: *Pseudergolis wedah* (Pseudergolinae), *Heliconius melpomene* (Heliconinae).

Partition Finder – Partition Finder identified 14 subsets.

Subset #	Substitution model	Gene fragments and codon positions
Subset 1	GTR+I+G	GAPDH_pos1, ArgKin_pos1, wingless_pos2, EF1a_pos1, RpS2_pos1
Subset 2	GTR+I+G	EF1a_pos2, ArgKin_pos2, DDC_pos2, RpS5_pos2, CAD_pos2, IDH_pos2, MDH_pos2, GAPDH_pos2
Subset 3	GTR+G	ArgKin_pos3
Subset 4	HKY+I+G	CAD_pos3, MDH_pos3
Subset 5	GTR+I+G	DDC_pos1, wingless_pos1, CAD_pos1, RpS5_pos1, MDH_pos1, IDH_pos1
Subset 6	GTR+I+G	COI-begin_pos3
Subset 7	GTR+I+G	COI-begin_pos1, COI-end_pos1
Subset 8	GTR+I+G	COI-begin_pos2, COI-end_pos2
Subset 9	GTR+G	COI-end_pos3
Subset 10	K80+I+G	DDC_pos3
Subset 11	GTR+I+G	EF1a_pos3
Subset 12	GTR+I+G	IDH_pos3, GAPDH_pos3

Subset 13	JC	RpS2_pos2
Subset 14	GTR+I+G	RpS2_pos3, RpS5_pos3, wingless_pos3

BEAST analysis – After multiple attempts to modify priors we could not obtain a good convergence of the MCMC. Hence, we decided to fix the topology. We performed an analysis with IQtree to search for the best topology. The topology was then enforced in our BEAST analysis and we only estimated the relative branch lengths. We also replaced the default prior for rates of substitutions by uniform prior ranging between 0 and 10 for the following case: subset9.cg. We used two molecular clocks: one for the mitochondrial gene fragments and one for the nuclear gene fragments. We used a birth-death tree prior. We performed two runs of 50 million generations, sampling trees and parameters every 5000 generations.

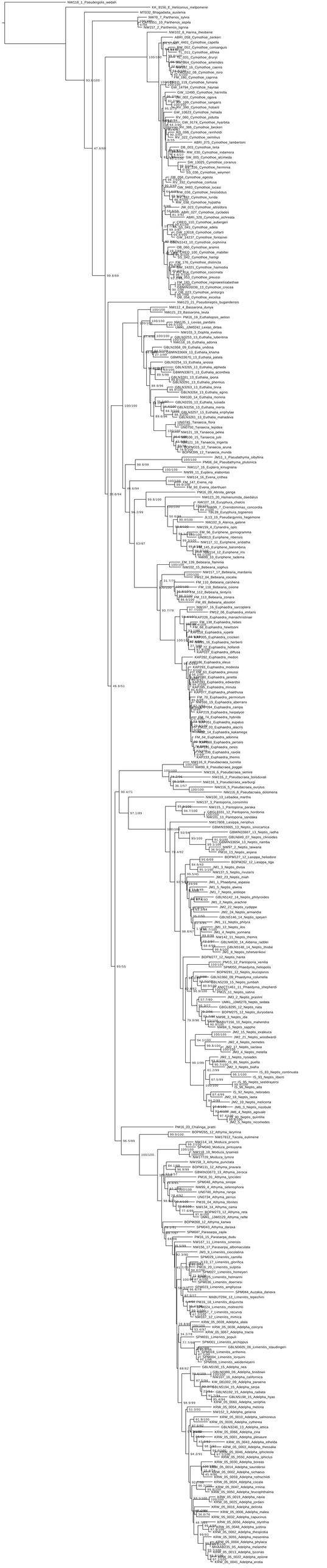
NW118_1_Pseudergolis_wedah
KK_9156_E_Heliconius_melpomene
MT032_Bhagadatta_austenia
NW70_7_Parthenos_sylvia
NW157_2_Parthenos_tigrina
NW102_8_Harma_theobene
ABRI_058_Cymothoe_zenkeri
GW_4401_Cymothoe_capella
GW_052_Cymothoe_consanguis
IL_011_Cymothoe_althea
IL_031_Cymothoe_druryi
GW_064_Cymothoe_amenides
NW102_16_Cymothoe_caenis
NW102_08_Cymothoe_isiro
GW_180_Cymothoe_caprina
CREO_119_Cymothoe_fumana
GW_14794_Cymothoe_haynae
GW_12490_Cymothoe_harmilla
GW_002_Cymothoe_ogova
RV_199_Cymothoe_sangaris
RV_390_Cymothoe_hobarti
GW_10623_Cymothoe_heliada
RV_060_Cymothoe_jodutta
GW_9174_Cymothoe_hyarbita
RV_386_Cymothoe_beckeri
RD_098_Cymothoe_reinholdi
RV_322_Cymothoe_oemilius
ABRI_075_Cymothoe_lambertoni
DB_003_Cymothoe_teita
RW_030_Cymothoe_indamora
SW_005_Cymothoe_alcimeda
SW_13025_Cymothoe_coranus
SW_026_Cymothoe_herminia
SS_036_Cymothoe_weymeri
DB_058_Cymothoe_egesta
RV_332_Cymothoe_confusa
GW_9483_Cymothoe_lucasi
RW_036_Cymothoe_hesiodotus
RW_032_Cymothoe_lurida
RW_038_Cymothoe_hypatha
JW_023_Cymothoe_altisidora
ABRI_027_Cymothoe_cyclades
ABRI_328_Cymothoe_ochreata
CREO_110_Cymothoe_aubergeri
SS_041_Cymothoe_adela
GW_13018_Cymothoe_collarti
GW_14237_Cymothoe_fontainei
GBMN3143_10_Cymothoe_orphnina
DB_060_Cymothoe_aramis
CREO_100_Cymothoe_mabillei
SS_042_Cymothoe_hartigi
FM_176_Cymothoe_distincta
GW_14221_Cymothoe_haimodia
FM_014_Cymothoe_coccinata
FM_053_Cymothoe_preussi
FM_183_Cymothoe_reginaeelisabethae
GBMIN16036_13_Cymothoe_crocea
DB_023_Cymothoe_anitorgis
DB_054_Cymothoe_excelsa
NW123_21_Pseudoneptis_bugandensis
NW112_4_Bassarona_dunya
NW121_23_Bassarona_teuta
PM16_19_Euthaliopsis_aetion
NW135_1_Lexias_pardalis
UMKL_JJW0242_Lexias_dirtea
NW103_3_Dophla_evelina
GBLN3253_13_Euthalia_lubentina
NW118_16_Euthalia_adonia
GBLN1958_09_Euthalia_undosa
GBMIN33669_13_Euthalia_khama
GBMIN33670_13_Euthalia_patala
GBLN3254_13_Euthalia_anosia
GBLN3265_13_Euthalia_alpheda
GBMIN33671_13_Euthalia_aconthea
GBLN3281_13_Euthalia_ipona
GBLN3291_13_Euthalia_phemius
GBLN3263_13_Euthalia_tinna
GBLN3264_13_Euthalia_agnis
NW100_14_Euthalia_monina
GBLN3255_13_Euthalia_lusiada
GBLN3256_13_Euthalia_merta
GBLN3257_13_Euthalia_eriphylae
GBLN3261_13_Euthalia_mahadeva
UN0745_Tanaecia_flora
UN0750_Tanaecia_lepidea
NW121_19_Tanaecia_pelea
NW100_15_Tanaecia_julii
NW121_16_Tanaecia_trigerta
BOPM315_12_Tanaecia_aruna
BOPM399_12_Tanaecia_munda
JM11_1_Pseudathyma_sibyllina
PM06_04_Pseudathyma_plutonica
NW117_16_Euptera_kinugnana
NW99_11_Euptera_elabontas
NW114_16_Evena_crithea
FM_147_Evena_niji
FM_93_Evena_obertlueri
PM16_09_Abrota_ganga
NW123_20_Hamanumida_daedalus
NW107_18_Euryphura_chalcis
NW99_7_Crenidomimas_concordia
TBL39_Euryphene_togoensis
JL13_19_Pseudargynnis_hegemone
NW102_9_Aterica_galene
NW159_4_Cynandra_opis
FM_96_Euriphene_gonioramma
UN0813_Euriphene_ribensis
NW117_11_Euriphene_aridatha
FM_145_Euriphene_barombina
NW114_12_Euriphene_iris
NW99_10_Euriphene_tadema
FM_139_Bebearia_flaminia
NW102_15_Bebearia_sophus
NW117_17_Bebearia_mardania
PM12_04_Bebearia_cocalia
FM_110_Bebearia_carshena
FM_118_Bebearia_oxione
FM_112_Bebearia_tentyris
FM_113_Bebearia_zonara
FM_89_Bebearia_absolon
NW167_16_Euphaedra_sarcoptera
PM12_06_Euphaedra_imitans
KAP226_Euphaedra_mariachristinae
FM_138_Euphaedra_hebes
FM_68_Euphaedra_hewitsoni
PM12_08_Euphaedra_xypete
KAP205_Euphaedra_crockeri
NW99_16_Euphaedra_herberti
FM_72_Euphaedra_hollandi
KAP037_Euphaedra_diffusa
KAP282_Euphaedra_medon
KAP186_Euphaedra_eleus
KAP293_Euphaedra_modesta
FM_63_Euphaedra_preussi
KAP190_Euphaedra_janetta
KAP203_Euphaedra_edwardsii
KAP185_Euphaedra_minuta
KAP077_Euphaedra_phaethusa
FM_70_Euphaedra_permixtum
NW100_19_Euphaedra_aberrans
KAP094_Euphaedra_zampa
KAP219_Euphaedra_harpalyce
FM_74_Euphaedra_hybrida
KAP051_Euphaedra_eupalus
NW123_03_Euphaedra_alacris
NW99_14_Euphaedra_kakamega
FM_64_Euphaedra_adonina
KAP060_Euphaedra_perseis
KAP195_Euphaedra_ceres
FM_136_Euphaedra_ravola
KAP233_Euphaedra_themis
NW116_9_Pseudacraea_lucretia
NW99_8_Pseudacraea_poggei
NW116_6_Pseudacraea_semire
NW116_2_Pseudacraea_boisduvali
NW116_3_Pseudacraea_warburgi
NW116_5_Pseudacraea_eurytus
NW116_8_Pseudacraea_dolomena
NW100_13_Lebadea_martha
NW137_3_Pantoporia_consimilis
NW115_1_Pantoporia_paraka
GBGL8331_12_Pantoporia_hordonia
NW101_13_Pantoporia_sandaka
NW17808_Lasippa_neriphus
GBMIN33665_13_Neptis_sinocartica
GBMIN33667_13_Neptis_radha
GBLN849_07_Neptis_clinioides
GBMIN33654_13_Neptis_namba
NW97_2_Neptis_taiwana
PM16_13_Neptis_anjana
BOPM127_12_Lasippa_heliodore
BOPM262_12_Lasippa_tiga
JM1_3_Neptis_divisa
NW137_5_Neptis_rivularis
JM2_23_Neptis_miah
JM1_1_Phaedyma_aspasia
JM1_5_Neptis_alwina
JM1_7_Neptis_antilope
GBLN5142_14_Neptis_philyroides
JM1_2_Neptis_arachne
JM2_22_Neptis_cydippe
JM2_24_Neptis_armandia
GBLN5146_14_Neptis_speyeri
JM1_11_Neptis_philyra
JM1_12_Neptis_ilos
JM1_4_Neptis_yunnana
NW142_11_Neptis_themis
GBLN4630_14_Aldania_raddei
GBLN5148_14_Neptis_thisbe
NW99_19_Neptis_ilshetverikovi
BOPM277_12_Neptis_harita
PM15_12_Pantoporia_venilia
SPM050_Phaedyma_heliopolis
BOPM281_12_Neptis_leucoporos
GBLN1960_09_Phaedyma_columella
GBLN5239_15_Neptis_jumbah
ANICT1461_11_Phaedyma_shepherdi
PM15_11_Neptis_satina
JM3_2_Neptis_praslini
UMKL_JJW0276_Neptis_sedata
GBGL8295_12_Neptis_nata
BOPM275_12_Neptis_duryodana
NW98_3_Neptis_ida
MABUT156_10_Neptis_mahendra
NW84_5_Neptis_sappho
JM2_15_Neptis_exaleuca
JM2_21_Neptis_woodwardi
JM2_4_Neptis_nemetes
JM2_17_Neptis_saclava
JM3_4_Neptis_metella
JM2_1_Neptis_nysiades
IS_86_Neptis_puella
JM2_3_Neptis_biafra
IS_83_Neptis_continuata
IS_93_Neptis_liberti
IS_95_Neptis_seeldrayersi
IS_96_Neptis_alta
IS_92_Neptis_nebrodes
JM2_18_Neptis_laeta
JM2_10_Neptis_melicerta
JM6_3_Neptis_nicobule
JM6_4_Neptis_agouale
JM_90_Neptis_quintilla
JM2_5_Neptis_nicomedes
PM16_03_Chalinga_pratti
BOPM265_12_Athyma_larymna
NW17812_Tacola_eulimene
NW99_10_Moduza_procris
SPM040_Moduza_pinnuvacia
NW118_10_Moduza_lysanias
NW17729_Moduza_lymire
NW158_3_Athyma_punctata
BOPM131_12_Athyma_pravara
GBMIN33673_13_Athyma_zeroca
PM16_01_Athyma_cyncides
SPM046_Athyma_sinope
NW99_4_Athyma_selenophora
UN0734_Athyma_ranga
UN0734_Athyma_perius
PM16_04_Athyma_libnites
NW134_14_Athyma_cama
BOPM273_12_Athyma_reta
UMKL_JJW0129_Athyma_nefte
BOPM268_12_Athyma_kanwa
SPM043_Athyma_daraxa
SPM047_Parasarpa_zayla
PM16_15_Parasarpa_dudu
NW167_11_Limenitis_sinensis
NW156_17_Parasarpa_albomaculata
JM3_9_Limenitis_ciocolatina
SPM029_Limenitis_glorifica
PM16_20_Limenitis_sulpitia
SPM027_Limenitis_homeyeri
SPM025_Limenitis_helmanni
SPM036_Limenitis_doerriesi
SPM023_Limenitis_amphyssa
SPM044_Auzakia_danava
MABUT294_12_Limenitis_lepechini
PM16_18_Limenitis_disjuncta
SPM024_Limenitis_moltrechti
SPM057_Limenitis_recurva
NW167_12_Limenitis_mimica
KRW_05_0028_Adelpha_alala
KRW_05_0036_Adelpha_corcyra
KRW_05_0067_Adelpha_tracta
SPM031_Limenitis_populi
SPM001_Limenitis_archippus
GBLN0605_06_Limenitis_staudingeri
SPM018_Limenitis_arthemis
SPM004_Limenitis_lorquini
SPM006_Limenitis_weidemeyerii
GBLN5190_15_Adelpha_nea
GBLN0389_06_Adelpha_bredowi
NW107_16_Adelpha_californica
KW_081002_09_Adelpha_paraena
GBLN5194_15_Adelpha_serpa
GBLN5192_15_Adelpha_radiata
GBLN5198_15_Adelpha_hyas
KRW_05_0060_Adelpha_seriphia
KRW_05_0054_Adelpha_melona
NW152_3_Adelpha_gelania
KRW_05_0010_Adelpha_salmoneus
KRW_05_0039_Adelpha_cytherea
GBLN3246_13_Adelpha_attica
KRW_05_0066_Adelpha_zina
KRW_05_0001_Adelpha_plesaure
KRW_05_0043_Adelpha_ethelda
KRW_05_0003_Adelpha_messana
KRW_05_0046_Adelpha_iphicleola
KRW_05_0550_Adelpha_iphiclus
KRW_05_0030_Adelpha_boreas
KRW_05_0014_Adelpha_saundersii
KRW_05_0002_Adelpha_sichaeus
KRW_05_0059_Adelpha_rothschildi
KRW_05_0024_Adelpha_cocala
KRW_05_0047_Adelpha_irmina
KRW_05_0050_Adelpha_leucophthalma
KRW_05_0019_Adelpha_naxia
KRW_05_0025_Adelpha_jordani
KRW_05_0013_Adelpha_delinita
KRW_05_0006_Adelpha_malea
KRW_05_0032_Adelpha_capucinus
KRW_05_0058_Adelpha_plymthia
KRW_05_0048_Adelpha_justina
KRW_05_0062_Adelpha_thesprotia
KRW_05_0055_Adelpha_mesentina
KRW_05_0004_Adelpha_phylaca
GBMAB235_05_Adelpha_melanthe
KRW_05_0020_Adelpha_epione
KRW_05_0041_Adelpha_erotia
100/100
93.6/100
47.6/60
99.8/69
100/100
35.6/94
98.8/99
46.6/94
99.8/100
94.2/99
63/87
93.7/78
46.8/51
90.4/71
97.1/89
95/55
96.5/89
100/100
98.9/99
94.2/91

Supplementary Figure 2. 10. (page before). Consensus tree for the Limenitidinae subclade from IQtree. Numbers at the nodes are SH-aLRT support (%) / ultrafast bootstrap support (%).

k) Satyrinae group II

Dataset – The dataset for the Satyrinae group II consisted of 169 taxa to which two outgroups were added: *Anaea troglodyta* (Charaxinae), *Brintesia circe* (Satyrinae).

Partition Finder – Partition Finder identified 10 subsets.

Subset #	Substitution model	Gene fragments and codon positions
Subset 1	TRN+I+G	wingless_pos2, ArgKin_pos1, RpS2_pos1, EF1a_pos1
Subset 2	TRN+I+G	RpS2_pos2, EF1a_pos2, RpS5_pos2, ArgKin_pos2, GAPDH_pos2, DDC_pos2
Subset 3	HKY+I+G	DDC_pos3, ArgKin_pos3, wingless_pos3
Subset 4	HKY+I+G	CAD_pos3, MDH_pos3
Subset 5	GTR+I+G	GAPDH_pos1, IDH_pos1, RpS5_pos1, MDH_pos1, CAD_pos1, DDC_pos1, wingless_pos1
Subset 6	GTR+I+G	MDH_pos2, COI-begin_pos2, COI-end_pos2, CAD_pos2, IDH_pos2
Subset 7	GTR+G	COI-begin_pos3, COI-end_pos3
Subset 8	GTR+I+G	COI-begin_pos1, COI-end_pos1
Subset 9	GTR+I+G	GAPDH_pos3, RpS5_pos3, EF1a_pos3
Subset 10	GTR+G	RpS2_pos3, IDH_pos3

BEAST analysis – In order to improve the quality of our runs we replaced the default priors for rates of substitutions by uniform prior ranging between 0 and 10 for the following cases: sub7.ag, at, gt, cg. We used one molecular clock per subset identified by Partition Finder and obtained good mixing and convergence. We used a birth-death tree prior. We performed three runs of 100 million generations, sampling trees and parameters every 10000 generations.

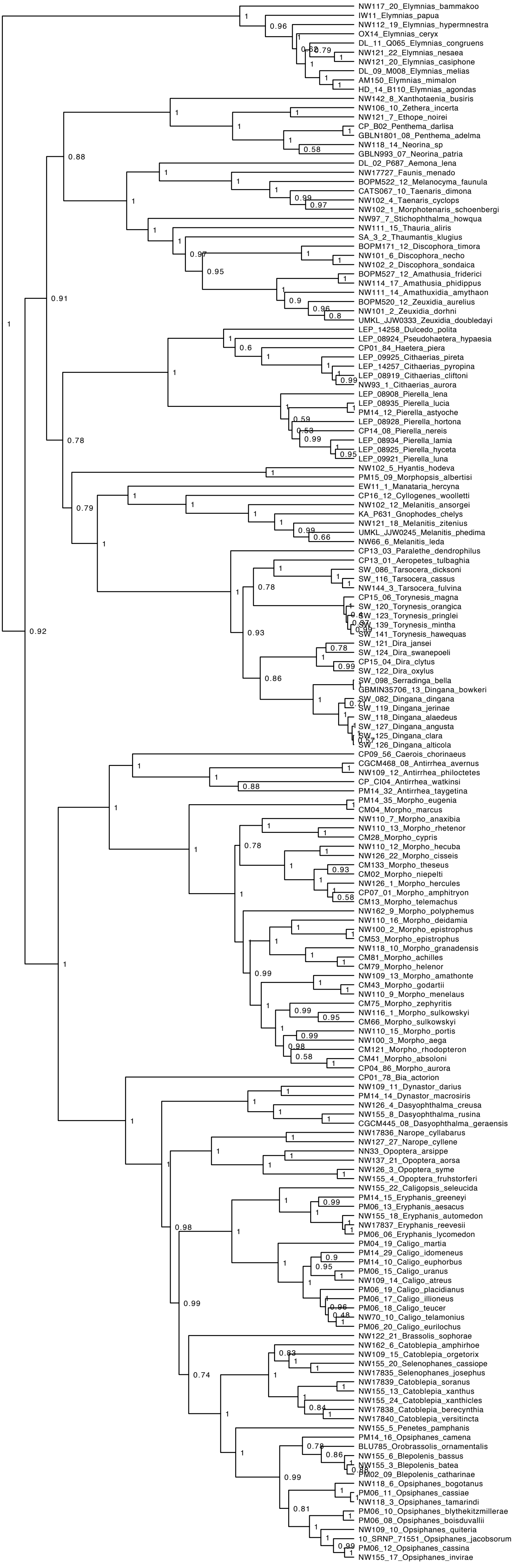
NW117_20_Elymnias_bammakoo
IW11_Elymnias_papua
NW112_19_Elymnias_hypermnestra
OX14_Elymnias_ceryx
DL_11_Q065_Elymnias_congruens
NW121_22_Elymnias_nesaea
NW121_20_Elymnias_casiphone
DL_09_M008_Elymnias_melias
AM150_Elymnias_mimalon
HD_14_B110_Elymnias_agondas
NW142_8_Xanthotaenia_busiris
NW106_10_Zethera_incerta
NW121_7_Ethope_noirei
CP_B02_Penthema_darlisa
GBLN1801_08_Penthema_adelma
NW118_14_Neorina_sp
GBLN993_07_Neorina_patria
DL_02_P687_Aemona_lena
NW17727_Faunis_menado
BOPM522_12_Melanocyma_faunula
CATS067_10_Taenaris_dimona
NW102_4_Taenaris_cyclops
NW102_1_Morphotenaris_schoenbergi
NW97_7_Stichophthalma_howqua
NW111_15_Thauria_aliris
SA_3_2_Thaumantis_klugius
BOPM171_12_Discophora_timora
NW101_6_Discophora_necho
NW102_2_Discophora_sondaica
BOPM527_12_Amathusia_friderici
NW114_17_Amathusia_phidippus
NW111_14_Amathuxidia_amythaon
BOPM520_12_Zeuxidia_aurelius
NW101_2_Zeuxidia_dorhni
UMKL_JJW0333_Zeuxidia_doubledayi
LEP_14258_Dulcedo_polita
LEP_08924_Pseudohaetera_hypaesia
CP01_84_Haetera_piera
LEP_09925_Cithaerias_pireta
LEP_14257_Cithaerias_pyropina
LEP_08919_Cithaerias_cliftoni
NW93_1_Cithaerias_aurora
LEP_08908_Pierella_lena
LEP_08935_Pierella_lucia
PM14_12_Pierella_astyoche
LEP_08928_Pierella_hortona
CP14_08_Pierella_nereis
LEP_08934_Pierella_lamia
LEP_08925_Pierella_hyceta
LEP_09921_Pierella_luna
NW102_5_Hyantis_hodeva
PM15_09_Morphopsis_albertisi
EW11_1_Manataria_hercyna
CP16_12_Cyllogenes_woolletti
NW102_12_Melanitis_ansorgei
KA_P631_Gnophodes_chelys
NW121_18_Melanitis_zitenius
UMKL_JJW0245_Melanitis_phedima
NW66_6_Melanitis_leda
CP13_03_Paralethe_dendrophilus
CP13_01_Aeropetes_tulbaghia
SW_086_Tarsocera_dicksoni
SW_116_Tarsocera_cassus
NW144_3_Tarsocera_fulvina
CP15_06_Torynesis_magna
SW_120_Torynesis_orangica
SW_123_Torynesis_pringlei
SW_139_Torynesis_mintha
SW_141_Torynesis_hawequas
SW_121_Dira_jansei
SW_124_Dira_swanepoeli
CP15_04_Dira_clytus
SW_122_Dira_oxylus
SW_098_Serradinga_bella
GBMIN35706_13_Dingana_bowkeri
SW_082_Dingana_dingana
SW_119_Dingana_jerinae
SW_118_Dingana_alaedeus
SW_127_Dingana_angusta
SW_125_Dingana_clara
SW_126_Dingana_alticola
CP09_56_Caerois_chorinaeus
CGCM468_08_Antirrhea_avernus
NW109_12_Antirrhea_philoctetes
CP_CI04_Antirrhea_watkinsi
PM14_32_Antirrhea_taygetina
PM14_35_Morpho_eugenia
CM04_Morpho_marcus
NW110_7_Morpho_anaxibia
NW110_13_Morpho_rhetenor
CM28_Morpho_cypris
NW110_12_Morpho_hecuba
NW126_22_Morpho_cisseis
CM133_Morpho_theseus
CM02_Morpho_niepelti
NW126_1_Morpho_hercules
CP07_01_Morpho_amphitryon
CM13_Morpho_telemachus
NW162_9_Morpho_polyphemus
NW110_16_Morpho_deidamia
NW100_2_Morpho_epistrophus
CM53_Morpho_epistrophus
NW118_10_Morpho_granadensis
CM81_Morpho_achilles
CM79_Morpho_helenor
NW109_13_Morpho_amathonte
CM43_Morpho_godartii
NW110_9_Morpho_menelaus
CM75_Morpho_zephyritis
NW116_1_Morpho_sulkowskyi
CM66_Morpho_sulkowskyi
NW110_15_Morpho_portis
NW100_3_Morpho_aega
CM121_Morpho_rhodopteron
CM41_Morpho_absoloni
CP04_86_Morpho_aurora
CP01_78_Bia_actorion
NW109_11_Dynastor_darius
PM14_14_Dynastor_macrosiris
NW126_4_Dasyophthalma_creusa
NW155_8_Dasyophthalma_rusina
CGCM445_08_Dasyophthalma_geraensis
NW17836_Narope_cyllabarus
NW127_27_Narope_cyllene
NN33_Opoptera_arsippe
NW137_21_Opoptera_aorsa
NW126_3_Opoptera_syme
NW155_4_Opoptera_fruhstorferi
NW155_22_Caligopsis_seleucida
PM14_15_Eryphanis_greeneyi
PM06_13_Eryphanis_aesacus
NW155_18_Eryphanis_automedon
NW17837_Eryphanis_reevesii
PM06_06_Eryphanis_lycomedon
PM04_19_Caligo_martia
PM14_29_Caligo_idomeneus
PM14_10_Caligo_euphorbus
PM06_15_Caligo_uranus
NW109_14_Caligo_atreus
PM06_19_Caligo_placidianus
PM06_17_Caligo_illioneus
PM06_18_Caligo_teucer
NW70_10_Caligo_telamonius
PM06_20_Caligo_eurilochus
NW122_21_Brassolis_sophorae
NW162_6_Catoblepia_amphirhoe
NW109_15_Catoblepia_orgetorix
NW155_20_Selenophanes_cassiope
NW17835_Selenophanes_josephus
NW17839_Catoblepia_soranus
NW155_13_Catoblepia_xanthus
NW155_24_Catoblepia_xanthicles
NW17838_Catoblepia_berecynthia
NW17840_Catoblepia_versitincta
NW155_5_Penetes_pamphanis
PM14_16_Opsiphanes_camena
BLU785_Orobrassolis_ornamentalis
NW155_6_Blepolenis_bassus
NW155_3_Blepolenis_batea
PM02_09_Blepolenis_catharinae
NW118_6_Opsiphanes_bogotanus
PM06_11_Opsiphanes_cassiae
NW118_3_Opsiphanes_tamarindi
PM06_10_Opsiphanes_blythekitzmillerae
PM06_08_Opsiphanes_boisduvallii
NW109_10_Opsiphanes_quiteria
10_SRNP_71551_Opsiphanes_jacobsorum
PM06_12_Opsiphanes_cassina
NW155_17_Opsiphanes_invirae

Supplementary Figure 2. 11. (page before). Maximum clade credibility tree for the Satyrinae group I subclade from BEAST. Posterior probabilities are indicated at the nodes.

l) Satyrinae group II

Dataset – The dataset for the Satyrinae group I consisted of 368 taxa to which two outgroups were added: *Amathusia phidippus* (Satyrinae), *Brintesia circe* (Satyrinae).

Partition Finder – Partition Finder identified 14 subsets.

Subset #	Substitution model	Gene fragments and codon positions
Subset 1	GTR+I+G	CAD_pos1, RpS5_pos1, MDH_pos1, IDH_pos1, GAPDH_pos1, ArgKin_pos1
Subset 2	HKY+I+G	wingless_pos2, ArgKin_pos2, EF1a_pos2, DDC_pos2
Subset 3	GTR+I+G	ArgKin_pos3, wingless_pos3
Subset 4	HKY+I+G	GAPDH_pos3, CAD_pos3, MDH_pos3
Subset 5	GTR+I+G	COI-begin_pos2, MDH_pos2, COI-end_pos2, CAD_pos2, IDH_pos2
Subset 6	GTR+I+G	COI-begin_pos3
Subset 7	GTR+I+G	COI-begin_pos1, COI-end_pos1
Subset 8	GTR+G	COI-end_pos3
Subset 9	GTR+I+G	DDC_pos3, IDH_pos3, RpS2_pos3, RpS5_pos3
Subset 10	SYM+I+G	RpS2_pos1, DDC_pos1
Subset 11	HKY+I+G	EF1a_pos3
Subset 12	TRN+I+G	wingless_pos1, EF1a_pos1
Subset 13	TRN+I+G	GAPDH_pos2, RpS5_pos2
Subset 14	SYM+I+G	RpS2_pos2

BEAST analysis – In order to improve the quality of our runs we replaced the default priors for rates of substitutions by uniform prior ranging between 0 and 10 for the following cases: sub14.at, gt and sub8.cg, gt. We used a single molecular clock linked across all partition to obtain good mixing and convergence. We used a birth-death tree prior. We performed two runs of 60 million generations, sampling trees and parameters every 6000 generations.

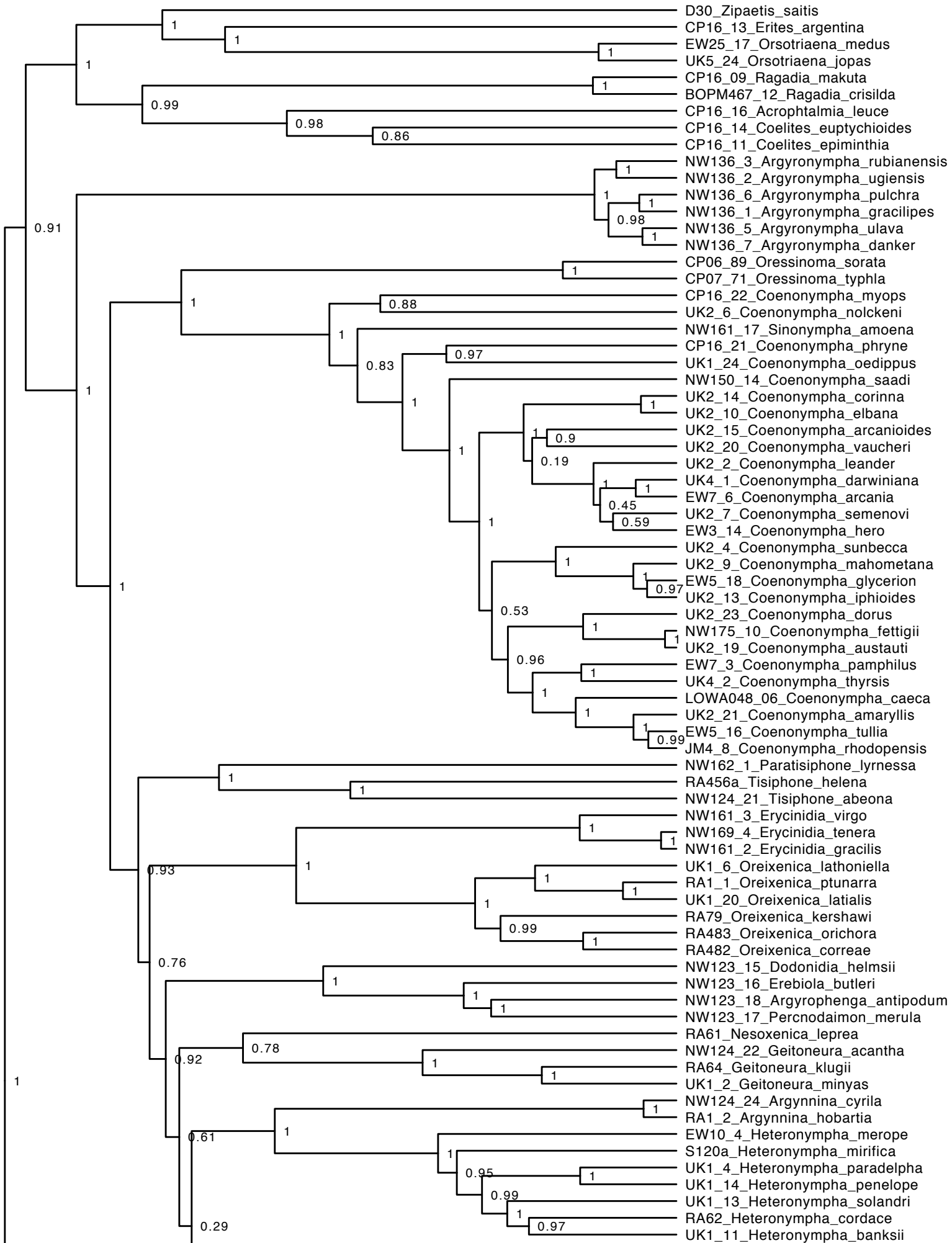
D30_Zipaetis_saitis
CP16_13_Erites_argentina
EW25_17_Orsotriaena_medus
UK5_24_Orsotriaena_jopas
CP16_09_Ragadia_makuta
BOPM467_12_Ragadia_crisilda
CP16_16_Acrophtalmia_leuce
CP16_14_Coelites_euptychioides
CP16_11_Coelites_epiminthia
NW136_3_Argyronympha_rubianensis
NW136_2_Argyronympha_ugiensis
NW136_6_Argyronympha_pulchra
NW136_1_Argyronympha_gracilipes
NW136_5_Argyronympha_ulava
NW136_7_Argyronympha_danker
CP06_89_Oressinoma_sorata
CP07_71_Oressinoma_typhla
CP16_22_Coenonympha_myops
UK2_6_Coenonympha_nolckeni
NW161_17_Sinonympha_amoena
CP16_21_Coenonympha_phryne
UK1_24_Coenonympha_oedippus
NW150_14_Coenonympha_saadi
UK2_14_Coenonympha_corinna
UK2_10_Coenonympha_elbana
UK2_15_Coenonympha_arcanioides
UK2_20_Coenonympha_vaucheri
UK2_2_Coenonympha_leander
UK4_1_Coenonympha_darwiniana
EW7_6_Coenonympha_arcania
UK2_7_Coenonympha_semenovi
EW3_14_Coenonympha_hero
UK2_4_Coenonympha_sunbecca
UK2_9_Coenonympha_mahometana
EW5_18_Coenonympha_glycerion
UK2_13_Coenonympha_iphioides
UK2_23_Coenonympha_dorus
NW175_10_Coenonympha_fettigii
UK2_19_Coenonympha_austauti
EW7_3_Coenonympha_pamphilus
UK4_2_Coenonympha_thyrsis
LOWA048_06_Coenonympha_caeca
UK2_21_Coenonympha_amaryllis
EW5_16_Coenonympha_tullia
JM4_8_Coenonympha_rhodopensis
NW162_1_Paratisiphone_lyrnessa
RA456a_Tisiphone_helena
NW124_21_Tisiphone_abeona
NW161_3_Erycinidia_virgo
NW169_4_Erycinidia_tenera
NW161_2_Erycinidia_gracilis
UK1_6_Oreixenica_lathoniella
RA1_1_Oreixenica_ptunarra
UK1_20_Oreixenica_latialis
RA79_Oreixenica_kershawi
RA483_Oreixenica_orichora
RA482_Oreixenica_correae
NW123_15_Dodonidia_helmsii
NW123_16_Erebiola_butleri
NW123_18_Argyrophenga_antipodum
NW123_17_Percnodaimon_merula
RA61_Nesoxenica_leprea
NW124_22_Geitoneura_acantha
RA64_Geitoneura_klugii
UK1_2_Geitoneura_minyas
NW124_24_Argynnina_cyrila
RA1_2_Argynnina_hobartia
EW10_4_Heteronympha_merope
S120a_Heteronympha_mirifica
UK1_4_Heteronympha_paradelpha
UK1_14_Heteronympha_penelope
UK1_13_Heteronympha_solandri
RA62_Heteronympha_cordace
UK1_11_Heteronympha_banksii

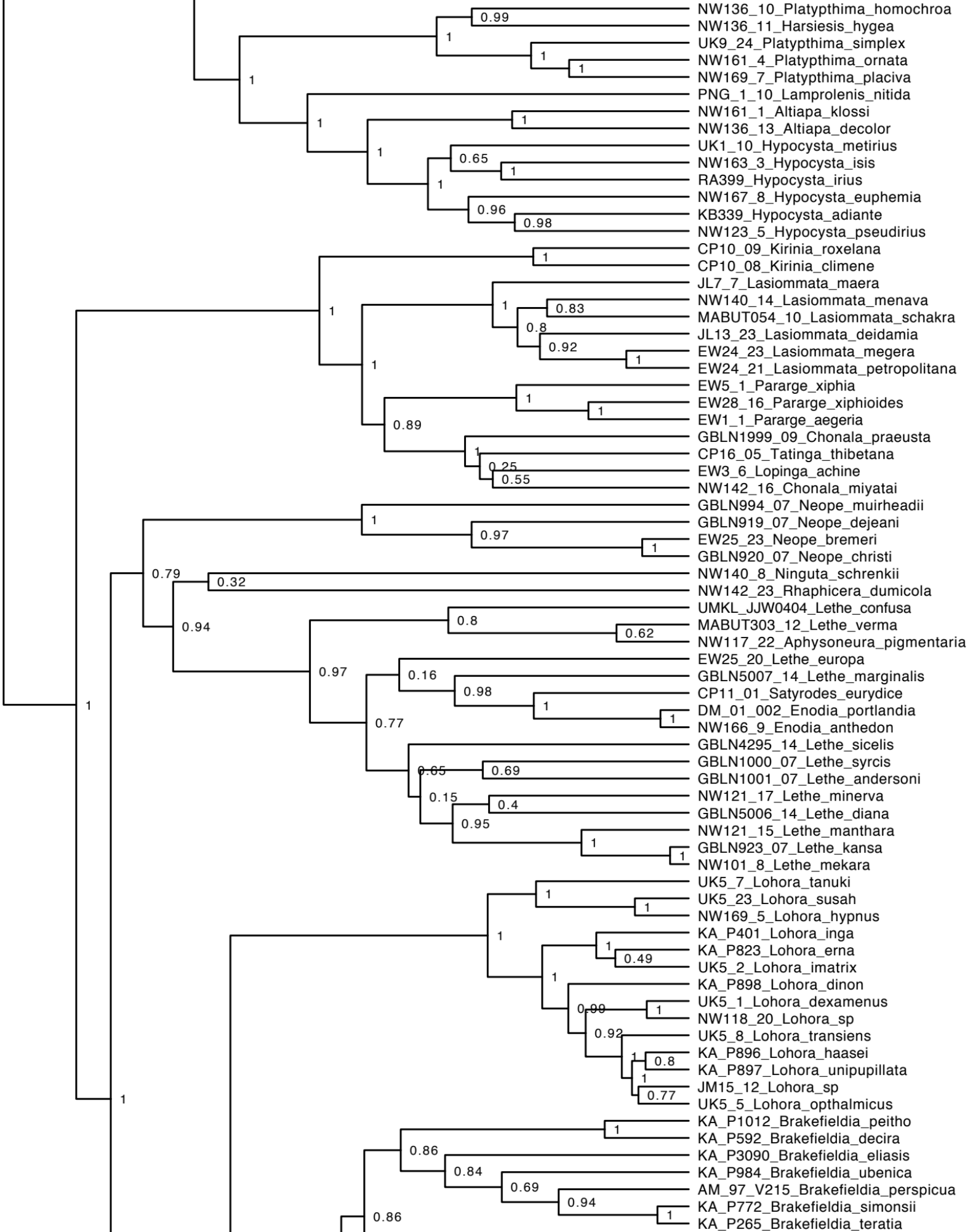
NW136_10_Platypthima_homochroa
NW136_11_Harsiesis_hygea
UK9_24_Platypthima_simplex
NW161_4_Platypthima_ornata
NW169_7_Platypthima_placiva
PNG_1_10_Lamprolenis_nitida
NW161_1_Altiapa_klossi
NW136_13_Altiapa_decolor
UK1_10_Hypocysta_metirius
NW163_3_Hypocysta_isis
RA399_Hypocysta_irius
NW167_8_Hypocysta_euphemia
KB339_Hypocysta_adiante
NW123_5_Hypocysta_pseudirius
CP10_09_Kirinia_roxelana
CP10_08_Kirinia_climene
JL7_7_Lasiommata_maera
NW140_14_Lasiommata_menava
MABUT054_10_Lasiommata_schakra
JL13_23_Lasiommata_deidamia
EW24_23_Lasiommata_megera
EW24_21_Lasiommata_petropolitana
EW5_1_Pararge_xiphia
EW28_16_Pararge_xiphioides
EW1_1_Pararge_aegeria
GBLN1999_09_Chonala_praeusta
CP16_05_Tatinga_thibetana
EW3_6_Lopinga_achine
NW142_16_Chonala_miyatai
GBLN994_07_Neope_muirheadii
GBLN919_07_Neope_dejeani
EW25_23_Neope_bremeri
GBLN920_07_Neope_christi
NW140_8_Ninguta_schrenkii
NW142_23_Rhaphicera_dumicola
UMKL_JJW0404_Lethe_confusa
MABUT303_12_Lethe_verma
NW117_22_Aphysoneura_pigmentaria
EW25_20_Lethe_europa
GBLN5007_14_Lethe_marginalis
CP11_01_Satyrodes_eurydice
DM_01_002_Enodia_portlandia
NW166_9_Enodia_anthedon
GBLN4295_14_Lethe_sicelis
GBLN1000_07_Lethe_syrcis
GBLN1001_07_Lethe_andersoni
NW121_17_Lethe_minerva
GBLN5006_14_Lethe_diana
NW121_15_Lethe_manthara
GBLN923_07_Lethe_kansa
NW101_8_Lethe_mekara
UK5_7_Lohora_tanuki
UK5_23_Lohora_susah
NW169_5_Lohora_hypnus
KA_P401_Lohora_inga
KA_P823_Lohora_erna
UK5_2_Lohora_imatrix
KA_P898_Lohora_dinon
UK5_1_Lohora_dexamenus
NW118_20_Lohora_sp
UK5_8_Lohora_transiens
KA_P896_Lohora_haasei
KA_P897_Lohora_unipupillata
JM15_12_Lohora_sp
UK5_5_Lohora_opthalmicus
KA_P1012_Brakefieldia_peitho
KA_P592_Brakefieldia_decira
KA_P3090_Brakefieldia_eliasis
KA_P984_Brakefieldia_ubenica
AM_97_V215_Brakefieldia_perspicua
KA_P772_Brakefieldia_simonsii
KA_P265_Brakefieldia_teratia

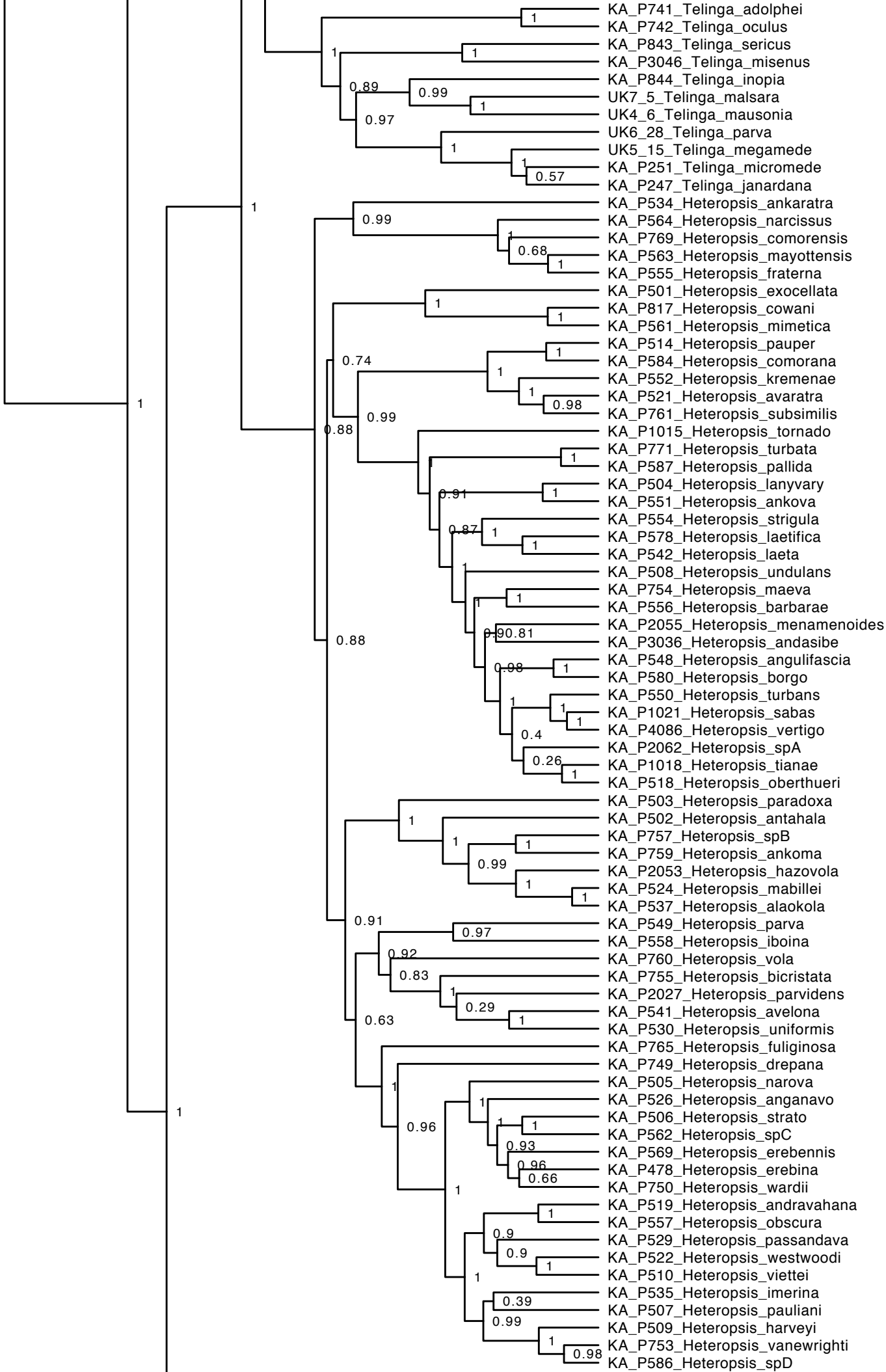
KA_P741_Telinga_adolphei
KA_P742_Telinga_oculus
KA_P843_Telinga_sericus
KA_P3046_Telinga_misenus
KA_P844_Telinga_inopia
UK7_5_Telinga_malsara
UK4_6_Telinga_mausonia
UK6_28_Telinga_parva
UK5_15_Telinga_megamede
KA_P251_Telinga_micromede
KA_P247_Telinga_janardana
KA_P534_Heteropsis_ankaratra
KA_P564_Heteropsis_narcissus
KA_P769_Heteropsis_comorensis
KA_P563_Heteropsis_mayottensis
KA_P555_Heteropsis_fraterna
KA_P501_Heteropsis_exocellata
KA_P817_Heteropsis_cowani
KA_P561_Heteropsis_mimetica
KA_P514_Heteropsis_pauper
KA_P584_Heteropsis_comorana
KA_P552_Heteropsis_kremenae
KA_P521_Heteropsis_avaratra
KA_P761_Heteropsis_subsimilis
KA_P1015_Heteropsis_tornado
KA_P771_Heteropsis_turbata
KA_P587_Heteropsis_pallida
KA_P504_Heteropsis_lanyvary
KA_P551_Heteropsis_ankova
KA_P554_Heteropsis_strigula
KA_P578_Heteropsis_laetifica
KA_P542_Heteropsis_laeta
KA_P508_Heteropsis_undulans
KA_P754_Heteropsis_maeva
KA_P556_Heteropsis_barbarae
KA_P2055_Heteropsis_menamenoides
KA_P3036_Heteropsis_andasibe
KA_P548_Heteropsis_angulifascia
KA_P580_Heteropsis_borgo
KA_P550_Heteropsis_turbans
KA_P1021_Heteropsis_sabas
KA_P4086_Heteropsis_vertigo
KA_P2062_Heteropsis_spA
KA_P1018_Heteropsis_tianae
KA_P518_Heteropsis_oberthueri
KA_P503_Heteropsis_paradoxa
KA_P502_Heteropsis_antahala
KA_P757_Heteropsis_spB
KA_P759_Heteropsis_ankoma
KA_P2053_Heteropsis_hazovola
KA_P524_Heteropsis_mabillei
KA_P537_Heteropsis_alaokola
KA_P549_Heteropsis_parva
KA_P558_Heteropsis_iboina
KA_P760_Heteropsis_vola
KA_P755_Heteropsis_bicristata
KA_P2027_Heteropsis_parvidens
KA_P541_Heteropsis_avelona
KA_P530_Heteropsis_uniformis
KA_P765_Heteropsis_fuliginosa
KA_P749_Heteropsis_drepana
KA_P505_Heteropsis_narova
KA_P526_Heteropsis_anganavo
KA_P506_Heteropsis_strato
KA_P562_Heteropsis_spC
KA_P569_Heteropsis_erebennis
KA_P478_Heteropsis_erebina
KA_P750_Heteropsis_wardii
KA_P519_Heteropsis_andravahana
KA_P557_Heteropsis_obscura
KA_P529_Heteropsis_passandava
KA_P522_Heteropsis_westwoodi
KA_P510_Heteropsis_viettei
KA_P535_Heteropsis_imerina
KA_P507_Heteropsis_pauliani
KA_P509_Heteropsis_harveyi
KA_P753_Heteropsis_vanewrighti
KA_P586_Heteropsis_spD

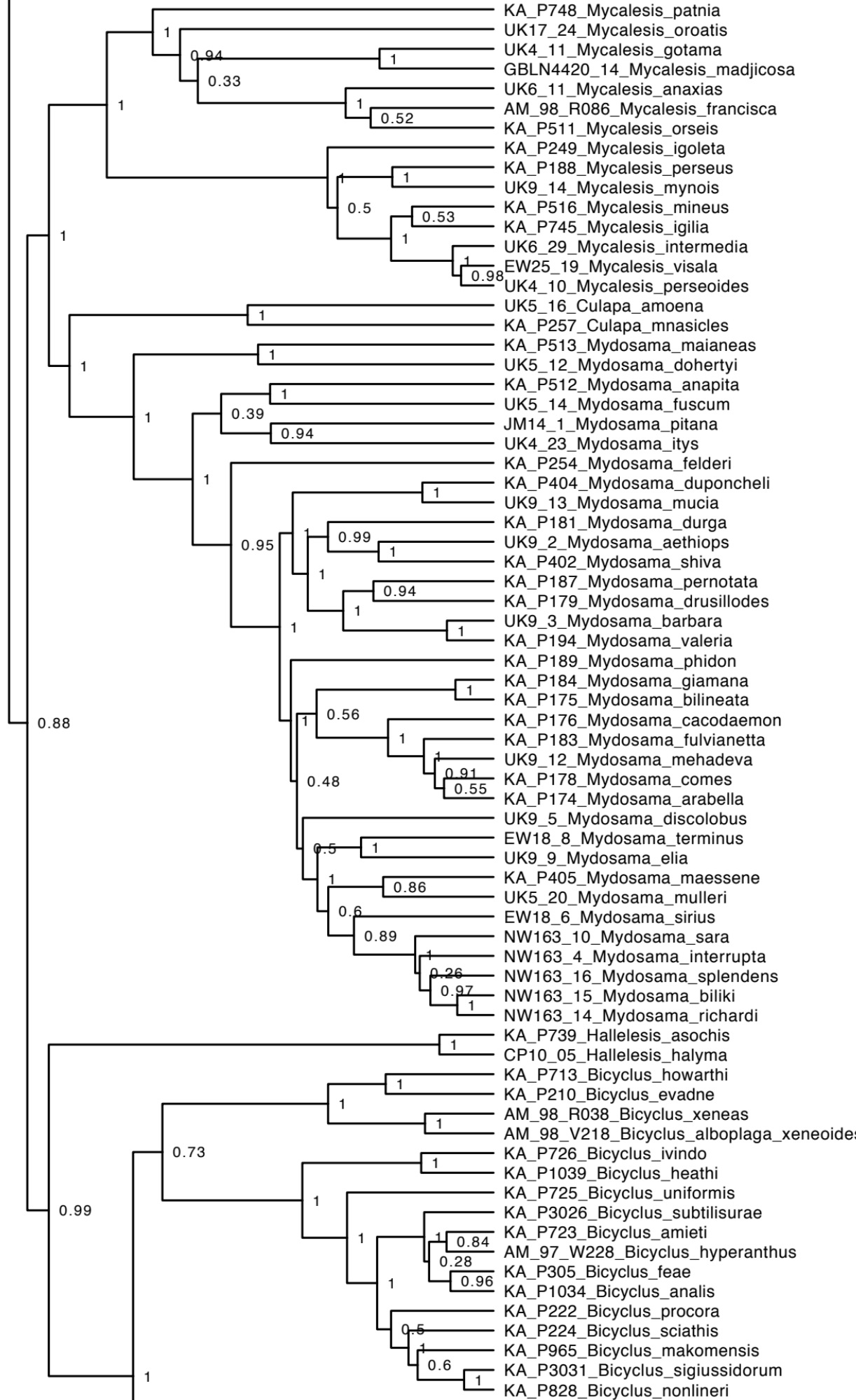
KA_P748_Mycalesis_patnia
UK17_24_Mycalesis_oroatis
UK4_11_Mycalesis_gotama
GBLN4420_14_Mycalesis_madjicosa
UK6_11_Mycalesis_anaxias
AM_98_R086_Mycalesis_francisca
KA_P511_Mycalesis_orseis
KA_P249_Mycalesis_igoleta
KA_P188_Mycalesis_perseus
UK9_14_Mycalesis_mynois
KA_P516_Mycalesis_mineus
KA_P745_Mycalesis_igilia
UK6_29_Mycalesis_intermedia
EW25_19_Mycalesis_visala
UK4_10_Mycalesis_perseoides
UK5_16_Culapa_amoena
KA_P257_Culapa_mnasicles
KA_P513_Mydosama_maianeas
UK5_12_Mydosama_dohertyi
KA_P512_Mydosama_anapita
UK5_14_Mydosama_fuscum
JM14_1_Mydosama_pitana
UK4_23_Mydosama_itys
KA_P254_Mydosama_felderi
KA_P404_Mydosama_duponcheli
UK9_13_Mydosama_mucia
KA_P181_Mydosama_durga
UK9_2_Mydosama_aethiops
KA_P402_Mydosama_shiva
KA_P187_Mydosama_pernotata
KA_P179_Mydosama_drusillodes
UK9_3_Mydosama_barbara
KA_P194_Mydosama_valeria
KA_P189_Mydosama_phidon
KA_P184_Mydosama_giamana
KA_P175_Mydosama_bilineata
KA_P176_Mydosama_cacodaemon
KA_P183_Mydosama_fulvianetta
UK9_12_Mydosama_mehadeva
KA_P178_Mydosama_comes
KA_P174_Mydosama_arabella
UK9_5_Mydosama_discolobus
EW18_8_Mydosama_terminus
UK9_9_Mydosama_elia
KA_P405_Mydosama_maessene
UK5_20_Mydosama_mulleri
EW18_6_Mydosama_sirius
NW163_10_Mydosama_sara
NW163_4_Mydosama_interrupta
NW163_16_Mydosama_splendens
NW163_15_Mydosama_biliki
NW163_14_Mydosama_richardi
KA_P739_Hallelesis_asochis
CP10_05_Hallelesis_halyma
KA_P713_Bicyclus_howarthi
KA_P210_Bicyclus_evadne
AM_98_R038_Bicyclus_xeneas
AM_98_V218_Bicyclus_alboplaga_xeneoides
KA_P726_Bicyclus_ivindo
KA_P1039_Bicyclus_heathi
KA_P725_Bicyclus_uniformis
KA_P3026_Bicyclus_subtilisurae
KA_P723_Bicyclus_amieti
AM_97_W228_Bicyclus_hyperanthus
KA_P305_Bicyclus_feae
KA_P1034_Bicyclus_analis
KA_P222_Bicyclus_procora
KA_P224_Bicyclus_sciathis
KA_P965_Bicyclus_makomensis
KA_P3031_Bicyclus_sigiussidorum
KA_P828_Bicyclus_nonlineri

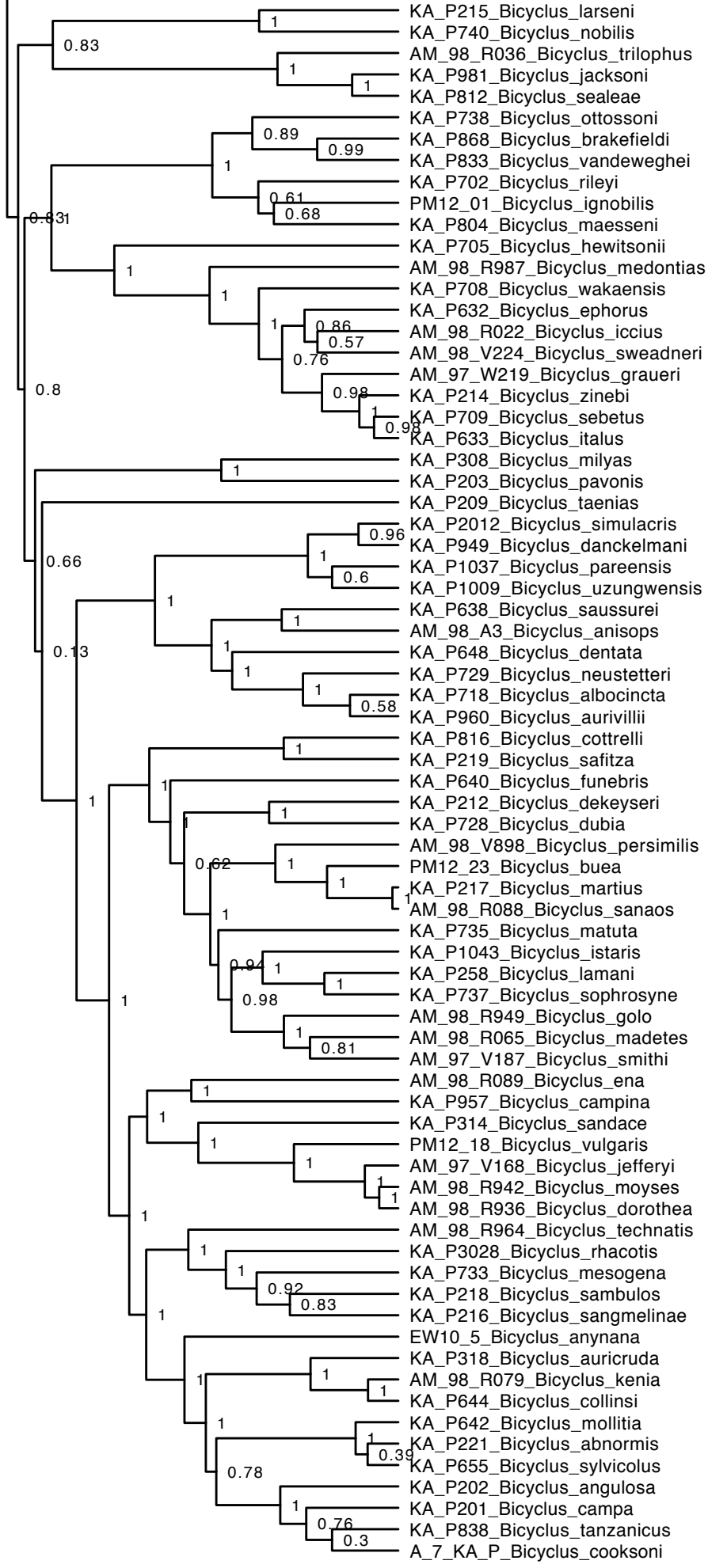
KA_P215_Bicyclus_larseni
KA_P740_Bicyclus_nobilis
AM_98_R036_Bicyclus_trilophus
KA_P981_Bicyclus_jacksoni
KA_P812_Bicyclus_sealeae
KA_P738_Bicyclus_ottossoni
KA_P868_Bicyclus_brakefieldi
KA_P833_Bicyclus_vandeweghei
KA_P702_Bicyclus_rileyi
PM12_01_Bicyclus_ignobilis
KA_P804_Bicyclus_maesseni
KA_P705_Bicyclus_hewitsonii
AM_98_R987_Bicyclus_medontias
KA_P708_Bicyclus_wakaensis
KA_P632_Bicyclus_ephorus
AM_98_R022_Bicyclus_iccius
AM_98_V224_Bicyclus_sweadneri
AM_97_W219_Bicyclus_graueri
KA_P214_Bicyclus_zinebi
KA_P709_Bicyclus_sebetus
KA_P633_Bicyclus_italus
KA_P308_Bicyclus_milyas
KA_P203_Bicyclus_pavonis
KA_P209_Bicyclus_taenias
KA_P2012_Bicyclus_simulacris
KA_P949_Bicyclus_danckelmani
KA_P1037_Bicyclus_pareensis
KA_P1009_Bicyclus_uzungwensis
KA_P638_Bicyclus_saussurei
AM_98_A3_Bicyclus_anisops
KA_P648_Bicyclus_dentata
KA_P729_Bicyclus_neustetteri
KA_P718_Bicyclus_albocincta
KA_P960_Bicyclus_aurivillii
KA_P816_Bicyclus_cottrelli
KA_P219_Bicyclus_safitza
KA_P640_Bicyclus_funebris
KA_P212_Bicyclus_dekeyseri
KA_P728_Bicyclus_dubia
AM_98_V898_Bicyclus_persimilis
PM12_23_Bicyclus_buea
KA_P217_Bicyclus_martius
AM_98_R088_Bicyclus_sanaos
KA_P735_Bicyclus_matuta
KA_P1043_Bicyclus_istaris
KA_P258_Bicyclus_lamani
KA_P737_Bicyclus_sophrosyne
AM_98_R949_Bicyclus_golo
AM_98_R065_Bicyclus_madetes
AM_97_V187_Bicyclus_smithi
AM_98_R089_Bicyclus_ena
KA_P957_Bicyclus_campina
KA_P314_Bicyclus_sandace
PM12_18_Bicyclus_vulgaris
AM_97_V168_Bicyclus_jefferyi
AM_98_R942_Bicyclus_moyses
AM_98_R936_Bicyclus_dorothea
AM_98_R964_Bicyclus_technatis
KA_P3028_Bicyclus_rhacotis
KA_P733_Bicyclus_mesogena
KA_P218_Bicyclus_sambulos
KA_P216_Bicyclus_sangmelinae
EW10_5_Bicyclus_anynana
KA_P318_Bicyclus_auricruda
AM_98_R079_Bicyclus_kenia
KA_P644_Bicyclus_collinsi
KA_P642_Bicyclus_mollitia
KA_P221_Bicyclus_abnormis
KA_P655_Bicyclus_sylvicolus
KA_P202_Bicyclus_angulosa
KA_P201_Bicyclus_campa
KA_P838_Bicyclus_tanzanicus
A_7_KA_P_Bicyclus_cooksoni

Supplementary Figure 2. 12. (page before). Maximum clade credibility tree for the Satyrinae group II subclade from BEAST. Posterior probabilities are indicated at the nodes.

m) Nymphalinae

Dataset – The dataset for the Nymphalinae consisted of 359 taxa to which two outgroups were added: *Chitoria ulupi* (Apaturinae), *Marpesia eleuchea* (Cyrestinae).

Partition Finder – Partition Finder identified 13 subsets.

Subset #	Substitution model	Gene fragments and codon positions
Subset 1	GTR+I+G	GAPDH_pos1, IDH_pos1, ArgKin_pos1, wingless_pos1, MDH_pos1, CAD_pos1
Subset 2	TRN+I+G	RpS5_pos2, MDH_pos2, CAD_pos2, DDC_pos2, ArgKin_pos2, IDH_pos2
Subset 3	GTR+I+G	ArgKin_pos3, DDC_pos3
Subset 4	HKY+I+G	CAD_pos3, MDH_pos3
Subset 5	GTR+I+G	COI-begin_pos3, COI-end_pos3
Subset 6	TRN+I+G	COI-begin_pos1
Subset 7	GTR+I+G	COI-begin_pos2, COI-end_pos2
Subset 8	TRN+I+G	COI-end_pos1
Subset 9	K80+I+G	wingless_pos2, DDC_pos1
Subset 10	GTR+I+G	wingless_pos3, EF1a_pos3
Subset 11	TRN+I+G	RpS5_pos1, EF1a_pos1, RpS2_pos1
Subset 12	JC+I+G	EF1a_pos2, GAPDH_pos2, RpS2_pos2
Subset 13	GTR+I+G	RpS5_pos3, IDH_pos3, RpS2_pos3, GAPDH_pos3

BEAST analysis – After multiple attempts to modify priors, MCMC runs did not converge. Hence, we decided to fix the topology. We performed an analysis with IQtree to search for the best topology. The topology was then enforced in our BEAST analysis and we only estimated the relative branch lengths. We used one molecular clock per subset identified by Partition Finder and obtained good mixing and convergence. We used a birth-death tree prior. We performed two runs of 60 million generations, sampling trees and parameters every 60000 generations.

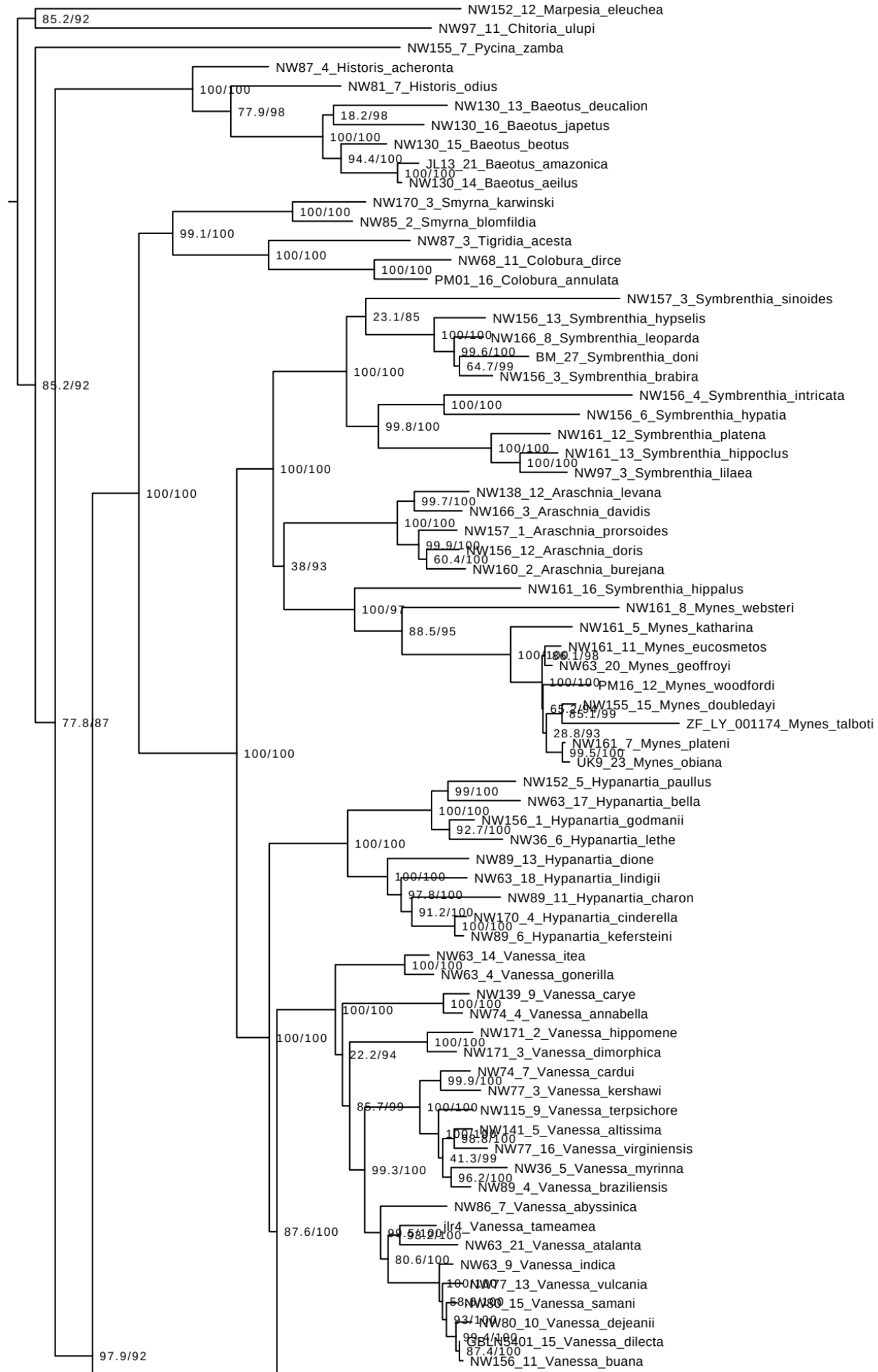
NW152_12_Marpesia_eleuchea
85.2/92
NW97_11_Chitoria_ulupi
NW155_7_Pycina_zamba
NW87_4_Historis_acheronta
100/100
NW81_7_Historis_odius
77.9/98
NW130_13_Baeotus_deucalion
18.2/98
NW130_16_Baeotus_japetus
100/100
NW130_15_Baeotus_beotus
94.4/100
JL13_21_Baeotus_amazonica
100/100
NW130_14_Baeotus_aeilus
NW170_3_Smyrna_karwinski
100/100
NW85_2_Smyrna_blomfildia
99.1/100
NW87_3_Tigridia_acesta
100/100
NW68_11_Colobura_dirce
100/100
PM01_16_Colobura_annulata
NW157_3_Symbrenthia_sinoides
23.1/85
NW156_13_Symbrenthia_hypselis
100/100
NW166_8_Symbrenthia_leoparda
99.6/100
BM_27_Symbrenthia_doni
64.7/99
NW156_3_Symbrenthia_brabira
100/100
85.2/92
NW156_4_Symbrenthia_intricata
100/100
NW156_6_Symbrenthia_hypatia
99.8/100
NW161_12_Symbrenthia_platena
100/100
NW161_13_Symbrenthia_hippoclus
100/100
NW97_3_Symbrenthia_lilaea
100/100
NW138_12_Araschnia_levana
99.7/100
NW166_3_Araschnia_davidis
100/100
NW157_1_Araschnia_prorsoides
99.9/100
NW156_12_Araschnia_doris
60.4/100
NW160_2_Araschnia_burejana
38/93
NW161_16_Symbrenthia_hippalus
100/97
NW161_8_Mynes_websteri
88.5/95
NW161_5_Mynes_katharina
NW161_11_Mynes_eucosmetos
100/100
NW63_20_Mynes_geoffroyi
100/100
PM16_12_Mynes_woodfordi
NW155_15_Mynes_doubledayi
85.1/99
ZF_LY_001174_Mynes_talboti
28.8/93
NW161_7_Mynes_plateni
99.5/100
UK9_23_Mynes_obiana
77.8/87
100/100
NW152_5_Hypanartia_paullus
99/100
NW63_17_Hypanartia_bella
100/100
NW156_1_Hypanartia_godmanii
92.7/100
NW36_6_Hypanartia_lethe
100/100
NW89_13_Hypanartia_dione
100/100
NW63_18_Hypanartia_lindigii
97.8/100
NW89_11_Hypanartia_charon
91.2/100
NW170_4_Hypanartia_cinderella
100/100
NW89_6_Hypanartia_kefersteini
NW63_14_Vanessa_itea
100/100
NW63_4_Vanessa_gonerilla
NW139_9_Vanessa_carye
100/100
100/100
NW74_4_Vanessa_annabella
NW171_2_Vanessa_hippomene
100/100
100/100
22.2/94
NW171_3_Vanessa_dimorphica
NW74_7_Vanessa_cardui
99.9/100
NW77_3_Vanessa_kershawi
85.7/99
100/100
NW115_9_Vanessa_terpsichore
NW141_5_Vanessa_altissima
96.8/100
NW77_16_Vanessa_virginiensis
41.3/99
99.3/100
NW36_5_Vanessa_myrinna
96.2/100
NW89_4_Vanessa_braziliensis
NW86_7_Vanessa_abyssinica
87.6/100
jlr4_Vanessa_tameamea
98.2/100
NW63_21_Vanessa_atalanta
80.6/100
NW63_9_Vanessa_indica
100/100
NW77_13_Vanessa_vulcania
58/100
NW80_15_Vanessa_samani
93/100
NW80_10_Vanessa_dejeanii
99.4/100
GBLN5401_15_Vanessa_dilecta
87.4/100
NW156_11_Vanessa_buana
97.9/92

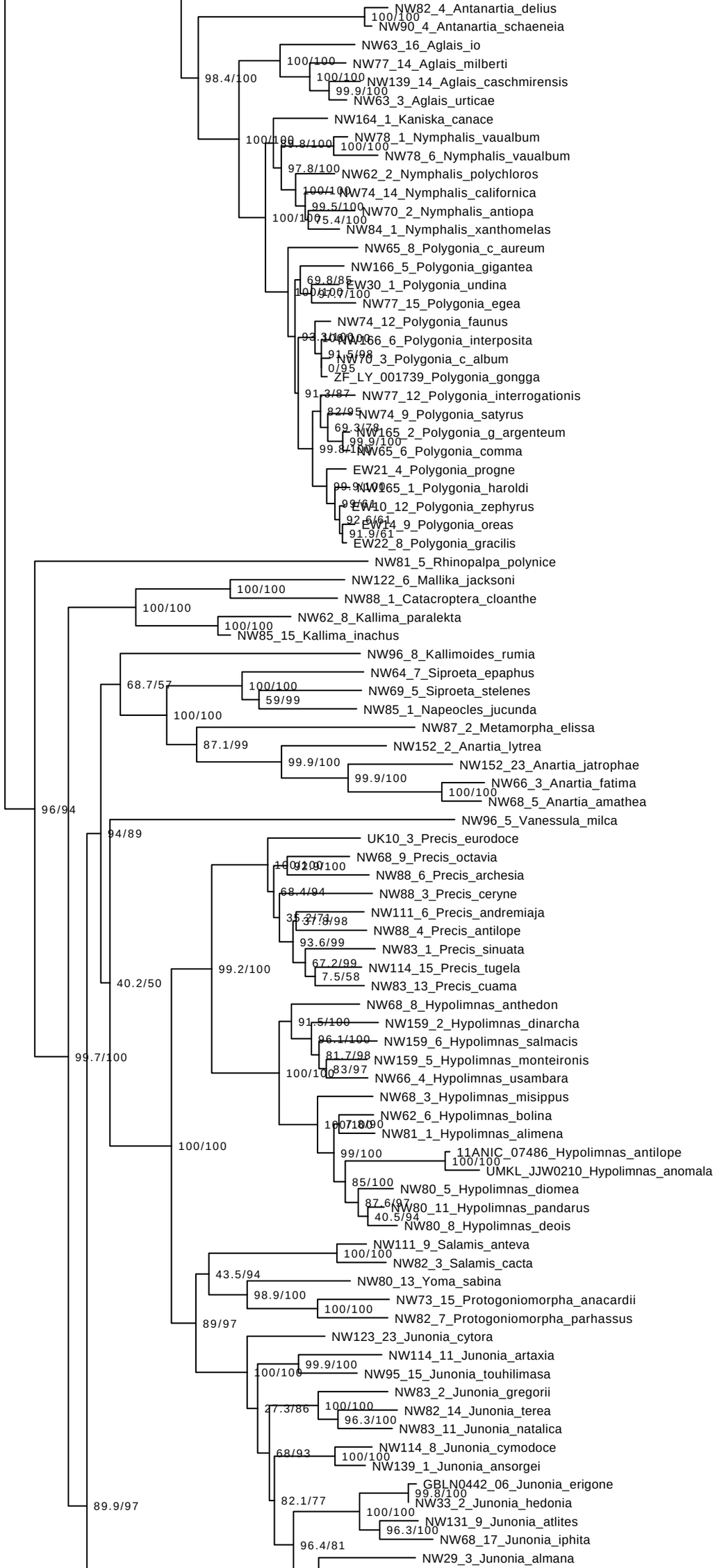
NW82_4_Antanartia_delius
100/100
NW90_4_Antanartia_schaeneia
NW63_16_Aglais_io
100/100
NW77_14_Aglais_milberti
98.4/100
100/100
NW139_14_Aglais_caschmirensis
99.9/100
NW63_3_Aglais_urticae
NW164_1_Kaniska_canace
100/100
NW78_1_Nymphalis_vaualbum
100/100
NW78_6_Nymphalis_vaualbum
97.8/100
NW62_2_Nymphalis_polychloros
100/100
NW74_14_Nymphalis_californica
99.5/100
NW70_2_Nymphalis_antiopa
100/100
NW84_1_Nymphalis_xanthomelas
NW65_8_Polygonia_c_aureum
NW166_5_Polygonia_gigantea
69.8/85
EW30_1_Polygonia_undina
100/100
NW77_15_Polygonia_egea
NW74_12_Polygonia_faunus
NW166_6_Polygonia_interposita
91.5/98
NW70_3_Polygonia_c_album
0/95
ZF_LY_001739_Polygonia_gongga
91.3/87
NW77_12_Polygonia_interrogationis
82/95
NW74_9_Polygonia_satyrus
69.3/78
NW165_2_Polygonia_g_argenteum
99.9/100
99.8/100
NW65_6_Polygonia_comma
EW21_4_Polygonia_progne
99.9/100
NW165_1_Polygonia_haroldi
99/61
EW10_12_Polygonia_zephyrus
92.6/61
EW14_9_Polygonia_oreas
91.9/61
EW22_8_Polygonia_gracilis
NW81_5_Rhinopalpa_polynice
NW122_6_Mallika_jacksoni
100/100
NW88_1_Catacroptera_cloanthe
100/100
NW62_8_Kallima_paralekta
100/100
NW85_15_Kallima_inachus
NW96_8_Kallimoides_rumia
NW64_7_Siproeta_epaphus
68.7/57
100/100
NW69_5_Siproeta_stelenes
59/99
NW85_1_Napeocles_jucunda
100/100
NW87_2_Metamorpha_elissa
87.1/99
NW152_2_Anartia_lytrea
99.9/100
NW152_23_Anartia_jatrophae
99.9/100
NW66_3_Anartia_fatima
100/100
NW68_5_Anartia_amathea
96/94
NW96_5_Vanessula_milca
94/89
UK10_3_Precis_eurodoce
NW68_9_Precis_octavia
100/100
92.9/100
NW88_6_Precis_archesia
68.4/94
NW88_3_Precis_ceryne
NW111_6_Precis_andremiaja
35.2/71
37.8/98
NW88_4_Precis_antilope
93.6/99
NW83_1_Precis_sinuata
67.2/99
NW114_15_Precis_tugela
7.5/58
NW83_13_Precis_cuama
99.2/100
40.2/50
NW68_8_Hypolimnas_anthedon
91.5/100
NW159_2_Hypolimnas_dinarcha
96.1/100
NW159_6_Hypolimnas_salmacis
81.7/98
NW159_5_Hypolimnas_monteironis
83/97
NW66_4_Hypolimnas_usambara
100/100
99.7/100
NW68_3_Hypolimnas_misippus
NW62_6_Hypolimnas_bolina
100/100
NW81_1_Hypolimnas_alimena
100/100
99/100
11ANIC_07486_Hypolimnas_antilope
100/100
UMKL_JJW0210_Hypolimnas_anomala
85/100
NW80_5_Hypolimnas_diomea
87.6/97
NW80_11_Hypolimnas_pandarus
40.5/94
NW80_8_Hypolimnas_deois
NW111_9_Salamis_anteva
100/100
NW82_3_Salamis_cacta
43.5/94
NW80_13_Yoma_sabina
98.9/100
NW73_15_Protogoniomorpha_anacardii
100/100
NW82_7_Protogoniomorpha_parhassus
89/97
NW123_23_Junonia_cytora
NW114_11_Junonia_artaxia
99.9/100
100/100
NW95_15_Junonia_touhilimasa
NW83_2_Junonia_gregorii
27.3/86
100/100
NW82_14_Junonia_terea
96.3/100
NW83_11_Junonia_natalica
68/93
NW114_8_Junonia_cymodoce
100/100
NW139_1_Junonia_ansorgei
GBLN0442_06_Junonia_erigone
99.8/100
82.1/77
NW33_2_Junonia_hedonia
100/100
NW131_9_Junonia_atlites
96.3/100
NW68_17_Junonia_iphita
89.9/97
96.4/81
NW29_3_Junonia_almana

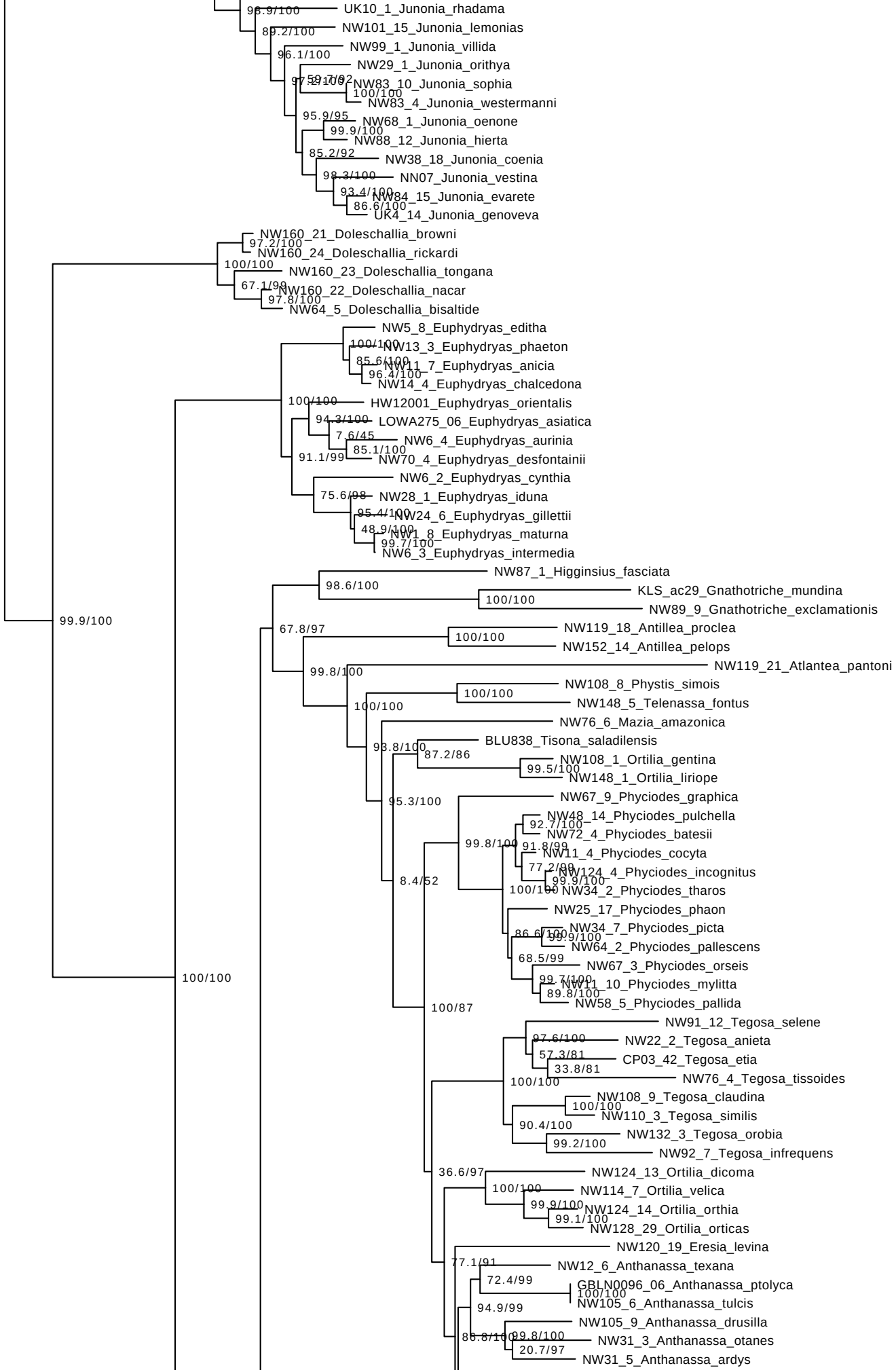
96.9/100
UK10_1_Junonia_rhadama
89.2/100
NW101_15_Junonia_lemonias
96.1/100
NW99_1_Junonia_villida
NW29_1_Junonia_orithya
97.2/100
59.7/92
NW83_10_Junonia_sophia
100/100
NW83_4_Junonia_westermanni
95.9/95
NW68_1_Junonia_oenone
99.9/100
NW88_12_Junonia_hierta
85.2/92
NW38_18_Junonia_coenia
98.3/100
NN07_Junonia_vestina
93.4/100
NW84_15_Junonia_evarete
86.6/100
UK4_14_Junonia_genoveva
NW160_21_Doleschallia_browni
97.2/100
NW160_24_Doleschallia_rickardi
100/100
NW160_23_Doleschallia_tongana
67.1/98
NW160_22_Doleschallia_nacar
97.8/100
NW64_5_Doleschallia_bisaltide
NW5_8_Euphydryas_editha
100/100
NW13_3_Euphydryas_phaeton
85.6/100
NW11_7_Euphydryas_anicia
96.4/100
NW14_4_Euphydryas_chalcedona
100/100
HW12001_Euphydryas_orientalis
94.3/100
LOWA275_06_Euphydryas_asiatica
7.6/45
NW6_4_Euphydryas_aurinia
85.1/100
91.1/99
NW70_4_Euphydryas_desfontainii
NW6_2_Euphydryas_cynthia
75.6/98
NW28_1_Euphydryas_iduna
95.4/100
NW24_6_Euphydryas_gillettii
48.9/100
NW1_8_Euphydryas_maturna
99.7/100
NW6_3_Euphydryas_intermedia
NW87_1_Higginsius_fasciata
98.6/100
KLS_ac29_Gnathotriche_mundina
100/100
NW89_9_Gnathotriche_exclamationis
99.9/100
67.8/97
NW119_18_Antillea_proclea
100/100
NW152_14_Antillea_pelops
NW119_21_Atlantea_pantoni
99.8/100
NW108_8_Phystis_simois
100/100
NW148_5_Telenassa_fontus
100/100
NW76_6_Mazia_amazonica
BLU838_Tisona_saladilensis
98.8/100
87.2/86
NW108_1_Ortilia_gentina
99.5/100
NW148_1_Ortilia_liriope
95.3/100
NW67_9_Phyciodes_graphica
NW48_14_Phyciodes_pulchella
92.7/100
NW72_4_Phyciodes_batesii
99.8/100
91.8/99
NW11_4_Phyciodes_cocyta
77.2/99
NW124_4_Phyciodes_incognitus
99.9/100
8.4/52
100/100
NW34_2_Phyciodes_tharos
NW25_17_Phyciodes_phaon
NW34_7_Phyciodes_picta
86.6/100
99.9/100
NW64_2_Phyciodes_pallescens
68.5/99
NW67_3_Phyciodes_orseis
100/100
99.7/100
NW11_10_Phyciodes_mylitta
89.8/100
NW58_5_Phyciodes_pallida
100/87
NW91_12_Tegosa_selene
97.6/100
NW22_2_Tegosa_anieta
57.3/81
CP03_42_Tegosa_etia
33.8/81
NW76_4_Tegosa_tissoides
100/100
NW108_9_Tegosa_claudina
100/100
NW110_3_Tegosa_similis
90.4/100
NW132_3_Tegosa_orobia
99.2/100
NW92_7_Tegosa_infrequens
36.6/97
NW124_13_Ortilia_dicoma
100/100
NW114_7_Ortilia_velica
99.9/100
NW124_14_Ortilia_orthia
99.1/100
NW128_29_Ortilia_orticas
NW120_19_Eresia_levina
77.1/91
NW12_6_Anthanassa_texana
72.4/99
GBLN0096_06_Anthanassa_ptolyca
100/100
NW105_6_Anthanassa_tulcis
94.9/99
NW105_9_Anthanassa_drusilla
86.8/100
99.8/100
NW31_3_Anthanassa_otanes
20.7/97
NW31_5_Anthanassa_ardys

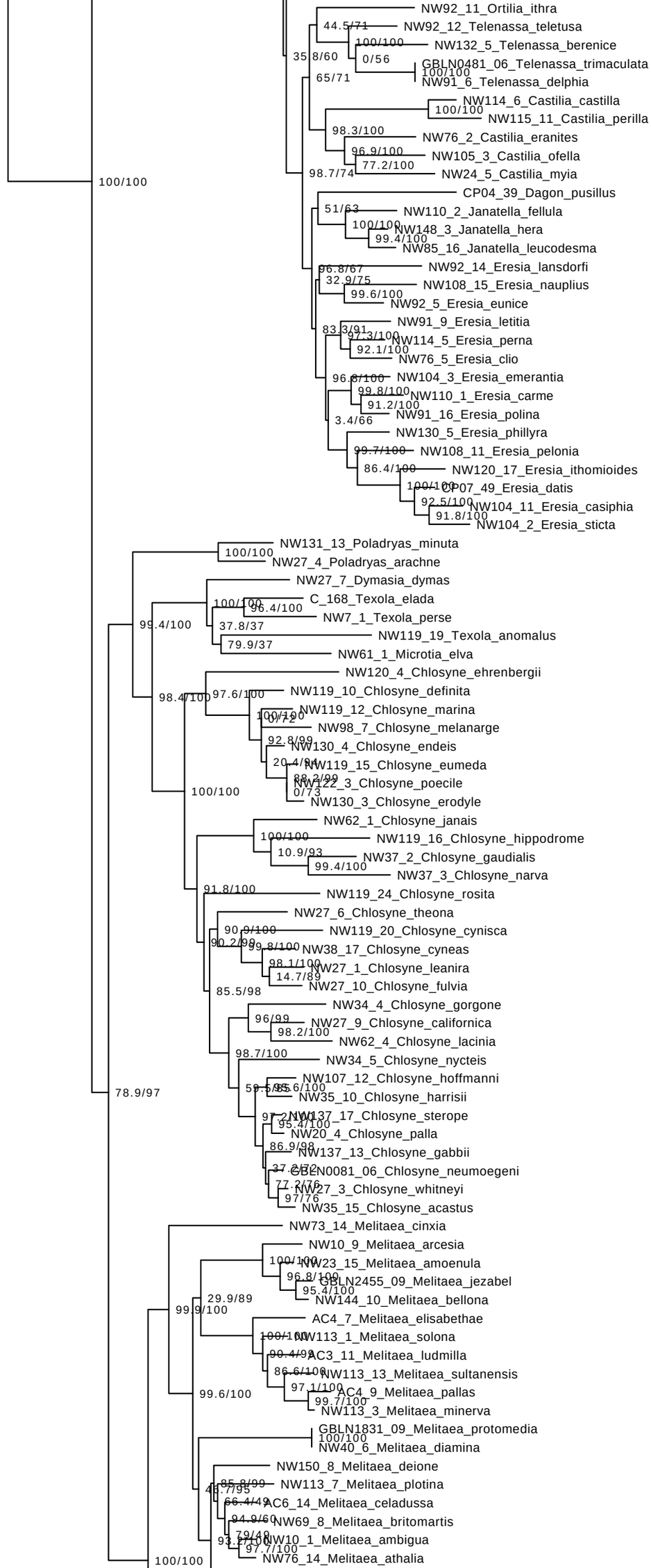
NW92_11_Ortilia_ithra
44.5/71
NW92_12_Telenassa_teletusa
100/100
NW132_5_Telenassa_berenice
35.8/60
0/56
GBLN0481_06_Telenassa_trimaculata
100/100
65/71
NW91_6_Telenassa_delphia
NW114_6_Castilia_castilla
100/100
NW115_11_Castilia_perilla
98.3/100
NW76_2_Castilia_eranites
96.9/100
NW105_3_Castilia_ofella
77.2/100
98.7/74
NW24_5_Castilia_myia
100/100
CP04_39_Dagon_pusillus
51/63
NW110_2_Janatella_fellula
100/100
NW148_3_Janatella_hera
99.4/100
NW85_16_Janatella_leucodesma
96.8/67
NW92_14_Eresia_lansdorfi
32.9/75
NW108_15_Eresia_nauplius
99.6/100
NW92_5_Eresia_eunice
NW91_9_Eresia_letitia
83.3/91
97.3/100
NW114_5_Eresia_perna
92.1/100
NW76_5_Eresia_clio
96.6/100
NW104_3_Eresia_emerantia
99.8/100
NW110_1_Eresia_carme
91.2/100
3.4/66
NW91_16_Eresia_polina
NW130_5_Eresia_phillyra
99.7/100
NW108_11_Eresia_pelonia
86.4/100
NW120_17_Eresia_ithomioides
100/100
CP07_49_Eresia_datis
92.5/100
NW104_11_Eresia_casiphia
91.8/100
NW104_2_Eresia_sticta
NW131_13_Poladryas_minuta
100/100
NW27_4_Poladryas_arachne
NW27_7_Dymasia_dymas
100/100
C_168_Texola_elada
96.4/100
NW7_1_Texola_perse
99.4/100
37.8/37
NW119_19_Texola_anomalus
79.9/37
NW61_1_Microtia_elva
NW120_4_Chlosyne_ehrenbergii
97.6/100
NW119_10_Chlosyne_definita
98.4/100
NW119_12_Chlosyne_marina
100/100
0/72
NW98_7_Chlosyne_melanarge
92.8/99
NW130_4_Chlosyne_endeis
20.4/94
NW119_15_Chlosyne_eumeda
88.2/99
NW122_3_Chlosyne_poecile
0/73
100/100
NW130_3_Chlosyne_erodyle
NW62_1_Chlosyne_janais
100/100
NW119_16_Chlosyne_hippodrome
10.9/93
NW37_2_Chlosyne_gaudialis
99.4/100
NW37_3_Chlosyne_narva
91.8/100
NW119_24_Chlosyne_rosita
NW27_6_Chlosyne_theona
90.9/100
NW119_20_Chlosyne_cynisca
90.2/99
99.8/100
NW38_17_Chlosyne_cyneas
98.1/100
NW27_1_Chlosyne_leanira
14.7/89
NW27_10_Chlosyne_fulvia
85.5/98
NW34_4_Chlosyne_gorgone
96/99
NW27_9_Chlosyne_californica
98.2/100
NW62_4_Chlosyne_lacinia
98.7/100
NW34_5_Chlosyne_nycteis
NW107_12_Chlosyne_hoffmanni
59.5/85
95.6/100
NW35_10_Chlosyne_harrisii
97.2/100
NW137_17_Chlosyne_sterope
95.4/100
NW20_4_Chlosyne_palla
86.9/98
NW137_13_Chlosyne_gabbii
37.2/72
GBLN0081_06_Chlosyne_neumoegeni
77.2/76
NW27_3_Chlosyne_whitneyi
97/76
NW35_15_Chlosyne_acastus
78.9/97
NW73_14_Melitaea_cinxia
NW10_9_Melitaea_arcesia
100/100
NW23_15_Melitaea_amoenula
96.8/100
GBLN2455_09_Melitaea_jezabel
95.4/100
NW144_10_Melitaea_bellona
29.9/89
99.9/100
AC4_7_Melitaea_elisabethae
100/100
NW113_1_Melitaea_solona
99.4/99
AC3_11_Melitaea_ludmilla
86.6/100
NW113_13_Melitaea_sultanensis
97.1/100
AC4_9_Melitaea_pallas
99.6/100
99.7/100
NW113_3_Melitaea_minerva
GBLN1831_09_Melitaea_protomedia
100/100
NW40_6_Melitaea_diamina
NW150_8_Melitaea_deione
85.8/99
NW113_7_Melitaea_plotina
46.7/95
66.4/49
AC6_14_Melitaea_celadussa
94.9/60
NW69_8_Melitaea_britomartis
79/48
93.2/100
NW10_1_Melitaea_ambigua
97.7/100
NW76_14_Melitaea_athalia
100/100

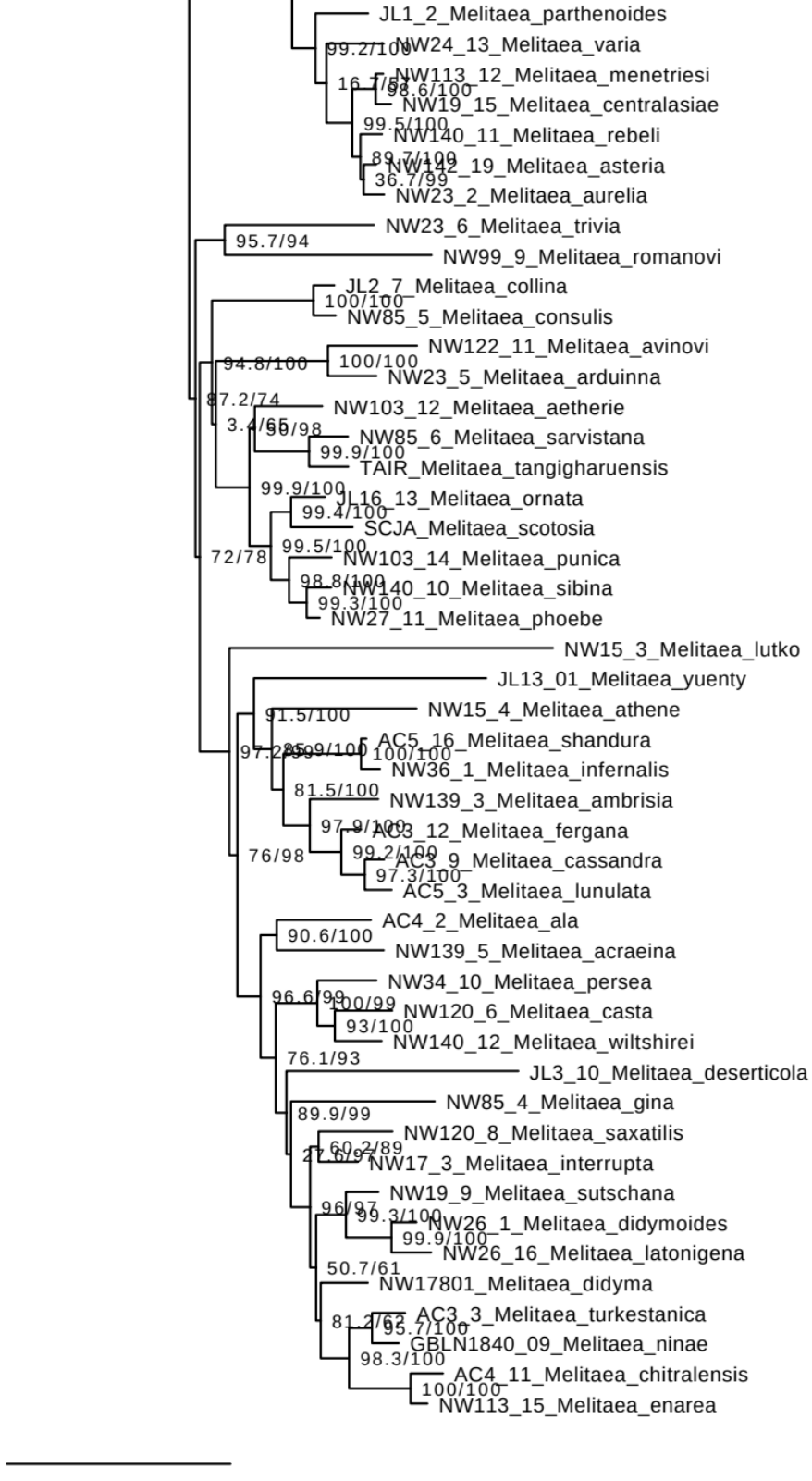
JL1_2_Melitaea_parthenoides
99.2/100
NW24_13_Melitaea_varia
NW113_12_Melitaea_menetriesi
98.6/100
NW19_15_Melitaea_centralasiae
99.5/100
NW140_11_Melitaea_rebeli
89.7/100
NW142_19_Melitaea_asteria
36.7/99
NW23_2_Melitaea_aurelia
NW23_6_Melitaea_trivia
95.7/94
NW99_9_Melitaea_romanovi
JL2_7_Melitaea_collina
100/100
NW85_5_Melitaea_consulis
NW122_11_Melitaea_avinovi
94.8/100
100/100
NW23_5_Melitaea_arduinna
87.2/74
NW103_12_Melitaea_aetherie
3.4/65
NW85_6_Melitaea_sarvistana
99.9/100
TAIR_Melitaea_tangigharuensis
99.9/100
JL16_13_Melitaea_ornata
99.4/100
SCJA_Melitaea_scotosia
99.5/100
72/78
NW103_14_Melitaea_punica
98.8/100
NW140_10_Melitaea_sibina
99.3/100
NW27_11_Melitaea_phoebe
NW15_3_Melitaea_lutko
JL13_01_Melitaea_yuenty
91.5/100
NW15_4_Melitaea_athene
AC5_16_Melitaea_shandura
100/100
NW36_1_Melitaea_infernalis
81.5/100
NW139_3_Melitaea_ambrisia
AC3_12_Melitaea_fergana
76/98
99.2/100
AC3_9_Melitaea_cassandra
97.3/100
AC5_3_Melitaea_lunulata
AC4_2_Melitaea_ala
90.6/100
NW139_5_Melitaea_acraeina
NW34_10_Melitaea_persea
100/99
NW120_6_Melitaea_casta
93/100
NW140_12_Melitaea_wiltshirei
76.1/93
JL3_10_Melitaea_deserticola
NW85_4_Melitaea_gina
89.9/99
NW120_8_Melitaea_saxatilis
60.2/89
NW17_3_Melitaea_interrupta
NW19_9_Melitaea_sutschana
96/97
99.3/100
NW26_1_Melitaea_didymoides
99.9/100
NW26_16_Melitaea_latonigena
50.7/61
NW17801_Melitaea_didyma
AC3_3_Melitaea_turkestanica
95.7/100
GBLN1840_09_Melitaea_ninae
98.3/100
AC4_11_Melitaea_chitralensis
100/100
NW113_15_Melitaea_enarea
0.04

Supplementary Figure 2. 13. (page before). Consensus tree for the Nymphalinae subclade from IQtree. Numbers at the nodes are SH-aLRT support (%) / ultrafast bootstrap support (%).

n) Pseudergolinae

Dataset – The dataset for the Pseudergolinae consisted of 6 taxa to which two outgroups were added: *Heliconius melpomene* (Satyrinae), *Marpesia eleuchea* (Cyrestinae).

Partition Finder – Partition Finder identified 10 subsets.

Subset #	Substitution model	Gene fragments and codon positions
Subset 1	TRN+G	wingless_pos1, DDC_pos1, ArgKin_pos1, MDH_pos1, RpS5_pos1, IDH_pos1, GAPDH_pos1, EF1a_pos1, RpS2_pos1
Subset 2	HKY+I	DDC_pos2, CAD_pos2, IDH_pos2, RpS5_pos2, ArgKin_pos2, EF1a_pos2, MDH_pos2, GAPDH_pos2
Subset 3	GTR+G	wingless_pos3, ArgKin_pos3, EF1a_pos3
Subset 4	TRN+G	CAD_pos3
Subset 5	GTR	CAD_pos1
Subset 6	HKY+G	COI-begin_pos3, COI-end_pos3
Subset 7	TRN+I	COI-begin_pos1, COI-end_pos1
Subset 8	HKY	COI-begin_pos2, COI-end_pos2
Subset 9	GTR+G	RpS5_pos3, DDC_pos3, RpS2_pos3, GAPDH_pos3, MDH_pos3, IDH_pos3
Subset 10	JC	RpS2_pos2, wingless_pos2

BEAST analysis – In order to improve the quality of our runs, we replaced the default priors for rates of substitutions by uniform prior ranging between 0 and 10 for the following cases: sub3.cg, sub5.at, cg, gt and sub9.ac, cg, gt. We used a single molecular clock linked across all partitions to obtain good mixing and convergence. We used a birth-death tree prior. We performed two runs of 30 million generations, sampling trees and parameters every 3000 generations.

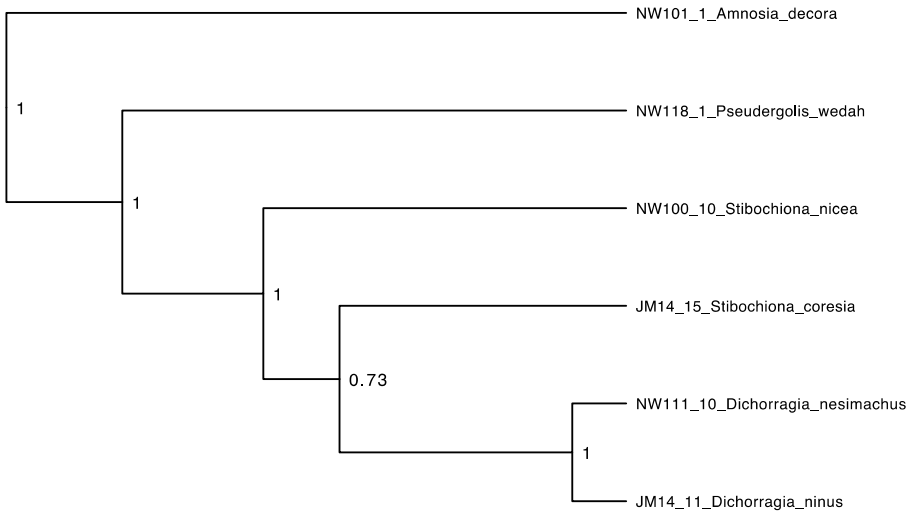

Supplementary Figure 2. 14. Maximum clade credibility tree for the Pseudergolinae subclade from BEAST. Posterior probabilities are indicated at the nodes.

o) Satyrini

Dataset – The dataset for the Satyrini consisted of 560 taxa to which two outgroups were added: *Amathusia phidippus* (Satyrinae), *Bicyclus anynana* (Satyrinae).

Partition Finder – Partition Finder identified 17 subsets.

Subset #	Substitution model	Gene fragments and codon positions
Subset 1	TRN+I+G	ArgKin_pos1, RpS2_pos1, EF1a_pos1, MDH_pos1
Subset 2	HKY+I+G	ArgKin_pos2, RpS5_pos2, MDH_pos2, GAPDH_pos2, IDH_pos2
Subset 3	GTR+I+G	ArgKin_pos3, wingless_pos3
Subset 4	HKY+I+G	CAD_pos3, MDH_pos3
Subset 5	GTR+I+G	GAPDH_pos1, RpS5_pos1, CAD_pos1, IDH_pos1
Subset 6	HKY+I+G	DDC_pos2, CAD_pos2, COI-end_pos2
Subset 7	GTR+I+G	COI-begin_pos3
Subset 8	SYM+I	COI-begin_pos1
Subset 9	GTR+I+G	COI-begin_pos2
Subset 10	GTR+G	COI-end_pos3
Subset 11	HKY+I+G	COI-end_pos1
Subset 12	K80+G	DDC_pos3, RpS2_pos3
Subset 13	SYM+G	DDC_pos1, wingless_pos1
Subset 14	GTR+I+G	EF1a_pos3
Subset 15	K80+I+G	RpS2_pos2, wingless_pos2, EF1a_pos2
Subset 16	GTR+I+G	GAPDH_pos3
Subset 17	GTR+I+G	IDH_pos3, RpS5_pos3

BEAST analysis – We used a single molecular clock linked across all partitions to obtain good mixing and convergence. We used one molecular clock per subset identified by Partition

Finder and obtained good mixing and convergence. We used a birth-death tree prior. We performed two runs of 100 million generations, sampling trees and parameters every 10000 generations.

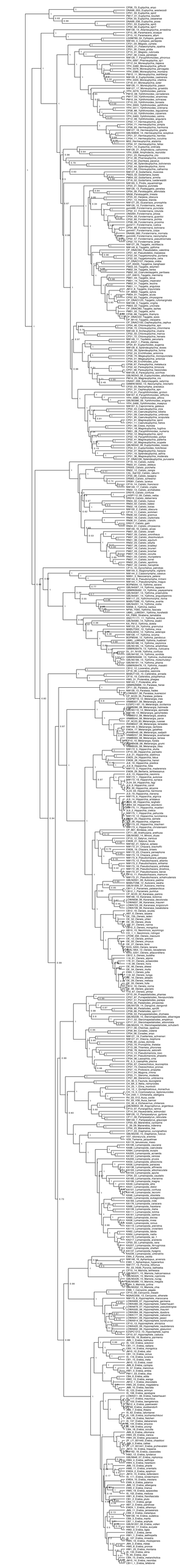
CP06_73_Euptychia_enyo
DNA96_005_Euptychia_westwoodi
CP01_33_Euptychia_spn2
PM17_01_Euptychia_boulleti
CP04_55_Euptychia_cesarense
DNA99_036_Euptychia_picea
CP01_53_Euptychia_spn5
CP02_58_Euptychia_spn7
NW136_14_Atlanteuptychia_ernestina
CP15_08_Paramacera_xicaque
CP15_10_Paramacera_allyni
LGSM789_04_Cyllopsis_gemma
NW165_3_Cyllopsis_pertepida
CP21_04_Megisto_cymela
EW25_21_Palaeonympha_opalina
CP01_30_Cissia_proba
CP15_01_Megisto_rubricata
CP07_58_Cissia_penelope
NW126_7_Paryphthimoides_phronius
YPH_0097_Pharneuptychia_sp1
CP12_04_Moneuptychia_itapeva
YPH_0480_Moneuptychia_giffordi
YPH_0376_Moneuptychia_pervagata
YPH_0385_Moneuptychia_montana
PM10_11_Moneuptychia_wahlbergi
NW126_9_Euptychoides_castrensis
YPH_0435_Moneuptychia_vitellina
CP18_01_Moneuptychia_soter
NW126_11_Moneuptychia_paeon
NW127_17_Moneuptychia_griseldis
YPH_0279_Yphthimoides_patricia
PM10_08_Yphthimoides_cerradensis
PM17_03_Yphthimoides_straminea
PM10_04_Yphthimoides_ochracea
CP10_03_Yphthimoides_borasta
YPH_0003_Yphthimoides_yphthima
YPH_0411_Yphthimoides_ordinaria
CP08_88_Yphthimoides_leguialimai
CP10_02_Yphthimoides_cipoensis
YPH_0463_Yphthimoides_celmis
CP12_08_Yphthimoides_angularis
CP02_17_Hermeuptychia_spn5
CP04_71_Hermeuptychia_pimpla
CP06_93_Hermeuptychia_harmonia
NW127_16_Hermeuptychia_gisella
GBLN3849_14_Hermeuptychia_sosybius
CP01_37_Hermeuptychia_hermes
CP04_11_Hermeuptychia_cuculina
M02_Hermeuptychia_atalanta
CP04_37_Hermeuptychia_fallax
CP01_14_Euptychia_ordinata
NW126_21_Amphidecta_calliomma
YPH_0306_Amphidecta_reynoldsi
CP01_23_Rareuptychia_clio
CP12_06_Pharneuptychia_innocentia
CP14_02_Zischkaia_pacarus
CP02_48_Splendeuptychia_boliviensis
CP02_44_Splendeuptychia_itonis
CP01_68_Chloreuptychia_catharina
NW127_8_Godartiana_muscosa
PM23_02_Godartiana_byses
PM04_02_Godartiana_armilla
CP16_02_Godartiana_luederwaldti
NW165_5_Pindis_squamistriga
CP23_21_Sepona_punctata
NW126_13_Posttaygetis_penelea
CP04_09_Parataygetis_albinotata
NN58_Parataygetis_lineata
CP23_22_Harjesia_obscura
CP01_13_Harjesia_blanda
NW127_20_Guaianaza_pronophila
NW126_10_Forsterinaria_necys
gsm488_Forsterinaria_punctata
CP02_51_Forsterinaria_rotunda
UN0264_Forsterinaria_pilosa
CP04_59_Forsterinaria_guaniloi
CP02_60_Forsterinaria_pichita
CP08_09_Forsterinaria_proxima
gsm211_Forsterinaria_rustica
CP04_88_Forsterinaria_boliviana
gsm447_Forsterinaria_coipa
DNA99_060_Forsterinaria_inornata
gsm449_Forsterinaria_neonympha
CP02_57_Forsterinaria_pseudinornata
CP02_72_Forsterinaria_antje
NW127_28_Taygetis_rectifascia
NW149_8_Taygetis_ypthima
CP_DNACI64_Pseudodebis_valentina
CP01_42_Pseudodebis_marpessa
CP22_04_Taygetomorpha_puritana
CP22_02_Taygetomorpha_celia
CP_DNACI107_Harjesia_oreba
LEP_00435_Taygetina_banghaasi
PM03_03_Taygetis_weymeri
PM02_04_Taygetis_kerea
PM02_02_Coeruleotaygetis_peribaea
LEP_04615_Taygetis_mermeria
PM01_04_Taygetis_larua
PM01_14_Taygetis_imperator
PM02_01_Taygetis_leuctra
PM01_11_Taygetis_angulosa
JM12_8_Taygetis_tripunctata
CP_M302_Taygetis_sylvia
PM04_01_Taygetis_acuta
CP02_63_Taygetis_chrysogone
CP_DNACI125_Taygetis_rufomarginata
NW108_3_Taygetis_virgilia
PM03_02_Taygetis_uncinata
CP_DNACI83_Taygetis_laches
PM01_02_Taygetis_echo
CP06_68_Taygetis_thamyra
CP_DNACI22_Taygetis_sosis
CP_M110_Taygetis_cleopatra
CP_DNACI100_Cepheuptychia_cephus
CP04_46_Chloreuptychia_spn
CP06_72_Chloreuptychia_chlorimene
NW149_9_Archeuptychia_cluena
CP02_50_Chloreuptychia_marica
CP01_72_Chloreuptychia_herseis
NW149_11_Taydebis_peculiaris
BR_AVLF_1_Prenda_clarissa
CP04_81_Euptychoides_eugenia
NW126_8_Splendeuptychia_doxes
CP02_39_Splendeuptychia_furina
CP02_24_Erichthodes_antonina
CP06_70_Megeuptychia_monopunctata
CP05_01_Megeuptychia_antonoe
CP04_65_Erichthodes_julia
CP06_67_Pareuptychia_metaleuca
CP02_42_Pareuptychia_binocula
CP01_66_Pareuptychia_hesionides
NW126_6_Pareuptychia_ocirrhoe
GBLN0343_06_Euptychoides_albofasciata
PM14_25_Magneuptychia_iris
DNA97_006_Satyrotaygetis_satyrina
GBMIN18050_13_Neonympha_mitchellii
CP22_03_Neonympha_areolatus
CP01_31_Cepheuptychia_spn
CP10_01_Paryphthimoides_grimon
NW167_6_Paryphthimoides_difficilis
YPH_0080_Yphthimoides_affinis
GBLN0386_06_Yphthimoides_erigone
YPH_0466_Yphthimoides_maepius
NW167_5_Capronnieria_galesus
CP02_43_Caeruleuptychia_ziza
CP01_55_Caeruleuptychia_lobelia
CP01_09_Caeruleuptychia_umbrosa
CP01_95_Caeruleuptychia_scopulata
CP01_91_Magneuptychia_spn4
CP01_11_Caeruleuptychia_helios
CP01_58_Cissia_myncea
CP01_18_Magneuptychia_fugitiva
PM01_28_Paryphthimoides_numeria
CP02_12_Magneuptychia_spn2
CP02_19_Paryphthimoides_poltys
CP02_41_Magneuptychia_pallema
CP01_32_Magneuptychia_ocypete
GBLN0342_06_Euptychoides_nossis
CP04_51_Euptychoides_hotchkissi
CP02_27_Magneuptychia_harpyia
CP01_19_Splendeuptychia_ashna
CP01_36_Magneuptychia_moderata
CP_DNACI39_Splendeuptychia_purusana
CP19_10_Calisto_nubila
RN03_01_Calisto_eleleus
DR003_Calisto_pulchella
RN02_12_Calisto_zangis
CAL_Sat102_Calisto_raburni
CP20_08_Calisto_tasajera
DR063_Calisto_schwartzi
DR081_Calisto_lyceius
CP19_14_Calisto_franciscoi
NW149_17_Calisto_crypta
RN02_14_Calisto_archebates
DR016_Calisto_confusa
LHISP112_09_Calisto_neiba
DR019_Calisto_debarriera
RN04_02_Calisto_hysius
RN03_02_Calisto_batesi
RN02_18_Calisto_loxias
NW150_2_Calisto_obscura
CP19_11_Calisto_sommeri
RN06_02_Calisto_grannus
RN02_16_Calisto_clydoniata
RN06_01_Calisto_clenchi
DR017_Calisto_galii
RN04_01_Calisto_chrysaoros
NW149_16_Calisto_arcas
PM07_02_Calisto_israeli
PM07_05_Calisto_smintheus
PM07_20_Calisto_dissimulatum
RN01_06_Calisto_aquilum
RN02_23_Calisto_sibylla
PM07_26_Calisto_bradleyi
PM07_16_Calisto_bruneri
PM07_03_Calisto_brochei
PM07_18_Calisto_occulta
RN01_05_Calisto_muripetens
PM07_11_Calisto_torrei
RN02_25_Calisto_apollinis
PM07_22_Calisto_herophile
CP15_16_Gyrocheilus_patrobas
NW144_5_Stygionympha_vigilans
NW144_2_Cassionympha_cassius
NW91_5_Neocoenyra_petersi
NW144_6_Pseudonympha_trimeni
NW144_1_Pseudonympha_magus
BOPM344_12_Ypthima_savara
GBLN4567_14_Ypthima_tappana
GBMIN39492_13_Ypthima_yayeyamana
GBLN4587_14_Ypthima_praenubila
GBLN4561_14_Ypthima_angustipennis
NW117_23_Ypthimomorpha_itonia
MABUT088_10_Ypthima_avanta
GBLN4201_14_Ypthima_zodia
NW98_5_Ypthima_baldus
NP95_Y065_Ypthima_fasciata
UMKL_JJW0341_Ypthima_horsfieldii
KA_P869_Strabena_tamatabia
ANICT1171_11_Ypthima_arctous
GBLN4580_14_Ypthima_esakii
KA_P612_Ypthima_doleta
NW153_24_Ypthima_grannulus
MABUT002_10_Ypthima_inica
GBGL8244_12_Ypthima_asterope
NW106_17_Ypthima_loryma
BOPM346_12_Ypthima_pandocus
UMKL_JJW0463_Ypthima_huebneri
GBLN5188_14_Ypthima_ceylonica
GBLN5185_14_Ypthima_amphithea
GBMIN39479_13_Ypthima_riukiuana
DL_01_N109_Ypthima_confusa
GBLN4192_14_Ypthima_sordida
GBMIN39498_13_Ypthima_multistriata
GBLN5189_14_Ypthima_motschulskyi
GBLN4191_14_Ypthima_phania
GBMIN39478_13_Ypthima_masakii
CB12_12_Loxerebia_phyllis
CP16_06_Loxerebia_saxicola
MABUT103_10_Callerebia_annada
CP16_19_Callerebia_polyphemus
HW5_31_Proterebia_phegea
NW143_7_Proterebia_afra
GBMIN26896_13_Paralasa_herse
CP11_05_Paralasa_styx
NW139_13_Paralasa_hades
LOWA057_06_Paralasa_kusnezovi
CP_AC23_35_Paralasa_jordana
EZSPM716_12_Melanargia_ines
VNMB307_08_Melanargia_arge
EZSPC1187_10_Melanargia_occitanica
VNMB286_08_Melanargia_halimede
GBLN5110_14_Melanargia_epimede
NW148_13_Melanargia_ganymedes
VNMB312_08_Melanargia_asiatica
VNMB544_08_Melanargia_parce
CP_AC23_83_Melanargia_russiae
IRANB447_08_Melanargia_teneates
NW149_3_Melanargia_lachesis
EW24_17_Melanargia_galathea
IRANB440_08_Melanargia_sadjadii
VNMB257_08_Melanargia_evartianae
VNMB393_08_Melanargia_larissa
CP10_10_Melanargia_hylata
IRANB438_08_Melanargia_grumi
VNMB535_08_Melanargia_titea
NW172_5_Hipparchia_stulta
CP10_06_Hipparchia_parisatis
JL9_21_Hipparchia_statilinus
EW25_24_Hipparchia_fatua
EW26_26_Hipparchia_hansii
JL8_19_Hipparchia_pisidice
JL9_6_Hipparchia_fidia
NW172_3_Hipparchia_maderensis
EW26_29_Berberia_lambessanus
JL9_13_Hipparchia_neomiris
NW173_1_Hipparchia_autonoe
NW172_19_Hipparchia_syriaca
JL24_04_Hipparchia_fagi
JL9_9_Hipparchia_caroli
JL8_30_Hipparchia_alcyone
JL24_03_Hipparchia_hermione
JL9_19_Hipparchia_mersina
NW175_6_Hipparchia_algirica
JL9_14_Hipparchia_aristaeus
JL24_06_Hipparchia_leighebi
JL24_02_Hipparchia_sbordonii
NW175_11_Hipparchia_muelleri
JL9_2_Hipparchia_cretica
NW175_1_Hipparchia_pellucida
NW172_12_Hipparchia_turcmenica
EW24_25_Hipparchia_semele
JL8_28_Hipparchia_volgensis
NW173_22_Hipparchia_blachieri
NW173_4_Hipparchia_christenseni
CP_B01_Brintesia_circe
CP11_06_Arethusana_arethusa
GBLN4362_14_Minois_dryas
CP10_12_Satyrus_iranicus
EW26_21_Satyrus_ferula
NW162_21_Satyrus_actaea
NW172_21_Chazara_bischoffii
EW26_19_Chazara_briseis
NW172_23_Chazara_persephone
NW173_13_Chazara_prieuri
NW173_6_Pseudochazara_pelopea
NW173_12_Pseudochazara_atlantis
NW173_2_Pseudochazara_williamsi
NW173_19_Pseudochazara_anthelea
NW172_26_Pseudochazara_droshica_
NW173_27_Pseudochazara_beroe
CP10_11_Pseudochazara_mamurra
NW173_21_Pseudochazara_schahrudensis
GBLN2001_09_Aulocera_padma
MABUT298_12_Aulocera_swaha
GBLN1009_07_Aulocera_merlina
CB11_2_Paroeneis_palaearcticus
CB12_1_Paroeneis_pumilus
CP_AC23_32_Karanasa_pamira
NW166_10_Karanasa_bolorica
LOWA638_06_Karanasa_decolorata
LOWA637_06_Karanasa_maureri
LOWA723_06_Karanasa_kirgizorum
LOWA728_06_Karanasa_kasakstana
CB12_19_Oeneis_sculda
AB7_6_Oeneis_tarpeia
OE_72b_Oeneis_lederi
OE_52_Oeneis_uhleri
OE_35_Oeneis_diluta
166_01_Oeneis_nanna
CB10_3_Oeneis_mongolica
AB10_15_Neominois_wyomingo
CD_1_1_Neominois_ridingsii
LPOW_050_Oeneis_macounii
OE_12_Oeneis_ammon
OE_02_Oeneis_chryxus
OE_27_Oeneis_bore
NVG_5203_Oeneis_tanana
BPAL1854_12_Oeneis_nevadensis
NVG_5201_Oeneis_altacordillera
CB12_5_Oeneis_buddha
119_61_Oeneis_alpina
176_01_Oeneis_actaeoides
116_06_Oeneis_hora
OE_46_Oeneis_elwesi
OE_54_Oeneis_mulla
EW4_1_Oeneis_jutta
119_42_Oeneis_tunga
OE_16_Oeneis_aktashi
OE_29_Oeneis_melissa
OE_55_Oeneis_fulla
CB12_16_Oeneis_norna
OE_48_Oeneis_glacialis
119_67_Oeneis_philipi
CP10_04_Praepedaliodes_phanias
CP07_87_Punapedaliodes_flavopunctata
CP07_51_Parapedaliodes_parepa
CP03_35_Pedaliodes_phrasiclea
GBLN4729_14_Dangond_dangondi
CP09_90_Pedaliodes_spn26
CP09_66_Pedaliodes_spn117
CP09_53_Panyapedaliodes_drymaea
GBLN5228_15_Steromapedaliodes_albarregas
CP17_02_Steromapedaliodes_empetrus
CP17_01_Steromapedaliodes_albonotata
GBLN5224_15_Steromapedaliodes_schuberti
CP17_06_Cheimas_opalinus
CP09_84_Corades_cistene
CP04_06_Corades_enyo
NW127_19_Foetterleia_schreineri
NW127_21_Eteona_tisiphone
CP06_94_Junea_dorinda
CP03_70_Pronophila_thelebe
CP13_08_Thiemeia_phoronea
CP09_78_Apexacuta_astoreth
CP13_13_Pseudomaniola_loxo
CP04_01_Pseudomaniola_phaselis
CP04_36_Lasiophila_cirta
PE_5_5_Lasiophila_piscina
CP04_67_Oxeoschistus_leucospilos
CP07_73_Oxeoschistus_pronax
CP07_15_Proboscis_propylea
CP17_04_Mygona_irmina
CP03_71_Steroma_modesta
CP07_89_Steremnia_umbracina
CH_30_5_Faunula_leucoglene
CH_8A_2_Nelia_nemyroides
CH_25_1_Elina_montrolii
CH_12_1_Quilaphoetosus_monachus
CH_15_5_Cosmosatyrus_leptoneuroides
CH_24A_1_Chillanella_stelligera
RV_03_V13_Auca_coctei
RV_03_V39_Auca_barrosi
CH_30_4_Etcheverrius_chiliensis
GBLN0654_06_Argyrophorus_argenteus
CP13_07_Punargentus_lamna
CP14_04_Haywardella_edmondsii
NW126_12_Pampasatyrus_gyrtone
CP17_09_Pampasatyrus_reticulata
NW149_7_Pampasatyrus_glaucope
CP03_63_Manerebia_cyclopina
E_39_09_Manerebia_inderena
CP04_23_Manerebia_lisa
CP17_03_Diaphanos_curvignathos
GBLN5230_15_Diaphanos_fuscus
V37_Idioneurula_eremita
V29_Tamania_jacquelinae
KA119_Ianussiusa_maso
KA106_Lymanopoda_caucana
KA98_Lymanopoda_caeruleata
KA84_Lymanopoda_euopis
KA205_Lymanopoda_acraeida
KA181_Lymanopoda_venosa
KA200_Lymanopoda_prusia
KA54_Lymanopoda_albocincta
KA56_Lymanopoda_panacea
KA136_Lymanopoda_affineola
KA193_Lymanopoda_albomaculata
KA104_Lymanopoda_apulia
CP04_22_Lymanopoda_caudalis
KA160_Lymanopoda_marianna
KA199_Lymanopoda_magna
KA49_Lymanopoda_altis
KA31_Lymanopoda_dietzi
KA101_Lymanopoda_confusa
KA146_Lymanopoda_lecromi
KA46_Lymanopoda_obsoleta
KA85_Lymanopoda_eubagioides
KA184_Lymanopoda_inde
KA176_Lymanopoda_caracara
KA66_Lymanopoda_hazelana
KA139_Lymanopoda_melia
KA111_Lymanopoda_tolima
KA161_Lymanopoda_samius
KA60_Lymanopoda_excisa
KA58_Lymanopoda_nivea
KA95_Lymanopoda_ionius
KA110_Lymanopoda_pieridina
KA115_Lymanopoda_vivienteni
KA62_Lymanopoda_labda
KA64_Lymanopoda_nadia
KA170_Lymanopoda_sp_1
KA217_Lymanopoda_araneola
CP03_33_Lymanopoda_rana
KA207_Lymanopoda_ferruginosa
KA87_Lymanopoda_shefteli
KA137_Lymanopoda_hyagnis
KA226_Lymanopoda_umbratilis
EW4_2_Pyronia_cecilia
NW148_16_Aphantopus_arvensis
EW2_1_Aphantopus_hyperantus
NW177_13_Pyronia_tithonus
RV_03_H546_Pyronia_bathseba
CP10_14_Maniola_telmessia
GBLN5371_15_Maniola_halicarnassus
GBLN5325_15_Maniola_cypricola
GBLN5426_15_Maniola_nurag
GBLN5389_15_Maniola_megala
EW4_5_Maniola_jurtina
GBLN5352_15_Maniola_chia
EW8_1_Cercyonis_pegala
CP15_09_Cercyonis_meadii
NGNAC056_13_Cercyonis_sthenele
NW173_8_Hyponephele_maroccana
LOWA909_07_Hyponephele_germana
LOWA480_06_Hyponephele_haberhaueri
LOWA879_07_Hyponephele_pseudokirgisa
LOWA500_06_Hyponephele_maureri
LOWA364_06_Hyponephele_dysdora
LOWA177_06_Hyponephele_cadusina
LOWA041_06_Hyponephele_jasavi
LOWA914_08_Hyponephele_korshunovi
CP10_13_Hyponephele_shirazica
LOWA420_06_Hyponephele_naubidensis
LOWA632_06_Hyponephele_glasunovi
EZSPC1212_10_Hyponephele_lupina
CP10_07_Hyponephele_cadusia
NW156_18_Boeberia_parmenio
JM9_1_Erebia_kalmuka
IS_122_Erebia_sokolovi
CB1_11_Erebia_radians
CB3_14_Erebia_mongolica
JM10_10_Erebia_sibo
CB1_13_Erebia_ocnus
IS_116_Erebia_turanica
CB1_15_Erebia_meta
JM10_13_Erebia_rossii
JM9_8_Erebia_cyclopia
IS_57_Erebia_mancinus
HW1_4_Erebia_embla
PM11_03_Erebia_disa
CB4_6_Erebia_edda
HW2_13_Erebia_wanga
JM12_1_Erebia_discoidalis
HW5_20_Erebia_magdalena
JM9_10_Erebia_fasciata
IS_123_Erebia_erinnyn
IS_106_Erebia_epistygne
LOWA311_06_Erebia_haberhaueri
IS_117_Erebia_maurisius
IS_103_Erebia_tsengelensis
JM12_4_Erebia_pawlowskii
IS_60_Erebia_stubbendorfi
JM9_7_Erebia_theano
IS_62_Erebia_lafontainei
IS_126_Erebia_kozhantschikovi
JM8_16_Erebia_fletcheri
IS_137_Erebia_dabanensis
IS_144_Erebia_anyuica
IS_128_Erebia_youngi
CB4_18_Erebia_occulta
JM9_6_Erebia_ottomana
HW4_23_Erebia_iranica
HW4_25_Erebia_graucasica
ZF_LY_001440_Erebia_chastilovi
JM9_3_Erebia_callias
ZF_LY_001441_Erebia_przhevalskii
JM10_16_Erebia_hispania
NW162_18_Erebia_cassioides
HW2_12_Erebia_tyndarus
GBLN946_07_Erebia_niphonica
HW4_4_Erebia_aethiops
HW4_5_Erebia_hewitsoni
JM8_13_Erebia_pharte
HW6_11_Erebia_orientalis
EW24_2_Erebia_epiphron
JM10_15_Erebia_kefersteini
IS_111_Erebia_kindermanni
EW24_10_Erebia_meolans
EW9_4_Erebia_palarica
JM8_12_Erebia_albergana
EW9_2_Erebia_triarius
HW5_19_Erebia_epipsodea
IS_102_Erebia_medusa
HW1_6_Erebia_flavofasciata
CB1_2_Erebia_pluto
CB3_11_Erebia_gorge
AB7_2_Erebia_pandrose
EW24_1_Erebia_sthennyo
JM9_11_Erebia_jeniseiensis
CB9_2_Erebia_melampus
NW139_16_Erebia_sudetica
CB9_3_Erebia_manto
CB7_1_Erebia_eriphyle
GBLN1207_08_Erebia_vidleri
NW162_17_Erebia_euryale
HW2_3_Erebia_ligea
EW24_7_Erebia_oeme
HW1_1_Erebia_aethiopella
IS_107_Erebia_mnestra
HW5_10_Erebia_rhodopensis
JM4_3_Erebia_melas
HW5_8_Erebia_pronoe
HW1_25_Erebia_montana
IS_133_Erebia_stiria
IS_65_Erebia_styx
CB4_15_Erebia_melancholica
JM10_14_Erebia_neoridas
CB11_1_Erebia_lefebvrei

Supplementary Figure 2. 15. (page before). Maximum clade credibility tree for the Satyrini subclade from BEAST. Posterior probabilities are indicated at the nodes.

5 - Grafting procedure

We built a posterior distribution of grafted trees by randomly sampling trees from the posterior distributions of both the backbone and the subclades. For each grafted tree, we (1) randomly picked a backbone from the posterior distribution without replacement, (2) randomly picked a tree from the posterior distribution of each subclade without replacement, (3) removed the two outgroups in the subclade tree, (4) rescaled the subclade trees to the crown age of the subclades in the backbone, (5) removed all the taxa representing the subclades in the backbone but one, (6) rescaled the branch length of the remaining taxa to the length of the stem leading to the subclades, and (7) grafted the subclade trees onto the corresponding stem branches. We repeated this process for 1000 random trees. Finally, we used TreeAnnotator v. 1.8.3 [9] to summarize the tree topology with median node age and 95% credibility interval of each node. Outgroups were finally removed and the resulting tree was used for all subsequent analyses.

Supplementary Tree 1. Nymphalidae backbone tree inferred with RAxML and time-calibrated using BEAST, with mean posterior node ages and 95% credibility intervals summarized. Available at: https://doi.org/10.5281/zenodo.5463912.

Supplementary Tree 2. Maximum clade credibility tree of all Nymphalidae included in this study, with mean posterior node ages and 95% credibility intervals estimated from the posterior distribution of 1000 grafted trees (1000 subclades posterior trees combined with 1000 backbone posterior trees). Available at: https://doi.org/10.5281/zenodo.5463912.

Supplementary Methods 3 - Inference of biogeographic history

We performed a maximum-likelihood estimate of geographical range evolution using the Dispersal-Extinction-Cladogenesis (DEC) model [16] as implemented in the C++ version [17] and recently extended to handle large phylogenetic trees such as the Nymphalidae, be faster even with a large number of possible ranges, and include new features (DECX model, [18]). We ran the classical DEC model to estimate ancestral states at all nodes and the main dispersal events between the biogeographic regions. We designed a biogeographic model spanning the evolutionary history of Nymphalidae (Late Cretaceous). We assigned extant species to nine biogeographic regions: Western Nearctic, Eastern Nearctic, Western Palearctic, Eastern Palearctic, Neotropics, Afrotropics, India, Southeast Asia, and Australasia (Supplementary Data 1). We designed a time-stratified model in which both the adjacency matrices and dispersal matrices varied between time periods. Time was divided into five time periods: 100-80, 80-60, 60-30, 30-10, 10-0 million years to account for increasing or decreasing connectivity between biogeographic regions through time (Supplementary Table 4. 1. and Supplementary Table 4. 2.). We used the results of the full model (i.e., including both connectivity matrix and dispersal multipliers) for subsequent analyses, but we performed additional analyses with different models to test the effect of our choices on the ancestral-state estimation.

Supplementary Table 3. 1. Dispersal multipliers matrices for five time-intervals used for ancestral biogeographic state estimation using DECX. WN=Western Nearctic, EN=Eastern Nearctic, NT=Neotropic, WP=Western Palearctic, EN=Eastern Palearctic, AF=Afrotropic, MD=Madagascar, IN=India, SEA=South East Asia, AU=Australasia.

0 - 10 Myr	WN	EN	NT	WP	EP	AF	MD	IN	SEA	AU
WN	1	1	1	0.01	1	0	0	0	0.01	0.01
EN	1	1	1	0.1	0.01	0.01	0	0	0	0
NT	1	1	1	0.01	0.01	0.01	0	0	0	0.01
WP	0.01	0.1	0.01	1	1	1	0	1	0	0
EP	1	0.01	0.01	1	1	0.5	0	1	1	0.01
AF	0	0.01	0.01	1	0.5	1	1	0.5	0.5	0.01
MD	0	0	0	0	0	1	1	0.1	0.01	0.01
IN	0	0	0	1	1	0.5	0.1	1	1	0.01
SEA	0.01	0	0	0	1	0.5	0.01	1	1	1
AU	0.01	0	0.01	0	0.01	0.01	0.01	0.01	0.01	1

10 - 30 Myr	WN	EN	NT	WP	EP	AF	MD	IN	SEA	AU
WN	1	1	0.5	0.01	1	0	0	0	0.01	0.01
EN	1	1	0.5	0.1	0.01	0.01	0	0	0	0
NT	0.5	0.5	1	0.01	0.01	0.01	0	0	0	0.01
WP	0.01	0.1	0.01	1	1	0	0.1	0	0.01	0

EP	1	0.01	0.01	1	1	0.5	0	0.5	1	0.01
AF	0	0.01	0.01	0	0.5	1	1	0.5	0.5	0.01
MD	0	0	0	0.1	0	1	1	0.1	0.01	0.01
IN	0	0	0	0	0.5	0.5	0.1	1	0.5	0.01
SEA	0.01	0	0	0.01	1	0.5	0.01	0.5	1	0.5
AU	0.01	0	0.01	0	0.01	0.01	0.01	0.01	0.5	1

30 - 60 Myr	WN	EN	NT	WP	EP	AF	MD	IN	SEA	AU
WN	1	1	0.1	0.01	1	0	0	0	0.01	0.01
EN	1	1	0.1	0.5	0.01	0.01	0	0	0	0
NT	0.1	0.1	1	0.01	0.01	0.1	0	0	0.01	0.1
WP	0.01	0.5	0.01	1	0.5	1	0	0.1	0	0
EP	1	0.01	0.01	0.5	1	0.1	0	0.1	1	0.01
AF	0	0.01	0.1	1	0.1	1	1	0.1	0.1	0.01
MD	0	0	0	0	0	1	1	0.1	0.01	0.01
IN	0	0	0	0.1	0.1	0.1	0.1	1	0.1	0.01
SEA	0.01	0	0.01	0	1	0.1	0.01	0.1	1	0.1
AU	0.01	0	0.1	0	0.01	0.01	0.01	0.01	0.1	1

60 - 80 Myr	WN	EN	NT	WP	EP	AF	MD	IN	SEA	AU
WN	1	1	0.1	0.01	1	0	0	0	0.01	0.01
EN	1	1	0.1	0.5	0.01	0.01	0	0	0	0
NT	0.1	0.1	1	0.01	0	0.5	0	0	0.01	0.5
WP	0.01	0.5	0.01	1	0.5	1	0	0.01	0	0
EP	1	0.01	0	0.5	1	0	0	0.01	1	0
AF	0	0.01	0.5	1	0	1	1	0.5	0.01	0.01
MD	0	0	0	0	0	1	1	0.5	0.01	0.01
IN	0	0	0	0.01	0.01	0.5	0.5	1	0.1	0.01
SEA	0.01	0	0.01	0	1	0.01	0.01	0.1	1	0.01
AU	0.01	0	0.5	0	0	0.01	0.01	0.01	0.01	1

80 - 100 Myr	WN	EN	NT	WP	EP	AF	MD	IN	SEA	AU
WN	1	0.5	0.01	0	0.5	0	0	0	0.01	0
EN	0.5	1	0.01	1	0.1	0.01	0	0	0	0
NT	0.01	0.01	1	0.01	0	0.5	0	0	0	0.5
WP	0	1	0.01	1	0.5	0.5	0	0	0	0
EP	0.5	0.1	0	0.5	1	0	0	0	1	0
AF	0	0.01	0.5	0.5	0	1	1	1	0.01	0.01
MD	0	0	0	0	0	1	1	1	0	0.01
IN	0	0	0	0	0	1	1	1	0	0.5
SEA	0.01	0	0	0	1	0.01	0	0	1	0.01
AU	0	0	0.5	0	0	0.01	0.01	0.5	0.01	1

Supplementary Table 3. 2. Adjacency matrices for five time-intervals used for ancestral biogeographic state estimation using DECX. WN=Western Nearctic, EN=Eastern Nearctic, NT=Neotropic, WP=Western Palearctic, EN=Eastern Palearctic, AF=Afrotropic, MD=Madagascar, IN=India, SEA=South East Asia, AU=Australasia.

0 - 10 Myr	WN	EN	NT	WP	EP	AF	MD	IN	SEA	AU
WN	1	1	1	0	1	0	0	0	0	0
EN	1	1	1	1	0	0	0	0	0	0
NT	1	1	1	0	0	0	0	0	0	0
WP	0	1	0	1	1	1	0	1	0	0

EP	1	0	0	1	1	0	0	1	1	0
AF	0	0	0	1	0	1	1	1	0	0
MD	0	0	0	0	0	1	1	0	0	0
IN	0	0	0	1	1	1	0	1	1	0
SEA	0	0	0	0	1	0	0	1	1	1
AU	0	0	0	0	0	0	0	0	1	1

10 - 30 Myr	WN	EN	NT	WP	EP	AF	MD	IN	SEA	AU
WN	1	1	1	0	1	0	0	0	0	0
EN	1	1	1	1	0	0	0	0	0	0
NT	1	1	1	0	0	1	0	0	0	0
WP	0	1	0	1	1	1	0	1	0	0
EP	1	0	0	1	1	0	0	1	1	0
AF	0	0	1	1	0	1	1	1	0	0
MD	0	0	0	0	0	1	1	0	0	0
IN	0	0	0	1	1	1	0	1	1	0
SEA	0	0	0	0	1	0	0	1	1	1
AU	0	0	0	0	0	0	0	0	1	1

30 - 60 Myr	WN	EN	NT	WP	EP	AF	MD	IN	SEA	AU
WN	1	1	1	0	1	0	0	0	0	0
EN	1	1	1	1	0	0	0	0	0	0
NT	1	1	1	0	0	1	0	0	0	1
WP	0	1	0	1	1	1	0	0	0	0
EP	1	0	0	1	1	0	0	0	1	0
AF	0	0	1	1	0	1	1	1	1	0
MD	0	0	0	0	0	1	1	1	0	0
IN	0	0	0	0	0	1	1	1	1	0
SEA	0	0	0	0	1	1	0	1	1	1
AU	0	0	1	0	0	0	0	0	1	1

60 - 80 Myr	WN	EN	NT	WP	EP	AF	MD	IN	SEA	AU
WN	1	1	0	0	1	0	0	0	0	0
EN	1	1	0	1	0	0	0	0	0	0
NT	0	0	1	0	0	1	0	0	0	1
WP	0	1	0	1	1	1	0	0	0	0
EP	1	0	0	1	1	0	0	0	1	0
AF	0	0	1	1	0	1	1	1	0	0
MD	0	0	0	0	0	1	1	1	0	0
IN	0	0	0	0	0	1	1	1	0	0
SEA	0	0	0	0	1	0	0	0	1	0
AU	0	0	1	0	0	0	0	0	0	1

80 - 100 Myr	WN	EN	NT	WP	EP	AF	MD	IN	SEA	AU
WN	1	1	0	0	1	0	0	0	0	0
EN	1	1	0	1	1	0	0	0	0	0
NT	0	0	1	0	0	1	0	0	0	1
WP	0	1	0	1	1	1	0	0	0	0
EP	1	1	0	1	1	0	0	0	1	0
AF	0	0	1	1	0	1	1	1	0	1
MD	0	0	0	0	0	1	1	1	0	1
IN	0	0	0	0	0	1	1	1	0	1
SEA	0	0	0	0	1	0	0	0	1	0

AU	0	0	1	0	0	1	1	1	0	1

Supplementary Figure 3. 1. (next page) Historical biogeography estimated by DECX. Pie-charts at the nodes are marginal probabilities of each biogeographic area, i.e., the relative frequency of an area summed across all probable ranges. WN=Western Nearctic, EN=Eastern Nearctic, NT=Neotropic, WP=Wetern Palearctic, EN=Eastern Palearctic, AF=Afrotropic, MD=Madagascar, IN=India, SEA=South East Asia, AU=Australasia.

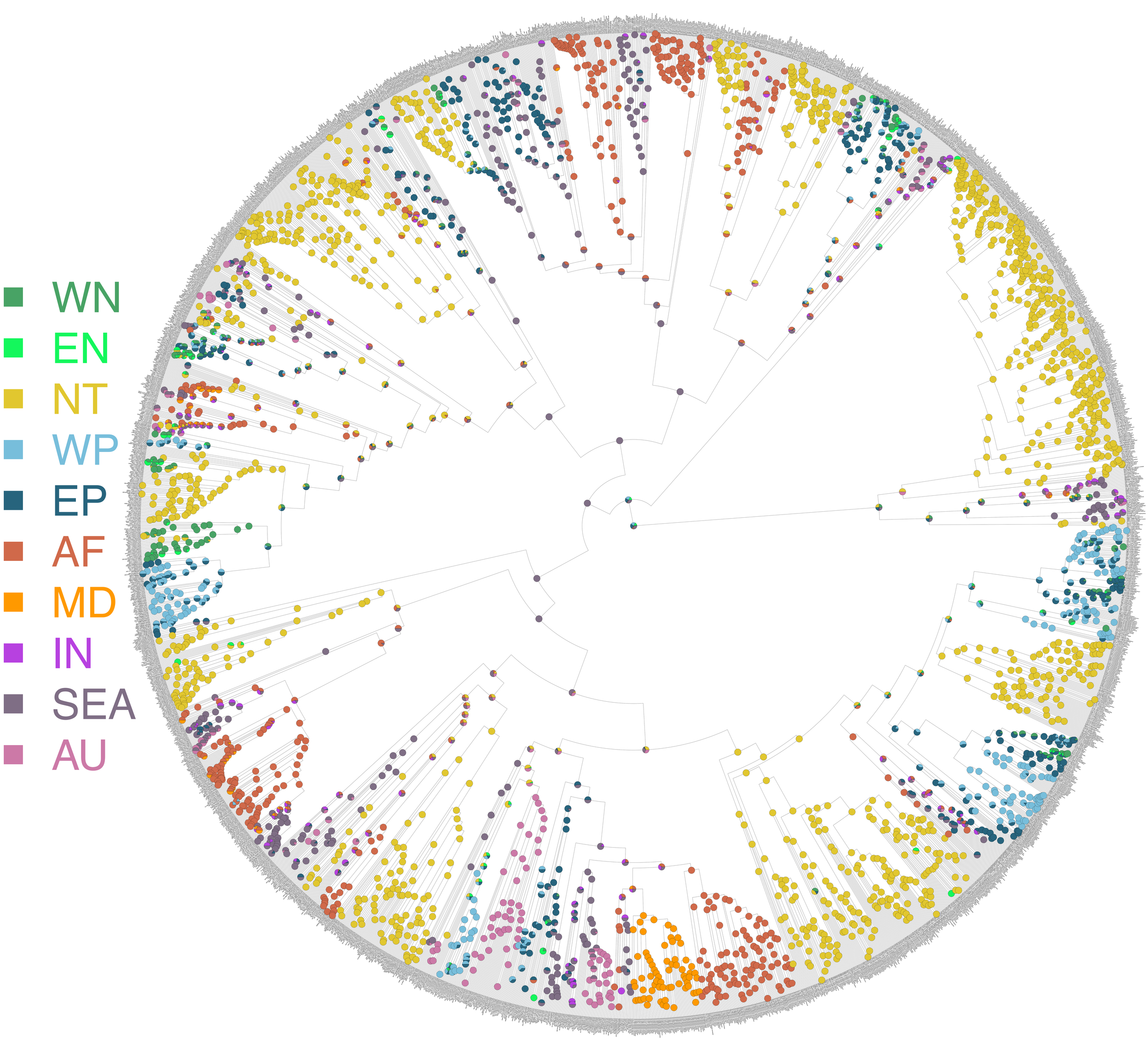
WN
EN
NT
WP
EP
AF
MD
IN
SEA
AU

Supplementary Methods 4 - Estimation of speciation and extinction rate

We estimated the temporal dynamics of speciation and extinction rates across our phylogeny using BAMM 2.5 [12–14]. We accounted for missing species by specifying the sampling fraction at the genus level. We used the R-package BAMMtools [13] to generate initial priors for speciation and extinction rates. We set the expected number of rate shifts (Poisson rate parameter) to 0.4 for our main analysis. Given the concerns about the sensitivity of BAMM to priors on posteriors ([15], but see [14]), we performed two additional BAMM analyses by setting the Poisson rate parameter to 0.2 (allowing fewer shifts) or 0.6 (allowing more shifts). All BAMM analyses ran 50 million generations with four reversible-jump MCMC, sampling the parameters every 50 000 generations. The outputs were then analyzed using the R-package BAMMtools. We checked that the MCMC converged with effective sample size after we discarded the first 10% of samples as burn-in. We extracted the best shift configuration by setting the expected number of shifts to five.

Supplementary Figure 4. 1. (next page) Results from BAMM analysis. Branches are colored according to the mean net diversification rate across the posterior distribution.

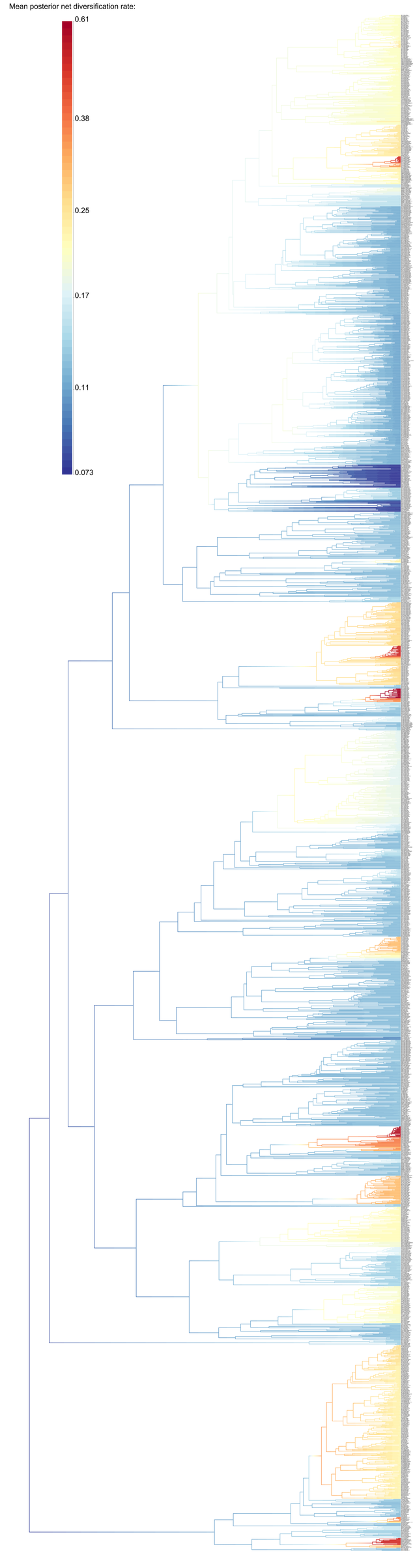
Mean posterior net diversification rate:
0.61
0.38
0.25
0.17
0.11
0.073

Supplementary Methods 5 - Biogeographic patterns of diversification: combining BAMM and DECX

We investigated the contribution of the three main processes explaining a regional species pool (dispersal, speciation, and extinction) to understand the disparity in extant species richness among biogeographic regions. We combined the speciation and extinction rates estimates for ancestral lineage obtained from BAMM with the biogeographic ranges and timing of dispersal events estimated with DECX to compare the accumulation of "out-of" *versus* "into" dispersal events, the average speciation rates and the average extinction rates among regions. We also integrated time in this analysis by computing these statistics for four different time intervals.

1 - Dispersal events

We divided time into four intervals: from 84 to 56 Myrs (Cretaceous-Paleocene: 28 Myrs-long), from 56 to 33.9 Myrs (Eocene: ~22 Myrs-long), from 33.9 to 23 Myrs (Oligocene: ~11 Myrs-long), and from 23 to 0 Myrs (Miocene-Present: ~23 Myrs-long). For each period of time we computed the sum of dispersal events among biogeographic regions. DECX does not implement biogeographic stochastic mapping and does not allow a simple use of ancestral state uncertainty in further analyses. Hence, we extracted the ranges with the highest probability at the nodes and identified the branches along which a dispersal event (range expansion) occurred. Then, to obtain a timing of dispersal events, we drew 1000 random timing of events along the branches for each event. For each replicate, we recorded the number of dispersal events between biogeographic regions occurring during each of the four periods of time. When a dispersal event occurred from a node occupying multiple areas, the source of the dispersal event was chosen by taking among the source area the one with the highest dispersal multiplier during that time period. In case there was two source areas with an equal multiplier we chose one randomly. Finally, we computed the average number of dispersal events across the 1000 stochastic timing of events and transform these sums of events into percentages of the total number of events during a period of time. For this analysis we reduced the number of areas from nine to six by combining Eastern and Western Nearctic into Nearctic, Eastern and Western Palearctic into Palearctic, India and Southeast Asia into Southeast Asia (Australasia was kept as a single area). Combining these areas improved the visualization of the results without actually loosing significant biogeographic information.

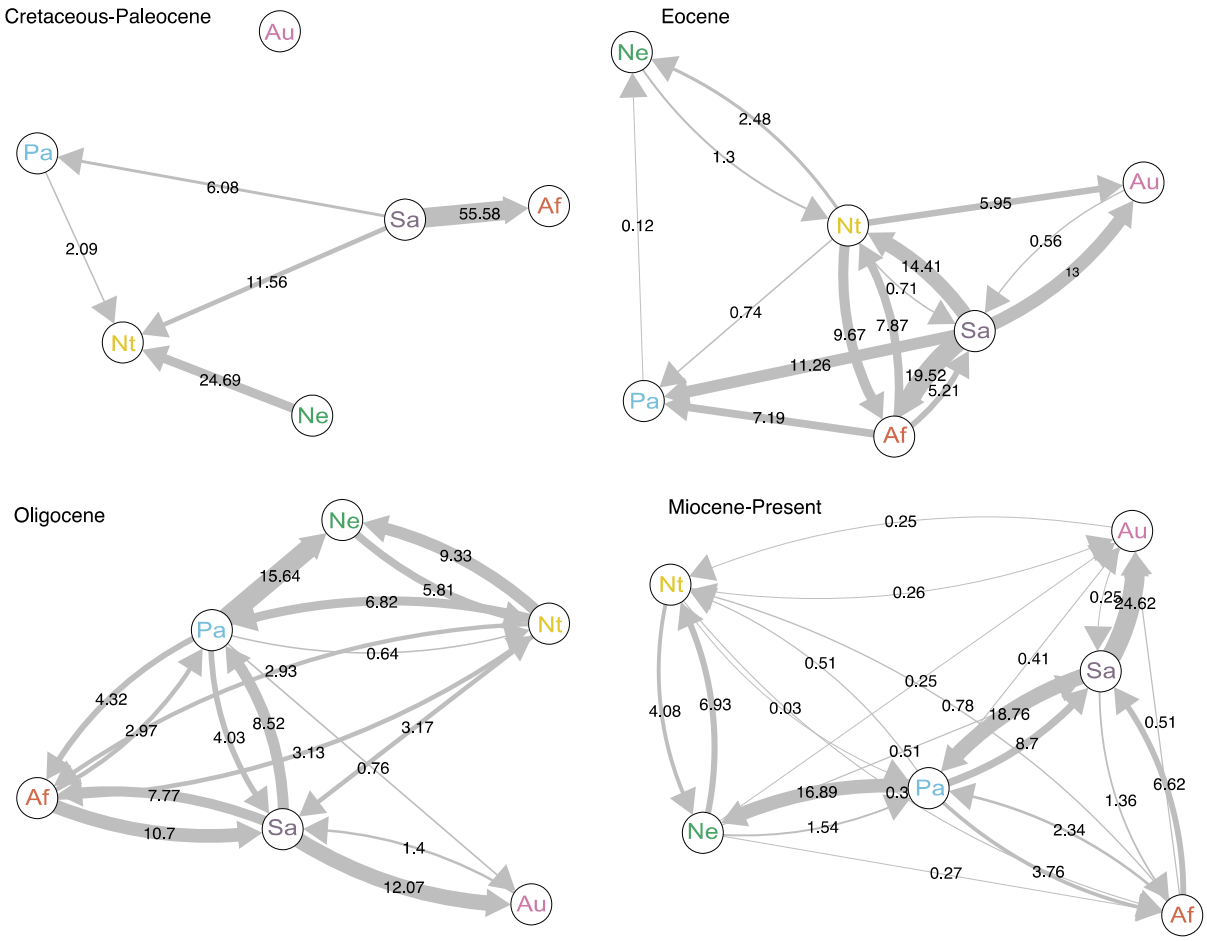

Supplementary Figure 5. 1. Full results of dispersal events during four time-intervals (Cretaceous-Paleocene, Eocene, Oligocene, Miocene-Present). Arrows indicate the direction of dispersal events. Thickness of the arrow is proportional to the amount of dispersal events occurring during the period of time. The number of dispersal events is the average number over 1000 stochastic timings of events. Numbers indicated are percentages of the total number of dispersal events during a specific period of time.

2 - Lineage-area frequency through time

We used DECX results to estimate the frequency of lineages sampled in the tree in each area through time. The number of lineages was computed within 0.5 My time-intervals. Here, in case of a dispersal event occurring along a branch, we took the midpoint of the branch as the timing of the dispersal event.

3 - Biogeography and diversification rates

We estimated how speciation and extinction rates varied through time within each biogeographic region by combining DECX ancestral range estimates and speciation/extinction rates estimation from BAMM.

a) Sliding window analysis

For the speciation and extinction rates we extracted the rates through time for all branches using the function dtRates (BAMMtools, [13]). The function dtRates discretized the phylogeny into time bins. Speciation and extinction rates of branches are then extracted for within each time window. The width of time bins is controlled by the parameter tau. In our case, we used a tau of 0.05, i.e., the topology was divided into 20 windows of equal size. In parallel, we inferred the ranges occupied along the branches from our ancestral range estimation (DECX analyses). For each branch we compared the ranges occupied at the upper node to the lower node. In the case of dispersal events occurring along the branch, we sampled another 100 stochastic timings of event for each dispersal event. Before the dispersal event, the lineage occupied the ancestral node ranges, and after the dispersal event, it occupied the descendent node range.

We used a sliding window analysis to obtain diversification rates through time for each biogeographic region. We computed the average speciation, extinction and net diversification rates per region within 4 My time-windows and shifting the window of 1 My. Within a time-window, if a lineage occupied an area, the rates estimated for this branch (or fraction of the branch in case of dispersal events) contributed to the average rate of the region. The average was computed by estimating the number of events in one area (rate*branch length) divided by the sum of branch lengths occupying this area during the same time-interval. The analysis was repeated for 100 stochastic timings of dispersal events.

b) Synthesizing diversification and dispersal

We computed the total number of "into" and "out-of" dispersal events for each biogeographic region within each of the four time-periods (Cretaceous-Paleocene, Eocene, Oligocene, Miocene-Present). Then, we summed for each region across the four time-periods the speciation rate, the extinction rate, the dispersal events into the region and the dispersal events out-of the region. We used this to generate a synthetic visualization of the processes having affected each region since the origin of Nymphalidae (Supplementary Figure 5. 3.).

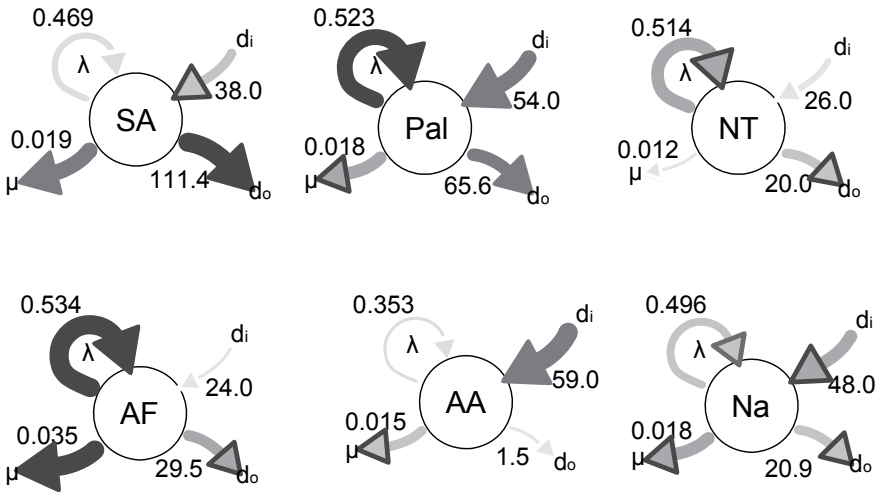

Supplementary Figure 5. 3. Relative influence of speciation rate (λ), extinction rate (μ), dispersal into (d_i), and dispersal out (d_o) across six biogeographic regions. Colour and thickness of the arrows are proportional to the statistic values when compared across regions. Speciation rate and extinction rate were calculated as the average speciation and extinction rates estimated from the sliding window analysis of BAMM results. Dispersal into and dispersal out parameters are the average sum of dispersal events into and out estimated for each biogeographic regions from our DECX analysis.

Supplementary Methods 6 – Visualization of dispersal and diversification "in real time"

It is difficult to visualize spatial and temporal patterns of diversification on large phylogenetic trees. Ancestral state biogeographic estimation in particular are difficult to synthesize, especially when uncertainty in ancestral ranges is accounted for. Here, we displayed a single realization of historical dispersal events through time on a map with present-day positions of continents for simplicity of implementation. We inferred migrations whenever descendant branches of a node were in different biogeographic regions than its ancestor and used time-stratified matrices to determine which region was more likely to be the source in cases where the ancestral branch was present in more than one location. When there were two or more regions that are equally likely to be the source according to the migration preference matrix we picked one at random.

Lines indicating migrations depart their region of origin at the time when the migrating branch begins (i.e., when the parental node splits into two). The tail of the migration line departs its origin when the head of the lineage is 30% of the way to its destination and all migrations are shown as taking the same amount of time. Regions without any lineages are displayed as white until colonization occurs.

The script used to generate the video is adapted from prior work [19], which uses the baltic module (https://github.com/evogytis/baltic) implemented in python and using matplotlib (cite https://ieeexplore.ieee.org/document/4160265).

Code available here: https://github.com/evogytis/nymphalidae-animation.

Animation can be seen here: https://youtu.be/97X5H1L8BWE and in Supplementary Movie 1.

We complemented this history of dispersal through time by also displaying the average net diversification rate through time by region estimated in a sliding window analysis (bottom left) and the relative frequency of lineages (sampled in the tree) in each region through time (bottom right).

In the case of net diversification rate, we reduced the number of regions by combining eastern and western Nearctic into "Nearctic", eastern and western Palearctic into "Palearctic", India and South-East Asia into "South-East Asia" and Afrotropics and Madagascar into "Afrotropics". We kept eastern Palearctic, western Palearctic, Afrotropics and Madagascar

separated for the lineage-frequency-through-time plot to better visualize their respective contribution to global diversity.

We complemented this history of dispersal through time by also displaying the average net diversification rate through time by region estimated by the sliding window analysis and the relative frequency of lineages (sampled in the tree) in each region through time. In the case net diversification rate, we reduced the number of regions by combining eastern and western Nearctic into "Nearctic", eastern and western Palearctic into "Palearctic", India and South-East Asia into "South-East Asia" and Afrotropics and Madagascar into "Afrotropics". We kept eastern Palearctic, western Palearctic, Afrotropics and Madagascar separated for the *lineage-frequency-through-time* plot to better visualize their respective contribution of the global diversity.

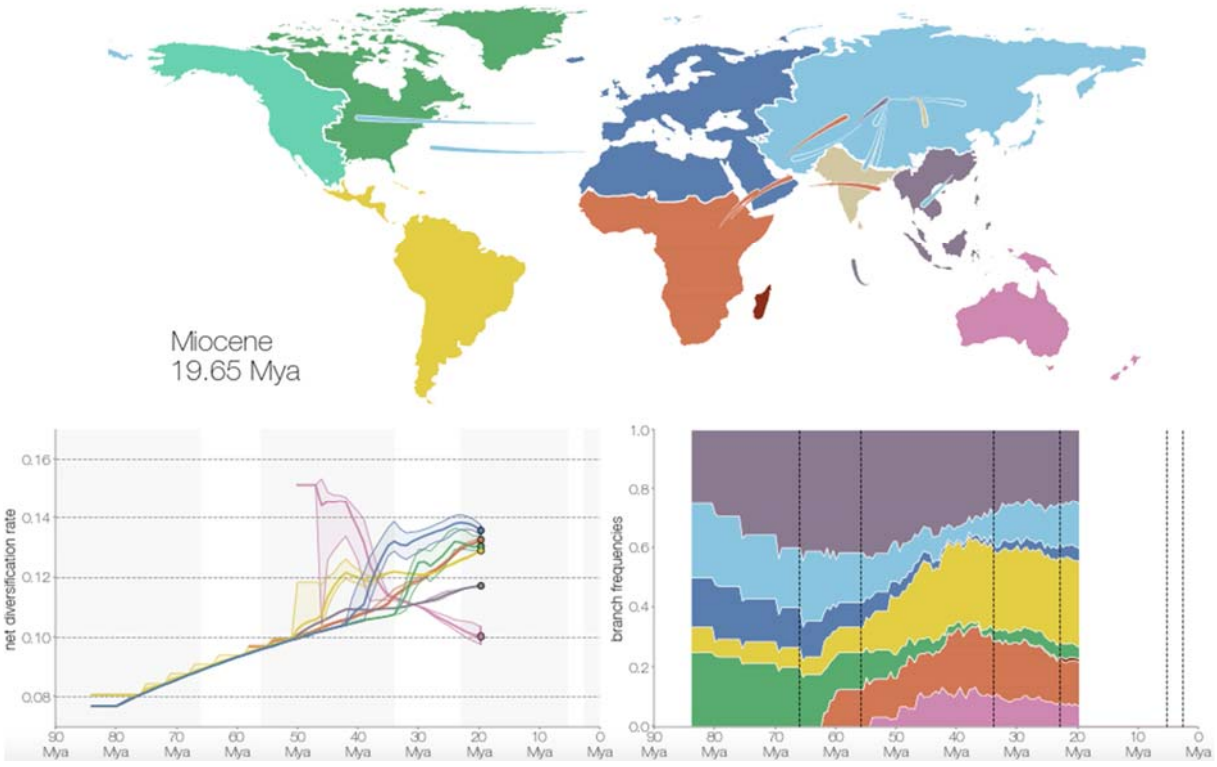

Supplementary Figure 6. 1. Snapshot of the animation. Upper plot: map of biogeographic regions used in the DECX model. Dispersal events are depicted by the "arrows" travelling from one area to another. Bottom left plot: Net diversification rate through time for the main biogeographic regions, estimated by the sliding window analysis. Bottom right plot: relative frequency lineages sampled in the tree in each biogeographic region through time.

Supplementary Methods 7 - Biogeographic patterns of diversification: regional diversification

We investigated the biogeographic pattern of diversification using an alternative approach consisting of focusing on the clades having diversified in one region only. We call these events hereafter "regional diversification".

1 - Dataset

Using the distribution of extant species and our inferred ancestral ranges we identified these regional diversification events and we computed a set of statistics to understand the processes explaining the current distribution of diversity.

We arbitrarily defined a local diversification event as a clade of at least four tips (i.e., extant taxa included in our tree) that diversified almost entirely in a single biogeographic region. We allowed rare events of range expansion, or recent dispersal events in one additional area. We also had to use a reduced number of regions: Neotropics, Afrotropics, Southeast Asia combined with Australasia, Palearctic, Nearctic. Australasia needed to be combined with South-East Asia because interchanges between the two regions happened too frequently. We identified 90 regional diversification events. For each of these events we estimated the fraction of diversity included in our tree and therefore the total number of extant species. This set of local diversifications accounted for an estimated 5373 species (and 2623 included tips) and ca. 90% of the estimated total diversity (92% of tips included in the tree).

2 - Data analyses

We designed the following tests to investigate whether (1) any difference in species richness; diversification rate and/or crown age existed between different regions, and whether (2) the age of the clade and/or diversification rate explained the variation in extant diversity within each region.

We fitted a model for each diversification event independently, in which speciation rate was modelled as an exponential function of time, while extinction rate remained constant [20] using the R-package RPANDA 1.5 [21]. We specified the appropriate sampling fraction and excluded the stem branch in the estimation of parameters. For each clade we estimated the extinction parameter (μ) and the two parameters for speciation: speciation rate at present (λ_0) and coefficient of time variation (α). Using these parameters, we also computed the speciation rate at the crown age (λ_{crown}), the net diversification at present ($netDiv_0$) and the net

diversification rate at the crown age ($netDiv_{crown}$). We tested for a difference between in species richness, crown age, $netDiv_0$, $netDiv_{crown}$ or α using a one-way anova for each parameter followed by a Tuckey test when significant. Then, we tested which parameter or parameter combination (crown age, $netDiv_0$, $netDiv_{crown}$ or α) best explained the variation in species richness within each region using a hierarchical partitioning analysis (Supplementary Table 7, Supplementary Figure 7). Models of all possible combinations of parameters were tested and compared using their AIC scores. All models within an AIC difference of 2 from lowest AIC score were considered equivalent and we reported in our discussion the simplest (less parameters) of these equivalent models.

Supplementary Table 7. Results of the hierarchical partitioning analysis performed for each biogeographic region. Models are ranked by increasing AIC score. The shaded model corresponds to the simplest model of all models within an AIC difference of 2 from the lowest AIC score. The difference of 2 AIC scores is also indicated. "Variable combinations" indicate the variables included in each model. alpha = speciation rate time-variation coefficient. netDiv0 = net diversification at present, netDivcrown = net diversification at the crown age.

a) Palearctic

Variable combinations				logLik	AIC	deltaAIC
crown age	alpha	netDiv0		-67.3	142.6	0
crown age	**netDiv0**			**-68.92**	**143.84**	**1.24**
crown age	alpha	netDiv0	netDivcrown	-67.02	144.04	1.44
crown age	netDiv0	netDivcrown		-68.89	145.79	3.19
crown age				-72.26	148.52	5.92
crown age	alpha			-71.63	149.26	6.66
crown age	netDivcrown			-72.1	150.2	7.6
crown age	alpha	netDivcrown		-71.63	151.26	8.66
alpha				-74.57	153.15	10.55
netDivcrown				-75.06	154.13	11.53
alpha	netDivcrown			-74.23	154.47	11.87
netDiv0	netDivcrown			-74.47	154.95	12.35
alpha	netDiv0			-74.57	155.15	12.55
alpha	netDiv0	netDivcrown		-74.18	156.36	13.76
netDiv0				-76.38	156.77	14.17
Theta				-77.17	158.34	15.74

b) Nearctic

Variable combinations				logLik	AIC	deltaAIC
crown age	**alpha**	**netDivcrown**		**125.73**	**-243.46**	**0**
crown age	netDiv0	netDivcrown		124.35	-240.71	2.75
alpha	netDiv0	netDivcrown		123.85	-239.71	3.75
crown age	alpha	netDiv0		123.23	-238.46	5
crown age	alpha	netDiv0	netDivcrown	123.23	-236.46	7
crown age	netDiv0			-1.74	9.48	252.94
crown age	alpha			-3.7	13.41	256.87
alpha	netDiv0			-6.35	18.71	262.17
crown age				-7.39	18.78	262.24
crown age	netDivcrown			-6.75	19.5	262.96
alpha				-10.47	24.95	268.41
alpha	netDivcrown			-10.33	26.67	270.13
netDivcrown				-14.84	33.68	277.14
netDiv0	netDivcrown			-14.49	34.99	278.45
netDiv0				-15.88	35.76	279.22

Theta				-15.96	35.92	279.38

c) Neotropics

Variable combinations				logLik	AIC	deltaAIC
crown age	netDiv0	netDivcrown		-128.22	264.44	0
crown age	alpha	netDivcrown		-128.57	265.15	0.71
crown age	netDiv0			-129.66	265.33	0.89
crown age	alpha	netDiv0	netDivcrown	-127.85	265.7	1.26
crown age				**-131.01**	**266.03**	**1.59**
crown age	netDivcrown			-130.08	266.16	1.72
crown age	alpha	alpha		-129.16	266.32	1.88
crown age	alpha			-130.99	267.99	3.55
netDiv0				-133.29	270.59	6.15
alpha				-134.2	272.4	7.96
alpha	netDiv0			-133.29	272.59	8.15
netDiv0	netDivcrown			-133.29	272.59	8.15
netDivcrown				-134.31	272.63	8.19
Theta				-134.32	272.65	8.21
alpha	netDivcrown			-134.09	274.19	9.75
alpha	netDiv0	netDivcrown		-133.29	274.58	10.14

d) Afrotropics

Variable combinations				logLik	AIC	deltaAIC
crown age	alpha	netDivcrown		-106.8	221.61	0
crown age				**-109.18**	**222.36**	**0.75**
crown age	netDiv0			-108.68	223.36	1.75
crown age	alpha	netDiv0	netDivcrown	-106.7	223.41	1.8

crown age	alpha		-108.78	223.56	1.95
crown age	netDivcrown		-109.03	224.07	2.46
crown age	netDiv0	netDivcrown	-108.22	224.45	2.84
crown age	alpha	netDiv0	-108.58	225.17	3.56
netDiv0			-117.24	238.49	16.88
alpha			-117.3	238.61	17
netDivcrown			-117.3	238.61	17
Theta			-117.31	238.62	17.01
alpha	netDiv0		-117.19	240.39	18.78
netDiv0	netDivcrown		-117.24	240.49	18.88
alpha	netDivcrown		-117.29	240.59	18.98
alpha	netDiv0	netDivcrown	-117.16	242.32	20.71

e) South-East Asia + Australasia

Variable combinations				logLik	AIC	deltaAIC
crown age				**-140.35**	**284.71**	**0**
crown age	netDivcrown			-139.99	285.99	1.28
crown age	netDiv0			-140.05	286.1	1.39
crown age	netDiv0	netDivcrown		-139.15	286.31	1.6
crown age	alpha			-140.31	286.62	1.91
crown age	alpha	netDiv0		-139.66	287.32	2.61
crown age	alpha	netDivcrown		-139.94	287.89	3.18
crown age	alpha	netDiv0	netDivcrown	-139.13	288.27	3.56
alpha				-142.2	288.4	3.69
netDiv0				-142.22	288.44	3.73
netDivcrown				-142.22	288.44	3.73
Theta				-142.22	288.45	3.74
alpha	netDivcrown			-142.16	290.33	5.62
alpha	netDiv0			-142.2	290.4	5.69
netDiv0	netDivcrown			-142.21	290.43	5.72
alpha	netDiv0	netDivcrown		-142.16	292.32	7.61

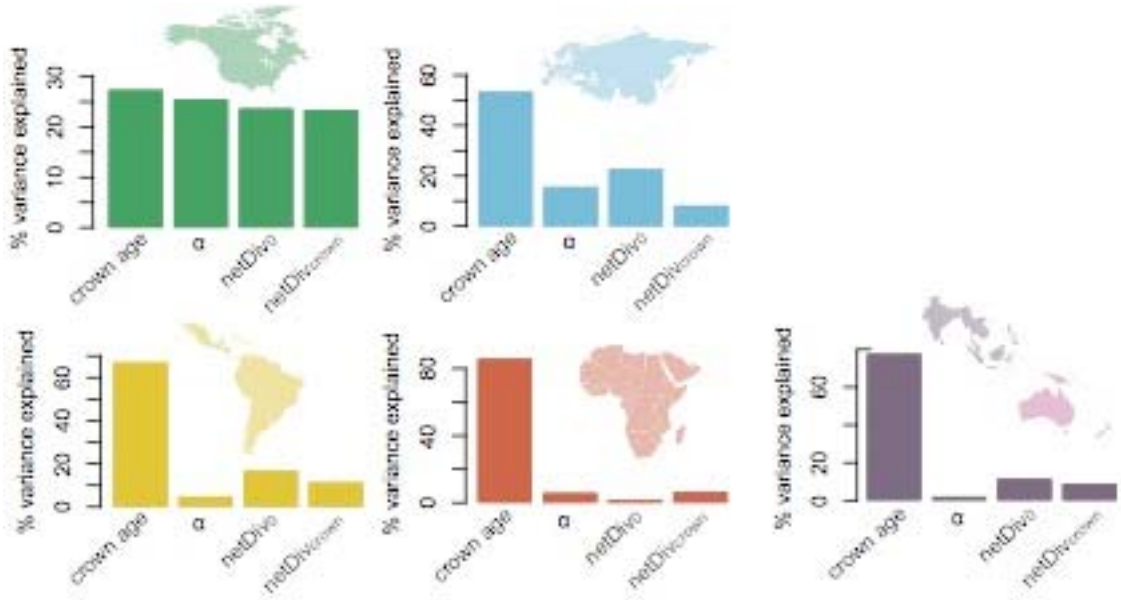

Supplementary Figure 7. Percentage of species richness variance for each region explained by crown age, α (coefficient of speciation rate time-variation), net diversification at present (netDiv0) and net diversification at the age of the crown (netDivcrown).

Supplementary References

1. Wahlberg, N. & Wheat, C. W. Genomic outposts serve the phylogenomic pioneers: designing novel nuclear markers for genomic DNA extractions of Lepidoptera. *Systematic Biology* **57**, 231–242 (2008).
2. Peña, C. & Malm, T. VoSeq: A Voucher and DNA Sequence Web Application. *PLoS ONE* **7**, e39071 (2012).
3. Ratnasingham, S. & Hebert, P. D. N. BARCODING: bold: The Barcode of Life Data System (http://www.barcodinglife.org): BARCODING. *Molecular Ecology Notes* **7**, 355–364 (2007).
4. Stamatakis, A. RAxML version 8: a tool for phylogenetic analysis and post-analysis of large phylogenies. *Bioinformatics* **30**, 1312–1313 (2014).
5. Jetz, W., Thomas, G. H., Joy, J. B., Hartmann, K. & Mooers, A. O. The global diversity of birds in space and time. *Nature* **491**, 444–448 (2012).
6. Tonini, J. F. R., Beard, K. H., Ferreira, R. B., Jetz, W. & Pyron, R. A. Fully-sampled phylogenies of squamates reveal evolutionary patterns in threat status. *Biological Conservation* **204**, 23–31 (2016).
7. Rabosky, D. L. *et al.* An inverse latitudinal gradient in speciation rate for marine fishes. *Nature* **559**, 392–395 (2018).
8. Chazot, N. *et al.* Priors and posteriors in bayesian timing of divergence analyses: the age of butterflies revisited. *Systematic Biology* **68**, 797–813 (2019).
9. Drummond, A. J., Suchard, M. A., Xie, D. & Rambaut, A. Bayesian phylogenetics with BEAUti and the BEAST 1.7. *Molecular Biology and Evolution* **29**, 1969–1973 (2012).
10. Jong, R. D. Fossil butterflies, calibration points and the molecular clock (Lepidoptera: Papilionoidea). *Zootaxa* **4270**, 1 (2017).

11. Lanfear, R., Frandsen, P. B., Wright, A. M., Senfeld, T. & Calcott, B. PartitionFinder 2: new methods for selecting partitioned models of evolution for molecular and morphological phylogenetic analyses. *Mol Biol Evol* msw260 (2016) doi:10.1093/molbev/msw260.
12. Rabosky, D. L. Automatic detection of key innovations, rate shifts, and diversity-dependence on phylogenetic trees. *PLoS ONE* **9**, e89543 (2014).
13. Rabosky, D. L. *et al.* BAMMtools: an R package for the analysis of evolutionary dynamics on phylogenetic trees. *Methods Ecol Evol* **5**, 701–707 (2014).
14. Rabosky, D. L., Mitchell, J. S. & Chang, J. Is BAMM Flawed? Theoretical and Practical Concerns in the Analysis of Multi-Rate Diversification Models. *Systematic Biology* **66**, 477–498 (2017).
15. Moore, B. R., Höhna, S., May, M. R., Rannala, B. & Huelsenbeck, J. P. Critically evaluating the theory and performance of Bayesian analysis of macroevolutionary mixtures. *Proc Natl Acad Sci USA* **113**, 9569–9574 (2016).
16. Ree, R. H. & Smith, S. A. Maximum likelihood inference of geographic range evolution by dispersal, local extinction, and cladogenesis. *Systematic Biology* **57**, 4–14 (2008).
17. Smith, S. A. Taking into account phylogenetic and divergence-time uncertainty in a parametric biogeographical analysis of the Northern Hemisphere plant clade Caprifolieae. *Journal of Biogeography* **36**, 2324–2337 (2009).
18. Beeravolu Reddy, C. & Condamine, F. *An extended maximum likelihood inference of geographic range evolution by dispersal, local extinction and cladogenesis*. http://biorxiv.org/lookup/doi/10.1101/038695 (2016) doi:10.1101/038695.
19. Dudas, G. *et al.* Virus genomes reveal factors that spread and sustained the Ebola epidemic. *Nature* **544**, 309–315 (2017).

20. Morlon, H., Parsons, T. L. & Plotkin, J. B. Reconciling molecular phylogenies with the fossil record. *Proceedings of the National Academy of Sciences* **108**, 16327–16332 (2011).
21. Morlon, H. *et al.* RPANDA: an R package for macroevolutionary analyses on phylogenetic trees. *Methods Ecol Evol* **7**, 589–597 (2016).